UDK 621.3:(53+54+621+66)(05)(497.1)=00 ISSN 0352-9045

INFORMACIJE MIDEM 2 ◦2000

Strokovno društvo za mikroelektroniko elektronske sestavne dele in materiale

Strokovna revija za mikroelektroniko, elektronske sestavne dele in materiale
Journal of Microelectronics, Electronic Components and Materials

INFORMACIJE MIDEM, LETNIK 30, ŠT. 2(94), LJUBLJANA, junij 2000

UDK 621.3:(53+54+621+66)(05)(497.1)=00 ISSN 0352-9045

INFORMACIJE MIDEM 2 ◦ 2000

INFORMACIJE MIDEM LETNIK 30, ŠT. 2(94), LJUBLJANA, JUNIJ 2000
INFORMACIJE MIDEM VOLUME 30, NO. 2(94), LJUBLJANA, JUNE 2000

Revija izhaja trimesečno (marec, junij, september, december). Izdaja strokovno društvo za mikroelektroniko, elektronske sestavne dele in materiale - MIDEM.
Published quarterly (march, june, september, december) by Society for Microelectronics, Electronic Components and Materials - MIDEM.

Naslov uredništva
Headquarters
Uredništvo Informacije MIDEM
Elektrotehniška zveza Slovenije
Dunajska 10, 1000 Ljubljana, Slovenija
tel.: +386 (0)1 5112 221
fax: +386 (0)1 5112 217
Iztok.Sorli@guest.arnes.si
http://paris.fe.uni-lj.si/midem/journal.htm

Letna naročnina znaša 12.000,00 SIT, cena posamezne številke je 3000,00 SIT. Člani in sponzorji MIDEM prejemajo Informacije MIDEM brezplačno.
Annual subscription rate is DEM 200, separate issue is DEM 50. MIDEM members and Society sponsors receive Informacije MIDEM for free.

Znanstveni svet za tehnične vede I je podal pozitivno mnenje o reviji kot znanstveno strokovni reviji za mikroelektroniko, elektronske sestavne dele in materiale. Izdajo revije sofinanci rajo Ministrstvo za znanost in tehnologijo in sponzorji društva.
Scientific Council for Technical Sciences of Slovene Ministry of Science and Technology has recognized Informacije MIDEM as scientific Journal for microelectronics, electronic components and materials.
Publishing of the Journal is financed by Slovene Ministry of Science and Technology and by Society sponsors.

Znanstveno strokovne prispevke objavljene v Informacijah MIDEM zajemamo v podatkovne baze COBISS in INSPEC.

Prispevke iz revije zajema ISI® v naslednje svoje produkte: Sci Search®, Research Alert® in Materials Science Citation Index™

Scientific and professional papers published in Informacije MIDEM are assessed into COBISS and INSPEC databases.

The Journal is indexed by ISI® for Sci Search®, Research Alert® and Material Science Citation Index™

Po mnenju Ministrstva za informiranje št.23/300-92 šteje glasilo Informacije MIDEM med proizvode informativnega značaja, za katere se plačuje davek od prometa proizvodov po stopnji 5 %.

Grafična priprava in tisk
Printed by
BIRO M, Ljubljana

Naklada
Circulation
1000 izvodov
1000 issues

Poštnina plačana pri pošti 1102 Ljubljana
Slovenia Taxe Percue

UDK621.3:(53+54+621+66), ISSN0352-9045 Informacije MIDEM 30(2000)2, Ljubljana

ZNANSTVENO STROKOVNI PRISPEVKI		PROFESSIONAL SCIENTIFIC PAPERS
G.W. Herzog, A. Reichmann, K. Reichmann, M. Ruplitsch-Lesnik, K Gatterer: Električne, magnetne in katalitske karakteristike materialov spinelnega in perovskitnega tipa, ki vsebujejo kobalt	71	G.W. Herzog, A. Reichmann, K. Reichmann, M. Ruplitsch-Lesnik, K Gatterer: Electronic, Magnetic and Catalytic Properties of Cobalt Containing Spinel and Perovskite Type Materials
L. Koller, M. Bizjak, B. Praček: Čiščenje tankih pasivacijskih prevlek na Ag kontaktnem materialu z vakuumskim razplinjevanjem	78	L. Koller, M. Bizjak, B. Praček: Cleaning of Thin Passivation Layers on the Ag Contact Material with Vacuum Outgassing
M. Knaipp, F. Unterleitner: Izbira termičnih robnih pogojev pri modeliranju inteligentnih močnostnih vezij	82	M. Knaipp, F. Unterleitner: Thermal Boundary Conditions in Smart Power Devices
D. Korošak, B. Cvikl:Modelski izračun odvisnosti induciranega naboja na vmesni plasti od zunanje napetosti na polprevodniških strukturah narejenih z metodo curka ioniziranih skupkov atomov	89	D. Korošak, B. Cvikl: Model Calculation of Ionized Cluster Beam Induced Bias Dependent Interface Charge
M. Milanovič, A. Roškarič, M. Auda: Polnilnik baterij zasnovan na dvojnem pretvorniku navzdol in pretvorniku navzgor	98	M. Milanovič, A. Roškarič, M. Auda: Battery Charger Based on Double-buck and Boost Converter
M. Komac: Tehnološko predvidevanje: instrument nabora družbeno in gospodarsko releventnih vsebin raziskovanja	105	M. Komac: Technology Foresight: a Convenient Tool for the Prioritization of Scientific Research
R. Osredkar, B. Gspan: Študija planarizacijskih lastnosti tankih BPSG plasti	110	R. Osredkar, B. Gspan: A Study of Planarizing Properties of Thin BPSG Films
KONFERENCE, POSVETOVANJA, SEMINARJI, POROČILA		**CONFERENCES, COLLOQUYUMS, SEMINARS, REPORTS**
L. Trontelj: Tridesetletnica Laboratorija za mikroelektroniko na Fakulteti za elektrotehniko v Ljubljani	113	L. Trontelj: Thirty Years of Laboratory of Microelectronics on Faculty of Electrical Engineering in Ljubljana
M. Hrovat: Šesti Groveov simpozij o gorivnih celicah	114	M. Hrovat: Sixth Grove Fuel Cell Symposium
M.Hrovat: Konferenca Micro Technologies 2000	118	M.Hrovat: Conference Micro Technologies 2000
I. Pompe: Kdor pride pozno, dobi kosti	121	I. Pompe: Who comes too late gets the bones
Pozdravni govor ob odprtju analitskega elektronskega mikroskopa JEM-2010 F, dne 22. junija 2000 na Institutu Jožef Stefan v Ljubljani	122	Speech at the Occasion of Inauguration of the Electronic Microscope JEM-2010 F on 22. June 2000 at the Jožef Stefan Institute
VESTI	123	**NEWS**
KOLEDAR PRIREDITEV	128	**CALENDAR OF EVENTS**
MIDEM prijavnica	129	MIDEM Registration Form
Slika na naslovnici: Učinkovite rešitve za izzive deregulirenega trga električne energije		Front page: Effective solutions for challenges for deregulated market of electric energy

VSEBINA **CONTENT**

36th INTERNATIONAL CONFERENCE ON MICROELECTRONICS, DEVICES AND MATERIALS

With the WORKSHOP on

ANALYTICAL METHODS IN MICROELECTRONICS AND ELECTRONIC MATERIALS

October 18. - 20. 2000
Postojna, SLOVENIA

http://paris.fe.uni-lj.si/midem/conference2000.htm

Elektrotehniška Zveza Slovenije

POSTOJNSKA JAMA

IEEE Slovenia Section

ELECTRONIC, MAGNETIC AND CATALYTIC PROPERTIES OF COBALT CONTAINING SPINEL AND PEROVSKITE TYPE MATERIALS

G.W. Herzog, A. Reichmann, K. Reichmann, M. Ruplitsch-Lesnik
Institut für Chemische Technologie Anorganischer Stoffe
and K. Gatterer
Institut für Physikalische und Theoretische Chemie
Technische Universität Graz

Keywords: spinel type materials, perovskite type materials, Co Cobalt spinel type materials Co_3O_4, Co Cobalt perovskite type materials $LaCoO_3$, electrical properties, magnetic properties, mechanical properties, correlations between properties, practical examples

Abstract: Correlations between electric, magnetic and catalytic properties of various Cobalt containing spinel and perovskite type materials (e.g. Co_3O_4, $LaCoO_3$) were investigated with respect to application in environmental catalysis. As a fast test reaction the CO oxidation with air up to 400°C was chosen and found to be initiated by high-spin Co^{2+} ions at the surface. Thus, catalytic activity depends strongly on the condition of materials preparation. From comparison of the activation energies of the oxidation rate and hopping bulk charges it is concluded, that an activated charge transfer between Co^{2+} and Co^{3+} ions at the surface is the rate determining step. However, the bulk conductance itself does not play any role for catalytic activity. A hindrance for broad application of perovskite type catalysts is the fast deactivation by SO_2. As it is chemisorbed and oxidized at the active Co^{2+} sites to give sulfate, SO_2 stops the CO oxidation immediately. Only a partial recovery is possible by heating at higher temperatures, therefore the substitution of Pt metal catalysts by such materials fails, when SO_2 is present in a waste gas.

Električne, magnetne in katalitske karakteristike materialov spinelnega in perovskitnega tipa, ki vsebujejo kobalt

Ključne besede: materiali tipa spinel, materiali tipa perovskite, Co Kobalt materiali tipa spinek Co_3O_4, Co Kobalt materiali tipa perovskite $LaCoO_3$, lastnosti električne, lastnosti magnetne, lastnosti katalitične, korelacija med lastnostmi, primeri praktični

Izvleček: Preiskovali smo korelacije med električnimi, magnetnimi in katalitskimi karakteristikami različnih materialov, ki vsebujejo kobaltove ione in imajo spinelno ali perovskitno strukturo, na primer Co_3O_4 in $LaCoO_3$. Za hitro testiranje smo izbrali oksidacijo CO v zraku pri 400°C. Ugotovili smo, da je reakcija katalizirana s Co^{2+} ioni z visokim spinom, ki se nahajajo na površini. To pomeni, da je aktivacijska energija katalize močno odvisna od priprave materiala. Iz primerjave aktivacijskih energij hitrosti oksidacije in »hopping« prevajanja v samem materialu smo ugotovili, da je aktiviran prenos naboja med Co^{2+} in Co^{3+} ioni na površini tisti, ki določa hitrost reakcije. Prevodnost samega materiala ne vpliva na katalitsko aktivnost.Možnost široke aplikacije katalizatorjev perovskitnega tipa pa preprečuje hitra deaktivacija teh katalizatorjev z SO_2. SO_2 se adsorbira na površini in na aktivnih Co^{2+} mestih oksidira v sulfat ter tako takoj prepreči oksidacijo CO. Katalitska aktivnost se lahko samo delno obnovi s segrevanjem pri povišani temperaturi. Zato zaenkrat ni možna zamenjava katalizatorjev na osnovi platine s takimi materiali, če je v odpadnih plinih prisoten SO_2.

INTRODUCTION

Since more than two decades Co containing spinels (e.g. Co_3O_4) and perovskites (e.g. $LaCoO_3$) are well-known materials of high catalytic activity /1, 2/, for instance for gas phase oxidation with air. Further, applications in gas sensors (for CO) were taken into consideration /3,4/. Unfortunately the relevance of these materials to environmental catalysis or other purposes seems to be extremely restricted and most of the existing literature is not very promising /5-7/. When applied to real gas mixtures, there is a high risk of poisoning. On the other hand, these or similar mixed valence materials are catalytically as active as Pt or Pd and a possible substitution of the latter by oxides is still a certain commercial challenge.

The outstanding catalytic activity is supposed to be connected with a special spin or bond situation of the Co ions, which can be two, three or fourfold charged /8-13/. Most of such ideas are based on mixed-valence and crystal field models, but a direct experimental correlation or evidence for a favored high spin action has never been obtained. A similar lack of knowledge exists for a possible correlation with electric properties, which would be vital for an extended use for sensor elements.

In general spinel and perovskite type materials can be tailored in a wide stoichiometric range, behaving either insulating, semiconducting or metallic in the catalytically interesting temperature range /14-16/. So the first aim of this work was to prepare thermally stable and active materials and to investigate, whether magnetic or electric correlations with catalytic activity can be found or not. In following this way, of course, special attention had to be paid to the interpretation of results because of the basic differences of bulk and surface properties.

The second aim of this work was to investigate the applicability of spinel and perovskite type materials for the CO oxidation in waste gases with a high level of SO_2, caused by the low cost incineration of S containing fuels. To gain more basic know-how for an eventual

application, catalytical experiments were carried out not only with powders but also with ceramic honey combs under realistic gas conditions, i.e. with reasonable space velocities /17,18/.

EXPERIMENTAL

For our investigations we chose materials, that were proved to be thermally stable in the temperature range up to 600°C. Those were:

1. Spinel type materials: $ZnNiMnO_4$, Co_3O_4.
2. Perovskite type materials: $LaCoO_3$, $LaNiO_3$, $LaNi_{1-x}Co_xO_3$, $LaAl_{1-x}Co_xO_3$, $LaTi_{1-x}Co_xO_3$, $La_{0,8}Sr_{0,2}CoO_3$.

Except Co_3O_4, which was purchased from MERCK (analytical grade), both spinel and perovskite type materials were prepared by coprecipitation of about 0,05m nitrate solutions with 3 m NaOH. After careful washing with deionised water and drying at 110°C, the calcination of hydroxides was carried out in air at different temperatures up to 1150°C for several hours. To characterize the powders the chemical stoichiometry was determined by wet chemical methods, BET surface was measured with a Quantachrome surface analyser and X-ray spectra were taken on a Siemens D5005 diffractometer. For susceptibility measurements the native powders were used of Co_3O_4, $LaCoO_3$ and $LaTi_{1-x}Co_xO_3$ at temperatures between 80K and 600K the magnetic susceptibility was measured with a modified Faraday balance. Low-temperature measure-ments between 4,2 and 80 K were performed with a Lake Shore 7121 magnetometer using liquid Helium for cooling. $KCr(SO_4)_2.12H_2O$ was used for calibration in both cases.

For electrical measurements the powders were pressed into pellets and sintered taking into account the range of stability. The DC bridge consisted of a Wenking Galvanostat LT-78 and a Knick Voltmeter. Catalytical measurements of the CO oxidation were usually made with spherical agglomerates of 0,1 to 1μm particles, sieved into a fraction of 0,5 to 1,25 mm, in an electrically heated double-tube reactor made of Pyrex glass with a inner diameter of 2 cm. The gas flow was kept constant by means of two Brooks mass flow meters 5858 TR at a space velocity of about 50 000 h^{-1}. Most experiments were carried out with a mixture of air (H_2O content <0,5vol%) and CO (0,1-1vol%). In some cases instead of air a water free mixture of 2% O_2 and 98% N_2 was used. The influence of SO_2 was studied by adding 0,1% SO_2 to the normal gas stream. The conversion of CO into CO_2 was continuously monitored by means of a CO/CO_2 IR detector Ultramat 22P from Siemens, varying the temperature stepwise. The reactor was usually filled with 2-5 g material equivalent to a height of about 1-3 cm.

Additionally small honey combs (2,5x2,5x10 cm with 25 channels) were prepared from powder mixtures of TiO_2/WO_3 (10%wt)/$LaCoO_3$ (20%wt) and SiO_2(90 %wt) /$LaCoO_3$(10 %wt) by extrusion, with the know-how and facilities of the catalyst producer FRAUENTAL KERAMIK, Austria. These honey combs were tested with a separate micro reactor, which was in use at the above mentioned company.

XPS data from literature show, that the Co content at the surface strongly depends on calcination temperature /19-21/. Therefore we varied additionally the calcination temperature of $LaCoO_3$ between 620 and 1150°C. Some calcined products were treated with water, because this significantly enhanced the catalytic activity. For comparison we included a commercial support coated with Pd (supplied by Kanzler Verfahrenstechnik, Austria) into our investigations.

RESULTS

Catalytic Properties

In the following figures all conversion/temperature curves refer to the gas inlet temperature, because the heat evolution during oxidation and thereby caused temperature distribution makes the kinetics a dynamical one. So self heating, formally acting as an autocatalytic reaction was the reason why we usually did not analyze the kinetics. But from several measurements approaching equilibrium temperatures, achieved with a smaller amount of catalyst and CO (reduced self-heating), we can roughly state, that up to a high degree the conversion curves correspond to an Arrhenius´ law of activation, excluding a transport limitation in the gas phase up to about 300°C. It is remarkable that activation energies of such a variety of materials like $LaCoO_3$, $LaNiO_3$, Co_3O_4, prepared at different calcination temperatures are almost equal and amount to 0,6±10%eV (fig. 1).

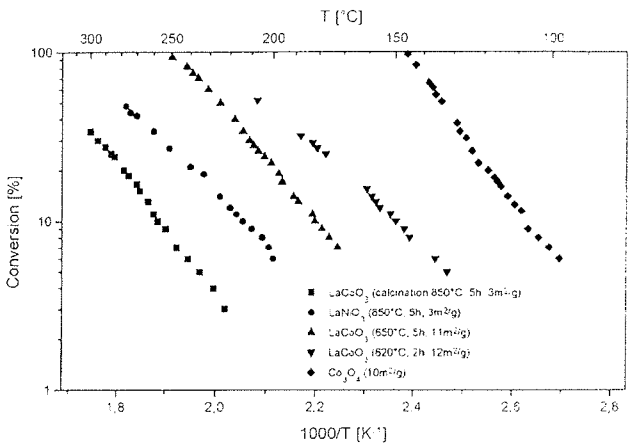

Fig. 1: Arrhenius´ evaluation of conversion curves.

As can be noticed from fig. 2, one of the most CO active substances except Pd covered supports is Co_3O_4. CO/CO_2 conversion starts below 100°C and reaches values of 100% at about 140°C, whereas $LaCoO_3$ needs at least 50° higher inlet temperature. The conversion curves of the Ni and Al substituted $LaCoO_3$ materials display one common feature: the higher the Co content in the bulk and hence at the surface, the more active is the material. Because of the much higher Co content, Co_3O_4 fits well into this simple model.

A similar conclusion can be drawn from the conversion behavior of the honey combs and the reground honey combs, showing no essential difference. Such honey

combs work like a mixture of powders. Furthermore, it does not matter, whether the ions substituted for Co in $LaCoO_3$ are active 3d-ions (Ni^{3+}) or not (Al^{3+}). But at this stage we cannot decide, which kind of Co ions with respect to valence and spin state at the surface is responsible for the catalytic oxidation. The support TiO_2/WO_3, which is the commercial basis for ceramic catalysts for NOx-reduction, is inactive for CO-oxidation and the activity depends only on the amount of $LaCoO_3$.

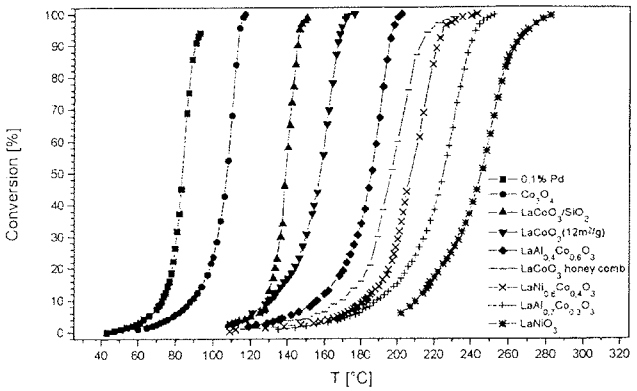

Fig. 2: Conversion curves of various materials (reactor filling 5 g).

Two preparation phenomena, which lead to a veritable increase of the catalytical activity are documented in figs. 3a and 3b. The first one concerns the calcination temperature and the second one the treatment of already calcined products with water. Calcination at lower temperatures leads to higher, surface-normalized reaction rates and treatment with water shifts the conversion curve to lower temperatures.

By normalization with respect to surface area for the conversion curves in fig.3a an activity ratio of 17:7:4 is found. X-ray analysis of these materials proved perovskite type structure and no additional impurity phases were found. For materials calcined at lower temperatures we assume, that these are more active because of unoxidized Co^{2+} species. On the other hand, the treatment with water (fig.3b) might have cleaning or dissolution effects, or the Co^{3+} ions are reduced to more active Co^{2+} ions approaching the case of Co_3O_4.

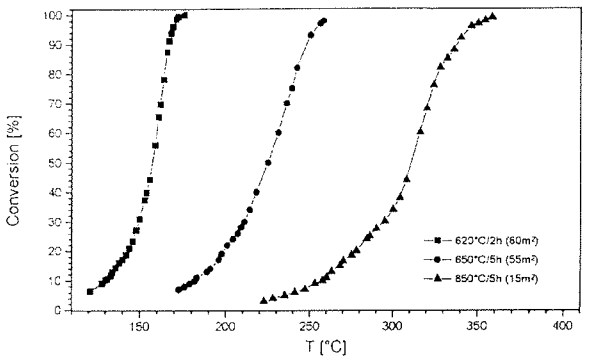

Fig. 3a: Conversion curves of 5g $LaCoO_3$ calcined at different temperatures.

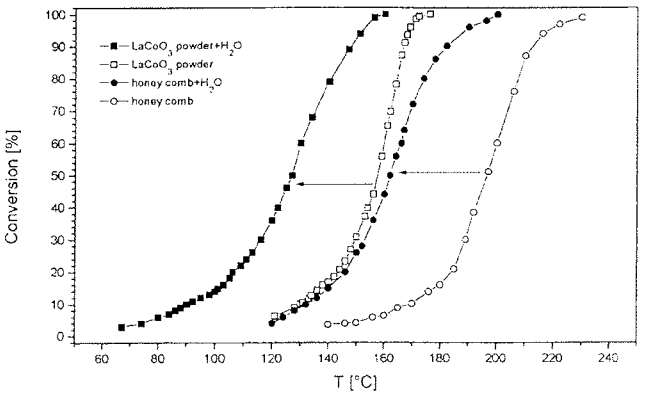

Fig. 3b: Shift of conversion curves by water treatment.

Some additional experiments were carried out with Sr^{2+}- and Ti^{4+}-substituted materials (fig. 4). Both the Sr^{2+} substitution of La^{3+} ions and the Ti^{4+} substitution of Co^{3+} ions shift the conversion to lower temperatures.

Here and in all other cases of Co and Ni containing catalysts the influence of SO_2 is extremely negative: The CO oxidation is completely stopped within a few minutes, indicating a lethal chemical adsorption of SO_2 or SO_3. As shown by $La_{0,8}Sr_{0,2}CoO_3$ in fig. 4 a certain but not total recovery is only achievable by heating up to temperatures above 600°C. Pd coated supports do not show this behavior and oxidize SO_2 into SO_3 in parallel to CO, even in a 2% O_2 containing gas.

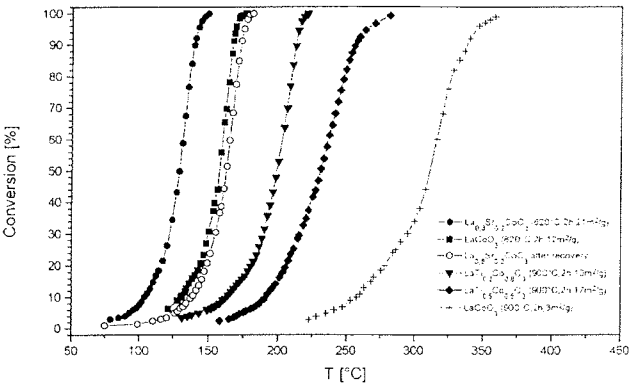

Fig. 4: Conversion influenced by substitution and SO_2 poisoning.

Electrical Properties

Referring to room temperature, the bulk conductivity of sintered pellets of the materials under investigation range from metallic (e.g. $LaNiO_3$) to semiconducting (e.g. $LaCoO_3$, $ZnNiMnO_4$) and low conducting materials (heavily Al and Ti doped $LaCoO_3$) (fig. 5).

In the catalytically interesting temperature range of 100 to 400°C, $LaCoO_3$ behaves semiconducting with an activation energy of about 0,55eV /22-24/. Above 400°C the behavior changes to a metallic type. Doping with Ti decreases the conductivity and increases the activation

energy to about 0,6-0,7eV /25-28/. Co_3O_4 also behaves semiconducting, but with an activation energy changing from low to high temperatures (0,3-0,7eV) /29, 30/. On the other hand, in a wide range $LaNiO_3$ is a Pauli type metallic conductor /31, 32/.

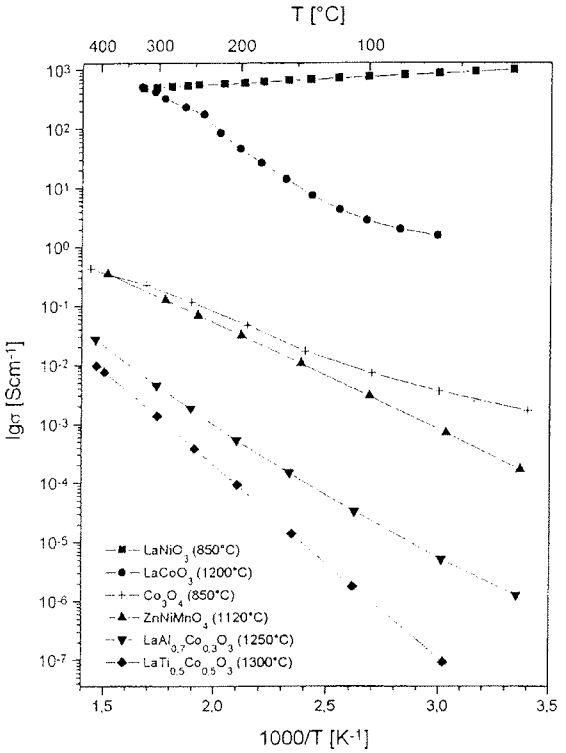

Fig. 5: Conductivity data of some active materials.

Most of the sintered Co and Ni containing materials conduct via activated hopping of electronic charges, i.e. small polarons. So one is tempted to assume, that the Arrhenius´ like conversion curves (fig. 1), which are proportional to the temperature dependence of the oxidation rate, are kinetically determined by the balance of hopping charges. Activation energies for hopping conduction and conversion rates are of the same order of magnitude (0,6 eV).

However, a simple inspection of the conductivity and activity data of $LaNiO_3$ reveals, that there is no direct correlation between electrical bulk and catalytical surface properties. This is also supported by the results obtained with Sr- and Ti-substituted $LaCoO_3$. As Sr-substitution increases the electronic conductivity and Ti-substitution decreases it, the enhanced catalytic activity in both cases shows that electronic conductivity does not have any influence on the conversion rate. So one is led to state, that bulk and surface regions are not coupled. If there is still an Arrhenius´ like temperature dependence, it must either be caused by a quite different activated step or by a charge transfer between Co^{2+} and Co^{3+} ions (Ni^{2+} and Ni^{3+} ions respectively) because of a restructured $LaCoO_3$ surface. In other words, we conclude, that in all cases the catalytic activity depends on a properly mixed valence state at the surface, as it is given in the case of the spinel Co_3O_4.

Magnetic Properties

Co_3O_4 is a mixed-valence compound with normal spinel structure. Co^{2+} ions are located at tetrahedrally and Co^{3+} ions at octahedrally oxygen coordinated lattice positions /33, 34/. It was first shown by Cossee /35/, that the observed magnetic susceptibility is consistent with a material, where Co^{2+} ions are high-spin (total spin S=3/2) with a spin-only moment of $\mu_{SO}=3.87\mu_B$ (equ.1) and Co^{3+} ions are low-spin (S=0) because of the strong octahedral crystal field.

$$\mu_{SO} = \sqrt{4S(S+1)} \cdot \mu_B = 3{,}87\mu_B \qquad (1)$$

μ_{SO}: spin-only moment
μ_B: Bohr magneton

The temperature dependence of the susceptibility (fig. 6) shows Curie-Weiss behavior (equ. 2). The evaluation including a diamagnetic correction with Pascal constants /36/ leads to an effective moment of $\mu_{eff}=4{,}57\mu_B$ (equ. 3). The deviation from the spin-only value 3,87 can be attributed satisfactorily to spin-orbit coupling /35/.

$$\chi = \frac{C}{T-\Theta} \qquad (2)$$

χ: Susceptibility
Θ: Weiss-Temperature (-109K)
C: Curie Constant (2,607 cm^3Kmol^{-1})

$$\mu_{eff} = \sqrt{8C} \cdot \mu_B = 4{,}57\mu_B \qquad (3)$$

μ_{eff} effective moment

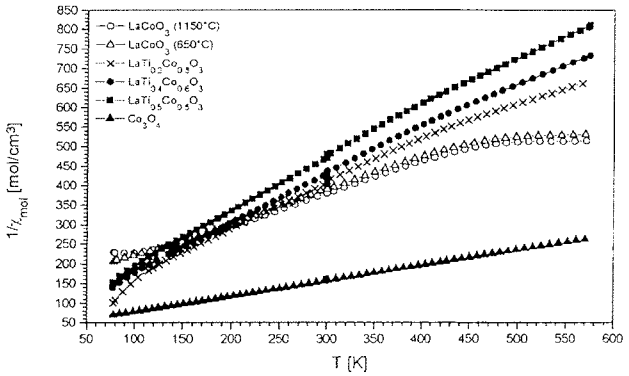

Fig. 6: Inverse molar susceptibilities.

The low-temperature susceptibility (fig. 7 curve a) goes through a maximum at about 40 K (Neel-temperature), which is consistent with an antiferromagnetic ordering of Co^{2+} spins /34/. A Co_3O_4 sample exposed to 0,1% SO_2 under conversion conditions (45 min, 310°C) has the same Neel-temperature, but shows an increase of the magnetic susceptibility towards lower temperatures (fig. 7 curve b). The absence of a field dependence excludes the presence of ferromagnetic impurities in the exposed sample. The additional component is paramagnetic and most probably surface $CoSO_4$. The

relative amount of $CoSO_4$ in the sample can be roughly estimated to about 0,2%, when the observed Curie constant of the paramagnetic component is compared with the one of $CoSO_4$.

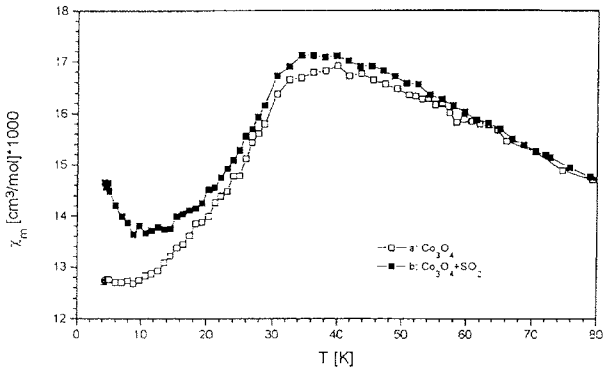

Fig.7: Low-temperature molar susceptibility of Co_3O_4 (a) and Co_3O_4 exposed to SO_2 (b)

On the other hand, Co^{3+} ions in $LaCoO_3$ occupy octahedral positions and their spin state changes in a wide temperature range /8, 9, 37/. The magnetic properties are governed by a subtle balance between the crystal field strength and the intra-atomic exchange energy, so that small temperature changes may cause conversion from low-spin to high-spin state and vice versa. The $1/\chi$ values of $LaCoO_3$ samples calcined at different temperatures are almost identical in the temperature range 150 to 600 K (fig 6). Above 400 K the inverse susceptibility reaches a temperature independent plateau, indicating a metal like phase /9, 38/. From 150 to 400 K the Curie-Weiss law applies, below 100 K severe discrepancies of the differently calcined materials occur. Samples calcined at temperatures above 900°C show a minimum in the $1/\chi$ curve, while those calcined below 900°C do not show a minimum. The $1/\chi$ curve decreases rapidly towards lowertemperatures and a notable field dependence is observed indicating an additional ferromagnetic phase /9, 38, 39/.

The presence of this ferromagnetism, which dominates the low-temperature susceptibility excludes a direct observation of the paramagnetic surface $CoSO_4$ species in SO_2 exposed $LaCoO_3$ samples. Curie Constants, C, Weiss temperatures, Θ and effective moments, μ_{eff}, of a Curie-Weiss analysis with diamagnetic correction are given in table 1.

According to a recent reinvestigation of $LaCoO_3$ /9/ the following conclusions can be drawn. The calculated effective moment for a 1:1 mixture of low- and high-spin Co^{3+} ions is 3,46 μ_B, however, smaller values are found experimentally. The reason for this difference could either be due to the presence of less than 50% high-spin Co^{3+} (μ_{S0}=4,9 μ_B) or to a partial replacement of the high-spin species by Co^{2+} (μ_{S0}=3,87 μ_B) or to both at the same time. The fact that the samples calcined at lower temperatures give the smaller effective moments is consistent with a larger amount of surface Co^{2+}, which also explains the observed field dependence.

Table 1: Curie-Weiss analysis

Sample	C [cm^3Kmol^{-1}]	Θ [K]	μ_{eff} [μ_B]
$LaCoO_3$ (1150°C/5h)	1,234	-158	3,14
$LaCoO_3$ (1050°C/5h)	1,240	-160	3,15
$LaCoO_3$ (950°C/5h)	1,229	-158	3,14
$LaCoO_3$ (850°C/5h)	1,211	-155	3,11
$LaCoO_3$ (750°C/5h)	1,204	-153	3,10
$LaCoO_3$ (650°C/5h)	1,194	-155	3,09
$LaTi_{0,2}Co_{0,8}O_3$ (900°C/2h)	0,888	-54	2,67
$LaTi_{0,4}Co_{0,6}O_3$ (900°C/2h)	0,837	-52	2,59
$LaTi_{0,5}Co_{0,5}O_3$ (900°C/2h)	0,762	-51	2,47
Co_3O_4	2,607	-109	4,57

For the catalytic activity of $LaCoO_3$ materials the existence of Co^{2+} at the surface is obviously of great importance. When the materials are calcined at lower temperatures a larger amount of unoxidized Co^{2+} species is retained causing higher activity (see fig. 3a). At the same time, treating the materials with water causes reduction of Co^{3+} to Co^{2+} thus, again enhancing the catalytic activity (see fig. 3b).

In the attempt to create Co^{2+} ions in $LaCoO_3$ we substituted Ti^{4+} for Co^{3+} ions. The inverse susceptibilities of three samples $LaTi_xCo_{1-x}O_3$ (x = 0,2, 0,4, 0,5) are also shown in fig. 6. Ti^{4+} is diamagnetic, hence a reduction of the susceptibility with increasing substitution is expected and is observed (table 1). The $1/\chi$ behavior is consistent with a metallic $LaCoO_3$ phase coexisting with paramagnetic Co^{2+} ions. The effective moment can be estimated according to

$$\mu_{eff} = \sqrt{x \cdot \mu_{S0}^2\left(Co^{2+}\right) + (1-2x) \cdot \mu_{eff}^2(LaCoO_3)} \cdot \mu_B \qquad (4)$$

Insertion of 3,87 for Co^{2+} and 3,10 for $LaCoO_3$ leads to the values 2,95 for x = 0,2, 2,81 for x = 0,4 and 2,73 for x = 0,5. From chemical analysis we know, that the com-

Table 2: Chemical analysis of Co oxidation state in $LaTi_{1-x}Co_xO_3$ materials

Perovskite	Average Co oxidation state			BET surface of calcined materials [m^2/g]
	nominal	observed		
		calcined 900°C	sintered 1250°C	
$LaCoO_3$ (620°C/2h)	3	2,86		12
$LaCoO_3$ (900°C/2h)	3	2,93		3
$LaTi_{0,2}Co_{0,8}O_3$	2,75	2,7	2,65	10
$LaTi_{0,4}Co_{0,6}O_3$	2,57	2,43	2,36	11
$LaTi_{0,4}Co_{0,6}O_3$	2,33	2,58	2,22	13
$LaTi_{0,5}Co_{0,5}O_3$	2	2,62	2,06	17

position given by x is not really achieved by a heat treatment at 900°C (table 2). So we understand why the applied estimation gives too high moments, but the trend is well reproduced. The strong increase and the field dependence of χ below 100 K again indicate the presence of Co^{2+} at the surface.

DISCUSSION

Although XPS spectra show a Co deficit, when calcination is carried out at low temperatures, XPS cannot differentiate between Co^{2+} and Co^{3+} ions. So one needs additional arguments for the decision, which of the Co ions or possibly both together create catalytical activity at the surface. Because of the stoichiometry and spinel type structure of Co_3O_4 both ions are present to a high extent in the bulk and at the surface, whereas in $LaCoO_3$ only Co^{3+} ions exist in the bulk. In a well crystallized perovskite lattice Co^{2+}/Co^{4+} ion pairs can be created by temperature dependent disproportion of Co^{3+}, but to a much smaller amount.

Under the real conditions of preparation some unreacted Co^{2+} portions may remain, for example, when nitrates decompose, but do not react completely. Another possibility is given by a reducing treatment with aqueous solutions or by decomposition at too high temperatures leaving an oxygen deficiency. It was recently proved experimentally, that Co^{2+} ions are responsible for catalytical activity in Co_3O_4, which was prepared with different Co^{2+} content /40/. As the spinel is the much better CO catalyst than the perovskite, we suppose that both ions need to be present for a fast reaction, operating via charge transfer after a first O_2 adsorption step.

The implementation of Co^{2+} ions in $LaCoO_3$ by substitution of Ti^{4+} ions at the calcination temperature 900°C enhances both the Co^{2+} content and the activity (table 2 and fig. 6). Thus we believe, that in all $LaCoO_3$ materials there is always a kind of mixed-valence surface phase present. The lower the calcination temperature the more mixed-valence states are formed. Moreover, the range of activation energy for electronic hopping process (0,4-0,7eV) fits well to the activation energy of the catalytical reaction (0,5-0,7eV).

CONCLUSIONS

From the experimental results of this work the following conclusions can be drawn. For any Co and Ni containing spinel or perovskite type material to be a good CO burning catalyst, it must contain mixed valences of 3d-ions at the surface, to facilitate a fast charge transfer when O_2/CO adsorption takes place.

It can be stated, that the catalytic activity is mainly influenced by the ratio of Co^{3+} and Co^{2+} at the surface of the material. A surface treatment of $LaCoO_3$ can be done by a partial reduction of already calcined products with aqueous solutions or calcination at low enough temperatures to get also large surface area. The limiting case of any improvement would be similar to the Co_3O_4 surface itself.

Although the activation energy of the CO oxidation corresponds to the activation energy of hopping charges in the bulk, no direct correlation with the DC bulk conductivity is observed. On the other hand, the magnetic susceptibility of native $LaCoO_3$ powders, calcined at low temperatures, indicate directly the presence of high-spin Co^{2+} (mixed valence states).

As anticipated before, SO_2 is a very strong inhibitor and blocks the exceptionally fast CO reaction instantly. Most probably it is chemisorbed at oxygen covered Co^{2+} sites and leads finally to sulfate formation. Decomposition of pure $NiSO_4$ and $CoSO_4$ takes place around 800°C, so that the problem of recovery at lower temperatures is evident and all catalysts of this type fail in low temperature applications of SO_2 containing waste gases. Quite the same SO_2 problem appears with honey combs and impregnated supports, otherwise being as fast as Pd coated supports. The Pd catalyst withstands SO_2, but during CO/CO_2 reaction it is oxidized to SO_3.

REFERENCES

/1/ L.G. Tejuca, U.L.E.Fierro, J.M.D.Tascon, Adv. Cat. 36 (1989) 237.

/2/ T. Seiyama, Catal. Rev. Sci. Eng. 34 (1992) 281-425.

/3/ C.M. Chiu, Y.H. Chang (Journal Paper) Thin Solid Films, 342 1-2 (1999) 15-19.

/4/ R. Sorita, T. Kawano, Sensors & Actuators B-Chemical, B36 1-3 (1996) 274-7.

/5/ R.J.H. Voorhoeve, D.W. Johnson Jr., J.P. Remeika, P.K. Gallagher, Science 195 (1977) 827.

/6/ Y.F.Yu Yao, J. Catal. 36 (1975) 266.

/7/ D.Y.Rao, D.K. Chakrabarty, Ind. J. Chem. 23A (1984) 375.

/8/ P.M. Raccah, J.B. Goodenough, Phys. Rev. 155 (1967) 932.

/9/ M.A. Senaris-Rodriguez, J.B. Goodenough, J. Solid State Chem. 116 (1995) 224.

/10/ R.J.V. Verhoeve, Advanced Materials in Catalysis, ed. by J.J. Burton, R.L. Garten, Academic Press, N.Y. 1977.

/11/ T. Shimizu, Chem. Lett. (1980) 1.

/12/ T. Arakawa, A. Yoshida, J. Shiokawa, Mat. Res. Bull. 15 (1980) 347.

/13/ O. Parkash et al., Mat. Res. Bull. 9 (1974) 1173.

/14/ A. Macher, K. Reichmann, O. Fruhwirth, K. Gatterer, G.W. Herzog, Informacije MIDEM 26 (1996) 79.

/15/ N. Katsarakis, O. Fruhwirth, W. Sitte, Fourth Euro Ceramics, ed. by G. Gusmano, E. Traversa, Faenza, Vol.5 (1995) 89.

/16/ O. Fruhwirth, A. Macher, K. Reichmann, H.G. Schuster, Third Euro Ceramics, ed. by P.Duran, J.F.Fernandez, Faenza, Vol.2 (1993) 395.

/17/ I. Binder-Begsteiger, G.W. Herzog, E. Megla, M. Tomann-Rosos, Chem. Ing. Tech. 62 (1990) 60.

/18/ M.Lesnik, Thesis, Technische Universität Graz 1994.

/19/ K.Tabata, I.Matsumoto, S.Kohiki, J. Mat. Science 22 (1987) 3037.

/20/ T.Nitadori, T.Ichiki, M.Misono, Bull. Chem. Soc. Jpn 61 (1988) 621.

/21/ E.A.Lombardo, K.Tanaka, I.Toyoshima, J. Catalysis 80 (1983) 340.

/22/ V.G.Bhide, D.S.Rajoria, G.R.Rao, C.N.R.Rao, Phys. Rev. B 6 (1972) 1021.

/23/ C.N.R.Rao, O.M.Parkash, P.Ganguly, J. Solid State Chem. 15 (1975) 186.

/24/ G.Thornton, B.C.Tofield, D.E.Williams, Solid State Comm. 44 (1982) 1213.

/25/ D.Bahadur, O.M.Parkash, J.Solid State Chem. 46 (1983) 197.

/26/ N.Ramadass, J.Gopalakrishnan, M.V.Sastri, J. Less Common Metals 65 (1979) 129.
/27/ A.Macher, Thesis, Technische Universität Graz, 1994.
/28/ K.Koumoto, H.Yaganida, J. Am. Chem. Soc. 64 (1981) 156.
/29/ J.A.Tareen, A.Malecki et al., Mater. Res. Bull. 19 (1984) 989.
/30/ J.B.Goodenough, J. Appl. Phys. 37 (1966) 1415.
/31/ K.Sreedhar, J.M.Honig et al., Physical Review B, 46 (1992) 6382.
/32/ N.Katsarakis, Thesis, Technische Universität Graz, 1996.
/33/ P.Cossee, J. Inorg. Nucl. Chem. 8 (1958) 483.
/34/ W.L.Roth, J. Phys. Chem. Solids 25 (1964) 1.
/35/ P. Cossee, A.E. van Arkel, J. Phys. Chem. Solids 15 (1960) 1.
/36/ E.A. Boudreaux, L.N. Mulay, Theory and Applications of Molecular Paramagnetism, J. Wiley, N.Y. 1976.
/37/ G.H.Jonker, J. Appl. Phys. 37 (1966) 1424.
/38/ K.Asai, et al., Physical Review B 50 (1994) 3025.
/39/ N. Menyuk, K.Dwight, P.M. Raccah, J. Phys. Chem. Solids 28 (1967) 549.
/40/ C. Oliva, L. Forni, L. Formaro, Appl. Spectroscopy 50 (1996) 1395.

Gerhard W. Herzog,
Angelika Reichmann,
Klaus Reichmann,
Martina Ruplitsch-Lesnik,
Institut für Chemische Technologie anorganischer Stoffe,
Technische Universität Graz
Stremayrgasse 16/III, A-8010 Graz
Tel.: ++43 316 873 8294
Fax.: ++43 316 873 8292
E-mail: f537mach@mbox.tu-graz.ac.at

Karl Gatterer
Institut für Physikalische und Theoretische Chemie
Technische Universität Graz
Technikerstrasse 4, A-8010 Graz
Tel.: ++43 316 873 8239
Fax: ++43 316 873 8225
E-mail: gatterer@ptc.tu-graz.ac.at

ACKNOWLEDGEMENT

The authors are indebted to FRAUENTAL KERAMIK, Frauenthal Austria, for stimulation and financial support of this work. The low-temperature magnetic equipment was provided by the Austrian Science Foundation (project number: P10713-CHE).

Prispelo (Arrived): 23.01.00 *Sprejeto (Accepted): 27.03.00*

CLEANING OF THIN PASSIVATION LAYERS ON THE Ag CONTACT MATERIAL WITH VACUUM OUTGASSING

L. Koller[1], M. Bizjak[2], B. Praček[3]
[1]Institute for Electronics and Vacuum Techniques, Ljubljana, Slovenia
[2]Iskra - Stikala, Kranj, Slovenia
[3]ITPO, Ljubljana, Slovenia

Keywords: electrical contacts, material for electrical contacts, surface treating, surface protection, passivation thin films, vacuum outgassing

Abstract: Metallic silver is relatively soft material and a good electric conductor. Therefore it is very suitable material for electric contacts. However, because silver is not resistant to the atmosphere containing H_2S, SO_2 and Cl_2, the surface of the silver contact material must be protected. Well known surface protection with the thin gold layer is too expensive to be economical. In our study we considered some cheaper passivation thin layers which could prevent the corrosive effects of the environment and at the same time assure good electric contact. We chose three different types of passivation thin layers. The first one was deposited by waxing in the Silverbrite solution, for the second layer chromizing was used while the titanium nitride layer was deposited by sputtering. The contact material used was AgNi0,15. Beside electrical properties of the material its clean surface is very important to achieve good electric contact and low level of contact resistance. In the high vacuum outgassing equipment designed and developed in our laboratory samples of silver contact material were outgassed for 48 hours in high vacuum ($1x10^{-7}$ mbar) at 200°C. Analysis of the outgassed substances with the quadrupole mass spectrometer showed that the outgassing rates of all the three passivation layers were low while the composition depended on the type of the layer. Then the thin layers were analyzed with the Auger electron spectroscopy.

Čiščenje tankih pasivacijskih prevlek na Ag kontaktnem materialu z vakuumskim razplinjevanjem

Ključne besede: kontakti električni, materiali kontaktov električnih, obdelava površinska, zaščita površin, plasti tanke pasivacijske, razplinjevanje vakuumsko

Izvleček: Srebro je dobra električno prevodna in sorazmerno mehka kovina. Zaradi tega je po elektromehanskih lastnostih primerna za električne kontakte. Ker pa je neobstojno v atmosferi s primesmi H_2S, SO_2 in Cl_2, je treba kontaktni material površinsko zaščititi. Izbrali smo tri pasivacijske zaščitne prevleke (prva je bila nanesena z voskanjem v raztopini SILVERBRITE, druga s kromatiranjem, tretja, titannitridna, pa je bila napršena) in jih nanesli na kontaktni material AgNi0,15. Za dober električni kontakt in nizko kontaktno upornost je poleg električnih lastnosti zelo pomembna tudi čista površina kontaktnega materiala. V laboratorijski razplinjevalni napravi, razviti doma, smo vzorce pasiviranega srebrnega kontaktnega materiala razplinjevali v visokem vakuumu $1x10^{-7}$mbar pri temperaturi 200°C. Analiza razplinjenih substanc je pokazala, da je velikost razplinjevanja vseh treh zaščitnih prevlek majhna, koncentracija plinskih nečistoč pa je odvisna od zaščitne plasti same. Nanose tankih zaščitnih prevlek po visokovakuumskem razplinjevanju smo analizirali še s spektrometrom Augerjevih elektronov.

1 Introduction

Recently the properties of the outgassed materials /1-3/ hermetically encapsulated into the electronic components attracted considerable attention. One of the main reasons for the failures of the electronic components is the surface contamination /4-7/ of the electric contacts. Contamination film increases the contact resistance and deteriorates the reliability of an electronic component. The most common contamination films are the oxides formed during the termal diffusion and outgassing processes. Besides oxide films the corrosion products and particles resulting from wearing are the main sources of contamination. The growth of industrialization together with the air pollution encounter the problem of the contact sulfating. The specific resistance of Ag_2S ranges from 10^3 Ωcm to 10^8 Ωcm at the room temperature (silver sulfide decomposes at about 300°C) so the sulfating of contacts increases the contact resistance. Contacts may be protected by thin gold plating but there are cheaper passivation coatings, too. We studied the outgassing properties of three possible useful protective thin layers on the contact surface of silver (AgNi0.15) contact material in order to decrease the influence of the surrounding atmosphere. All three layers were outgassed in high vacuum at the increased temperature. The mass spectrometer was used to determine the composition of the outgassed products. Purity and the composition of the protective layers were determined by the Auger spectroscopy.

2 Experimental

To protect the silver based contact material AgNi0.15 three different types of thin layers were used:

- Passivation by waxing. Test samples were treated in the water solution named Silverbrite /8/.
- Passivation by chromizing. Layers were made by anode oxidation according to the receipt /9/.
- Passivation by solid layer. Solid layer Ti/TiN was formed by sputtering /10/.

All the passivation thin layers were outgassed in high vacuum $1x10^{-7}$ mbar at the temperature 200°C 48 hours in the vacuum outgassing comora /11/. Products of the outgassing procedure were analysed with the quadrupole mass spectrometer (masses from 1 to 100) TRANSPECTOR GAS ANALYSIS SYSTEM - MODEL C100, F LEYBOLD Inficon Inc. Mass spectra were taken twice: after half an hour and after 48 hours of outgassing. Purity and composition of three surface layers after the outgassing were determined by the Auger spectros-

copy (AES). AES spectrometer /12/ (PEI, SAM, Model 545A) with the static primary electron beam with the energy of 3 keV, the beam current of 0.5 μA, and the beam diameter of about 40 μm was used for the analysis. Etching was performed on the surface area of 10 mm x 10 mm with the two Ar^+ ion beams with the energy of 1 keV. The incidence angle of the ion beam was 47°. The etching velocity was about 1.7 nm/min and was calibrated with the standard Ni/Cr sample. For determining the element concentration (except for the nitrogen concentration where the factor was calculated from the standard sample of stehiometric TiN) the sensitivity factors were taken from the spectroscope manufacturer (PEI) manual.

3 Results and discussion

The composition of gasses evaporated out of the heated surface of samples made of the passivated contact material AgNi0.15 is presented in mass spectra in Figures 1 to 6. Mass spectra of the outgassed products from the silver contact material AgNi0.15 coated with the thin passivation layer in the Silverbrite solution are presented in Fig.1 after 30 minutes and in Fig. 2 after 48 hours of outgassing, respectively. Spectrum in Fig. 2 shows that after 48 hours of outgassing at 200°C and at the total pressure $2x10^{-7}$ mbar nearly all the evaporable contaminants and hydrogen H_2 are removed. The same conclusion can be drawn for the outgassing of cromated contact material (Figures 3 and 4). When the contact material AgNi0.15 was passivated by the solid layer Ti/TiN (mass spectra in Figures 5 and 6) greater amount of contaminants than in the first two cases is noticed on the surface before the beginning of the outgassing. After the 48 hours of outgassing at 200°C the contaminants are not removed completely. At the same time the strong hydrogen peak is observed. During the procedure of sputtering considerable amount of molecules are built in the protective layer. Also, when the procedure of sputtering is finished the

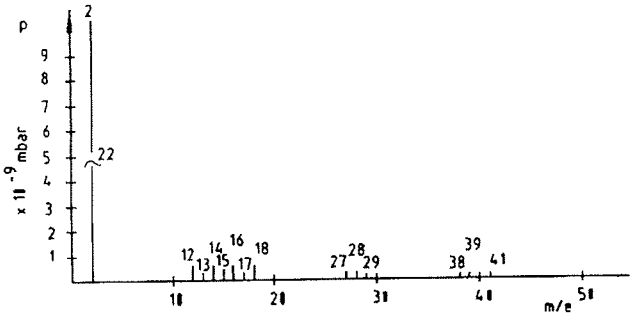

Figure 1. Mass spectrum of the outgassed products from the silver contact material AgNi0.15 waxed in the Silverbrite solution after 30 minutes of ougassing ($2x10^{-7}$ mbar, 25°C).

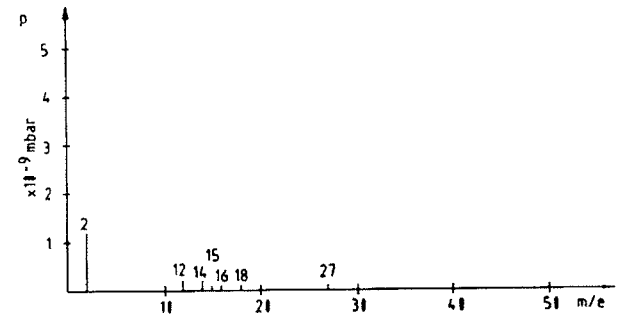

Figure 2. Mass spectrum of the outgassed products from the silver contact material AgNi0.15 waxed in the Silverbrite solution after 48 hours of ougassing ($2x10^{-7}$ mbar, 200°C).

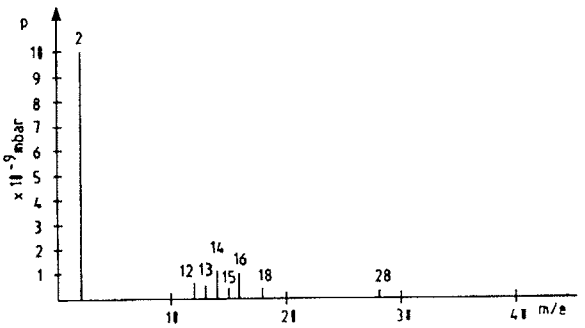

Figure 3. Mass spectrum of the outgassed products from the cromated silver contact material AgNi0.15 after 30 minutes of ougassing ($4x10^{-7}$ mbar, 25°C).

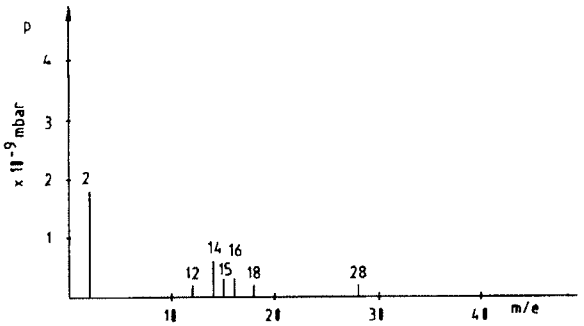

Figure 4. Mass spectrum of the outgassed products from the cromated silver contact material AgNi0.15 after 48 hours of ougassing ($1.8x10^{-7}$ mbar, 200°C).

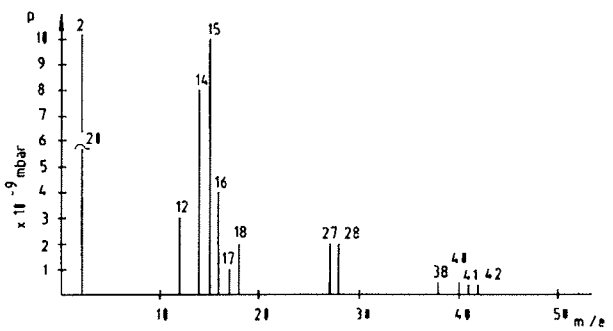

Figure 5. Mass spectrum of the outgassed products from the sputtered silver contact material AgNi0.15 with the titanium nitride Ti/TiN after 30 minutes of ougassing ($8x10^{-7}$ mbar, 25°C).

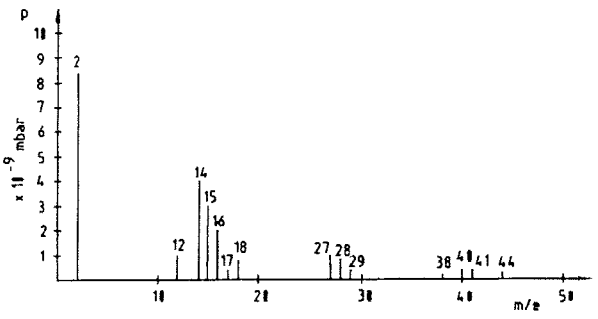

Figure 6. Mass spectrum of the outgassed products from the sputtered silver contact material AgNi0.15 with the titanium nitride Ti/TiN after 48 hours of ougassing (4x10^{-7} mbar, 200°C).

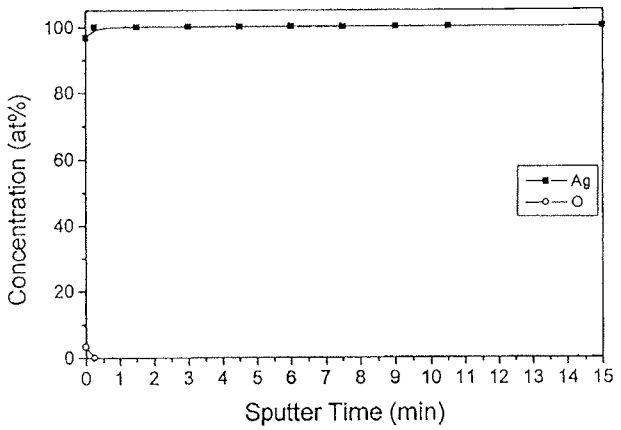

Figure 7. Profile diagram of the silver contact material AgNi0.15 waxed in the Silverbrite solution after the outgassing.

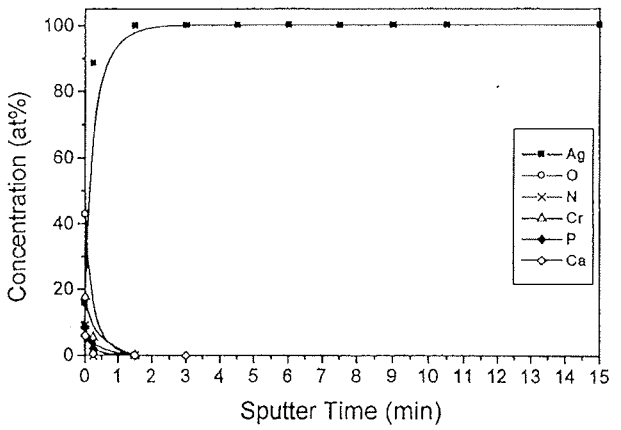

Figure 8. Profile diagram of the cromated silver contact material AgNi0.15 after the outgassing.

protective layer is rather active so that larger amount of gas can be absorbed. Contamination of the layer depends very much on the technology of the procedure. Results of the AES analysis as three profile diagrams are presented in Figures 7, 8 and 9. Profile diagrams of

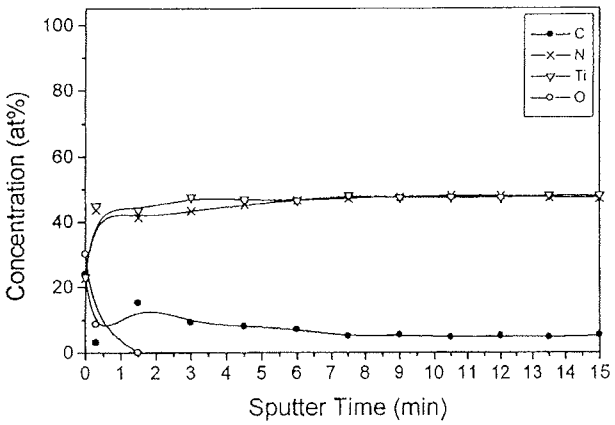

Figure 9. Profile diagram of the sputtered silver contact material AgNi0.15 with the titanium nitride Ti/TiN after the outgassing.

the waxed silver contact material AgNi0.15 (Fig. 7) after the outgassing shows the extremely clean surface with just the traces of oxygen. Profile diagram of the cromated silver contact material AgNi0.15 (Fig. 8) after the outgassing shows the passivation layer which is less than 1 nm thick and consists mainly of chromium with small concentrations of nitrogen, phosphorus and calcium on the surface. The surface is oxidized to a great deal while there is no oxygen inside the layer. Profile diagram of the silver contact material AgNi0.15 passivated by the Ti/TiN solid layer (Fig. 9) after the outgassing shows that titan nitride layer is slightly oxidized only at the surface. Inside the layer the carbon incorporated during the formation of the layer is detected.

4 Conclusions

Outgassing properties of three conducting passivation thin layers on the silver contact material AgNi0.15 are studied. First passivation layer was deposited by waxing in the Silverbrite solution, the next one by chromizing using the electrochemical procedure, while the third one (Ti/TiN) was deposited by sputtering.

Outgassing was performed in high vacuum (1x10^{-7} mbar, 200°C, 48 hours), the mass spectrometer was used to determine the composition of the outgassed products. Thin passivated protective layers after the outgassing was studied with the use of the Auger spectroscopy.

Our studies show that all the three passivation thin layers considered are suitable for protection of silver contact material. The layers produced are very clean with low outgassing rate and are not expensive.

5 References

/1/ M Wutz, H Adam, W Walcher, in Theory and Practice of Vacuum Technology, Friedr. Vieweg & Sohn, Braunschweig/Wiesbaden, 1989.

/2/ L Koller, M Jenko, S Spruk, B Praček, S Vrhovec, Vacuum, 1995, 46, 827.

/3/ L Koller, S Vrhovec, M Jenko, Kovine, zlitine, tehnologije, 1995, 29, 515.

/4/ R Holm, in Electric Contacts Handbook, Springer, New York, 1967.

/5/ M Bizjak, L Koller, K Požun, J Leskovšek, ICEC'98 Offenbach, VDE-Verlag 1998, 47.

/6/ SK Chawla, JK Payer, J. Electrochem. Soc., 1990, 137.

/7/ J Schirnikat, H-J Gewatter, L Kiesewetter, F & M 1996, 104, 515.

/8/ Doduco Datenbuch, 2. Aufl. Pforzheim, 7, 1997.

/9/ Navodilo za uporabo "Cromating AG-797100", Kemična tovarna Podnart.

/10/ B Navinšek, P Panjan, J Krušič, Service and Coating Technology, 1998, 98, 809.

/11/ L Koller, M Bizjak, K Požun, Kovine, zlitine, tehnologije, 1999, 32, 155.

/12/ B Praček, Kovine, zlitine, tehnologije, 1996, 30, 53.

Lidija Koller, univ. dipl. inž. kemije
Inštitut za elektroniko in vakuumsko tehniko
Teslova 30
1000 Ljubljana
številka raziskovalca:1703
tel. 061/177-66-58
faks 061/126-45-78
E-pošta: joze.koller@uni-lj.si

domači naslov:
Cesta na Laze 15
1000 Ljubljana
tel. 061 / 159-7661

Dr. Martin Bizjak, univ. dipl. inž. fizike
Iskra - Stikala,
4000 Kranj
številka raziskovalca: 3930
tel. 064/37-22-26
faks 064/37-22-59
E-pošta: iskra.stikala-rd@siol.net

domači naslov:
Sveti Duh 275,
Škofja Loka
tel. 061/159-7661

B. Praček, univ. dipl. inž. metalurgije
Inštitut za tehnologijo površin in optoelektroniko,
Teslova 30,
1000 Ljubljana
številka raziskovalca: 9105
tel. 061/126-45-92
faks 061/126-45-93

Prispelo (Arrived): 01.02.00 *Sprejeto (Accepted): 27.03.00*

THERMAL BOUNDARY CONDITIONS IN SMART POWER DEVICES

Martin Knaipp, Franz Unterleitner,
Austria Mikrosysteme International AG, Unterpremstätten, Austria

Keywords: semiconductors, smart power devices, device models, thermal boundary conditions, selfheating, state of the art, device simulations, comparisons between formalisms, DD formalism, Drift Diffusion formalism, HD formalism, HydroDynamic formalism, SOR, Safe Operation Regime, increased temperature, degradation of device operation, permanent device failure, practical examples, experimental results

Abstract: This work gives a review of the state of the art device simulation including selfheating effects. A comparison between the Drift-Diffusion and Hydrodynamic formalism is given. Especially the influence of non-local effects in the lattice heating is shown. The influence of the interface and contact conditions on the final lattice temperature is described. It is shown that only a correct formulation of the boundary conditions enables energy conservation of the simulated device. But even in case of energy conservation, the contact conditions are the critical uncertainty in the description of the device behaviour.

Izbira termičnih robnih pogojev pri modeliranju inteligentnih močnostnih vezij

Ključne besede: polprevodniki, naoprave močnostne inteligentne, modeli naprav, pogoji termični mejni, samosegrevanje, stanje razvoja, simulacije naprav, primerjave med formalizmi, DD formalizem drita difuzije, HD formalizem hidrodinamični, SOR režim delovanja varnega, temperatura povišana, degradacija delovanja naprave, izpad naprave trajni, primeri praktični, rezultati eksperimentalni

Izvleček: V prispevku opisujemo trenutno stanje na področju termične simulacije elektronskih elementov z upoštevanjem efektov samosegrevanja. Podajamo primerjavo med tokovno-difuzijskim in hidrodinamičnim pristopom. Še posebej poudarimo vpliv nelokalnih efektov pri segrevanju kristalne mreže, kakor tudi vpliv kontaktov in medpovršin na končno temperaturo kristalne mreže. Pokažemo, da le s pravilno izbiro robnih pogojev omogočimo ohranitev energije simuliranega elementa. Vendar celo v takem primeru so pogoji na kontaktih kritična neznanka pri pravilnem opisu obnašanja elementa.

I. Introduction

In modern semiconductor devices the selfheating effects play the major role in the specification of the safe operation regime (SOR). The increase of the lattice temperature during the operation can cause a complete different device behaviour, an accelerated degradation or even a permanent device failure (e.g. second breakdown). At least the local lattice temperature of the chip is a critical factor which determines if the IC fulfill its specification.

To optimize the system performance, sophisticated device simulations are needed which should also include selfheating effects. Typical devices where selfheating plays a major role are smart power devices, electrostatic discharge structures (ESD) and structures with low thermal conductivity components like silicon on insulator devices (SOI).

Modern device simulators are tools to solve nonlinear coupled partial differential equation systems. Their numerical behaviour is optimized for the semiconductor equations to find a solution in the shortest time with an accuracy which can be defined by the user. The numerical discretisation scheme is so sophisticated that even variations in the carrier concentrations in a range of 20 orders of magnitude can be solved. This is not trivial and major efforts are carried out to find new robust numerical schemes to solve the specified equation systems /1/. The feedback from the device lattice temperature to the electrical behaviour is given by the various physical models which depend on the lattice temperature. Some examples are the carrier mobility, the densities of states and the band edge energies /2,4,5/.

The calculated solution inside the device strongly depends on the given boundary conditions. The specification of these conditions is not easy and has to be done by the user. The specification of electrical conditions is quite simple. In most time the potential drop in the interconnect metal (backend) can be neglected to describe the electrical device properties in a moderate current regime. The development of power devices is often done with a large scaled interconnect to avoid any potential drop in the metal or poly lines.

However the thermal boundary conditions cannot be defined as simple as the electrical case. The thermal influence of the backend cannot be reduced, and much knowledge is necessary to estimate realistic thermal conditions. In addition it is not easy to decide to which metal or poly line the user should simulate the devices. At least the final SOR is determined by the complete packaging of the device. This thermal packaging includes a temperature drop in the packaging material, in the bonding wires of the IO cells and in the pins of the chip. All these materials finally determine the local device temperature and therefore the boundary conditions of the semiconductor.

To simulate a modern semiconductor device the user has to provide the simulating structure to the device simulator. In the general case this structure consists of several segments. Each segment corresponds to a certain material. Typical materials are silicon, poly lines, oxides, interconnect dielectric, etc. However it is not always useful to describe even the complete silicon with one segment /3/. A typical example is the hetero bipolar transistor (HBT) with a silicon/germanium (SiGe) base. The major reason to describe silicon with several seg-

ments is the simulation time which can be kept low while including all necessary models. In case of the HBT only the base is evaluated with the sophisticated SiGe models while in the other segments the plain silicon models are used.

II. Segment Models

In this section a review of the heat source term is given within the Hydrodynamic (HD) and Drift-Diffusion (DD) model /2,5/.

The equation to describe the lattice temperature is the lattice heat flow equation (1). On the right hand side the heat source term H corresponds to a power density which heats up the device segments. The formulation of the heat source term depends on the used equation set. The complete equation (1) describes the transient behaviour of the selfheating. The heat conductivity κ depends weakly on the lattice temperature. The second term on the left side of (1) describes the time dependent part of the equation where the thermal heat capacity ρ defines the material dependent properties. In case of a stationary solution of the selfheating problem, the second term on the left side of (1) vanishes.

$$-\mathrm{div}\left(\kappa_L(T_L)\right)\cdot \mathrm{grad}\left(T_L(\vec{r},t)\right)+\rho_L\cdot c_p\cdot\frac{\partial T_L}{\partial t}=H(\vec{r},t) \tag{1}$$

In case of the DD model the source term is given in (2). When a stationary simulation is done, H only depends on the position. For pure silicon the electron and hole band edges E_C and E_V are often assumed to be constant. Only in high doped regions the band gap narrowing has to be included. In case of recombination, the recombination rate R_{net} is multiplicated with the bandgap E_g to give the recombination heat.

$$H(\vec{r})=\mathrm{grad}\left(\frac{E_c}{q}-\psi\right)\cdot\vec{J_n}+\mathrm{grad}\left(\frac{E_v}{q}-\psi\right)\cdot\vec{J_p}+R_{net}\cdot E_g \tag{2}$$

In the HD model the heat source term H is given in (3). The first two terms of (3) describe the carrier energy which is transferred to the lattice. The amount of the energy is proportional to the difference of the carrier and the lattice temperature. This means that the carriers can give their thermal energy to the lattice even if they are not accelerated by an electric field. The hot carriers relax with the cold lattice and the first two terms of (3) are therefore called relaxation terms. The terms $H_{n,eff}$ and $H_{p,eff}$ describe the net recombination heat of the corresponding carrier system. It is assumed that the recombination term heats up the lattice in case of recombination and cools down the lattice in case of carrier generation. The calculation of these terms is not easy because it is not so clear how to split the recombination or generation heat between the carrier energy systems and the lattice heat system. At least in case of high currents the heat transfer caused by recombination or generation is small compared to the energy transfer of the relaxation terms.

It is important to note that in space charge regions the carriers are heated up by the electric field. In these regions the final carrier temperatures can reach several thousand Kelvin. The reason why the semiconductor does not melt is the low energy density of the carriers because of their low concentration. On the other hand, in regions with high carrier densities (e.g. in case of high injection) only a moderate carrier heating can be achieved.

$$H(\vec{r})=\frac{3\cdot k_B}{2}\cdot\left(n\cdot\frac{T_n-T_L}{\tau_{\varepsilon,n}}+p\cdot\frac{T_p-T_L}{\tau_{\varepsilon,p}}\right)-H_{n,eff}-H_{p,eff} \tag{3}$$

As long as the carriers give their thermal energy to the lattice, the first two terms of (3) are positive values. However, it is possible that carrier temperatures are below the lattice temperature as shown in the example section.

III. Interface and Contact Models

A) Interface Model

The interface model described in this section deals with the interface of two adjacent semiconductor segments. In the general case there are different values of the band edge energies on each side. An example is the emitter/base interface of a Si/SiGe HBT device, where a carrier current crosses the interface. The boundary condition for the potential at the interface is simple because there is no interface dipole charge and so the electrostatic potential on each side of the interface must be the same. However the carriers move at their band edge energies which might change abruptly at the interface.

Because of this abrupt change the heat source term for the DD model according to (2) leads to an infinite large power density at the interface. Fortunately the heat transfer must not be calculated explicitly. The limes of this boundary problem leads to a surface divergence of the lattice thermal heat flux density S, which in turn changes the slope of the lattice temperature at the interface. On both sides of the interface the lattice temperatures are set equal. Equation (1) therefore reads for the DD hetero interface model:

$$\mathrm{div}\kappa_L\cdot\mathrm{grad}(T_L)=\mathrm{div}\cdot\vec{S_L}=\frac{\vec{J_n}}{q}\cdot(E_{c1}-E_{c2})+\frac{\vec{J_p}}{q}\cdot(E_{v1}-E_{v2}) \tag{4}$$

In case of the HD model the non-local effects have to be taken into account. This means that the abrupt change of the band edge energies cause a surface divergence of the carrier energy flux and not of the lattice thermal heat flux. The change of the carrier energy flux at the interface defines the shape of the carrier concentrations and their temperatures across the interface. Again the lattice temperatures on both sides of the interface are equal. At least the HD interface model only affects the carrier energy flux, and the lattice is only incorporated by the volume model according to (3).

B) Contact model

The two commonly used thermal contact models are the isothermal contact condition and the condition of a thermal contact resistance. These two conditions can be applied for ideal electrical conductors, for ideal electrical isolators and real electrical conductors (e.g. adjacent semiconductor segments). The option for adjacent semiconductor segments makes it possible to calculate the selfheating only in defined segments, to achieve shorter simulation times. The isothermal condition specifies a certain contact temperature for the contact boundary. This corresponds to a Dirichlet boundary problem of (1).

In contrast the specification of a thermal contact resistance defines a Neumann boundary problem for the energy flux of (1). The physical meaning of this condition is that the amount of heat flux, which crosses the boundary, is proportional to the difference of the boundary temperature and the temperature of a specified thermal heat sink.

The specification of these setup conditions seems to be simple, but each condition can lead to numerical and physical problems if a wrong specification is used. In case of the isothermal condition it is possible to simulate an overheated device with an arbitrary small current. The reason therefore is a too small chosen contact area, which leads to wrong simulation results. If a thermal resistance is defined and the resistance is too high, the device may heat up to arbitrary high temperatures even if the device current is low and the contact areas are large. This can result from an inaccurate definition of the simulation structure as described in a previous section.

If an electric current crosses the boundary, the simple thermal contact models have to be extended to electro/thermal contact models. These models include the energy transfer when the carriers move from the contact metal to the semiconductor. The energy diagram of the metal/n-doped semiconductor contact is shown in Fig.1.

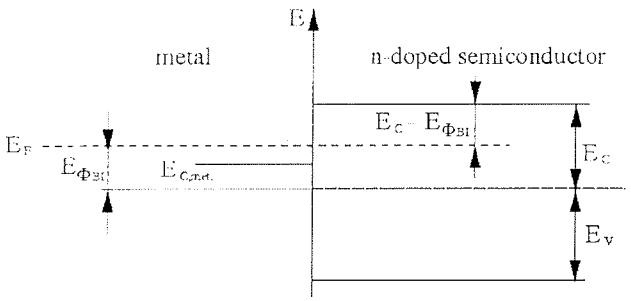

Fig.1: Bandedge energy diagram on a metal/n-doped semiconductor contact.

In case of a contact current the carriers gain or loose energy because of the difference between the metal Ferminiveau E_F and the corresponding conducting band E_C or E_V of the semiconductor. It should be noted that the intrinsic level of the semiconductor is shifted by the Build-In energy $E_{\Phi BI}$. In case of a n-doped semiconductor the barrier of the electrons is much lower compared to the barrier of the holes. If we assume a n-doped device with nearly equivalent electron and hole currents, it is easy to see that the hole current gives the main part of the carrier contact heating or cooling.

A similar contact bandedge energy diagram can be given for a p-doped semiconductor. Only when all current semiconductor/metal boundaries are incorporated by this model, an energy conservation of the device can be shown as described in (5).

In this equation the electrical power dissipation of m electrical contacts is equal to the lattice heat flux of n thermal contacts. The vector A corresponds to the boundary normal area and defines the sign of the power

$$\sum_{i=1}^{m} \vec{A}_i \cdot \vec{J}_i \cdot U_i = \sum_{j=1}^{n} \vec{A}_j \cdot \vec{S}_{L,j} \qquad (5)$$

dissipation. Equation (5) also holds for hetero devices and even for multi segment structures.

IV Examples

This section will give two examples which should show the effects explained in the previous sections. First a simple two segment silicon diode with an abrupt p/n junction is described. The second example shows the selfheating of a hetero bipolar field transistor. Both were simulated with the stationary semiconductor equation set, which means that there is no transient thermal and electrical behaviour .

A) The Diode

The example was chosen because a bias applied in forward direction results in high electron and hole currents. This allows to verify the contact and interface conditions as described in section II. The device is modeled as a two segment structure with a step junction at the segment interface and a constant doping in each segment of about 1.0e17cm^{-3}. Two contact resistances are applied with values of R_{th} = 6.9e-5 [K cm^2/W] on each side. The device has a length of 60 μm and a contact area of 6 μm^2.

Fig.2 shows the diode with an applied forward voltage of +0.6 V at the anode (left side). The left part of the figure shows the lattice heating while the right side shows the band edge potentials of the device. The most upper line of the band edge potentials corresponds to the hole potential which is followed by the device potential and the lowest line corresponds to the electron potential. In thermal equilibrium that means without an applied voltage, the potential drop at the junction corresponds to the Built-In potential which is about 0.82V. One should be aware that in the vicinity of the junction the potentials are continual functions without any unsteadiness at the physical junction. The right side of Fig. 2 shows that at a contact bias of 0.6V the junction voltage drop is already reduced to 0.22V. This voltage drop causes a high diffusion current over the junction with an electron to hole current ratio of nearly 2.5. This ratio is mainly determined by the different mobilities of

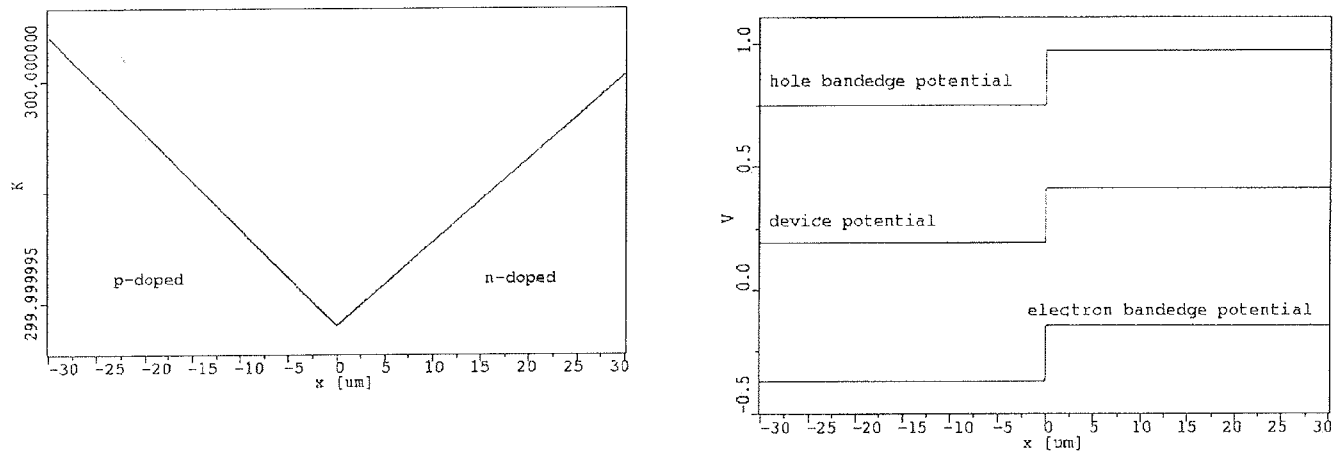

Fig. 2: Lattice temperature (left diagram) and band edge potentials (right diagram) of a diode in forward direction. The applied cathode voltage is 0.6V. The electrons move from the right to the left.

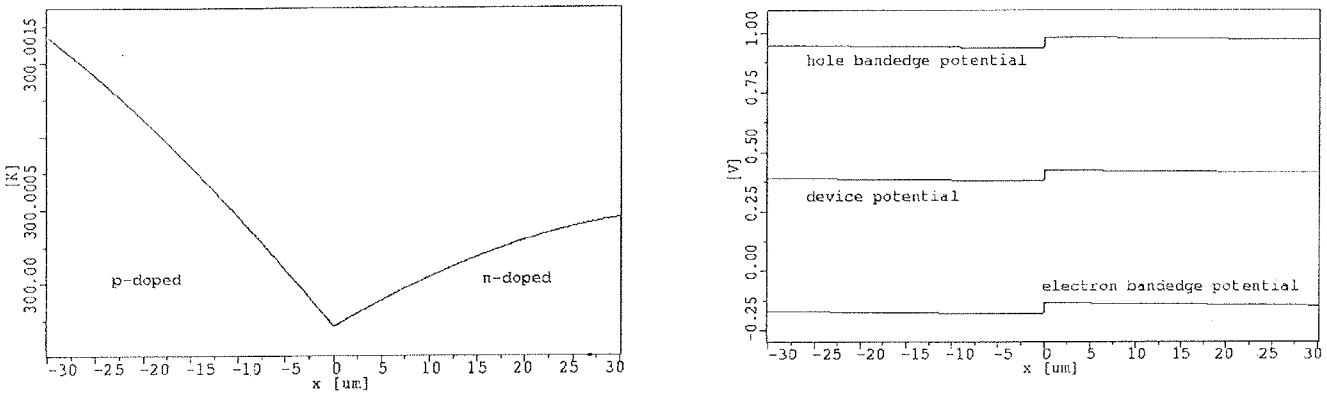

Fig. 3: Lattice temperature (left diagram) and band edge potentials (right diagram) of a diode in forward direction. The applied cathode voltage is 0.8V. The electrons move from the right to the left.

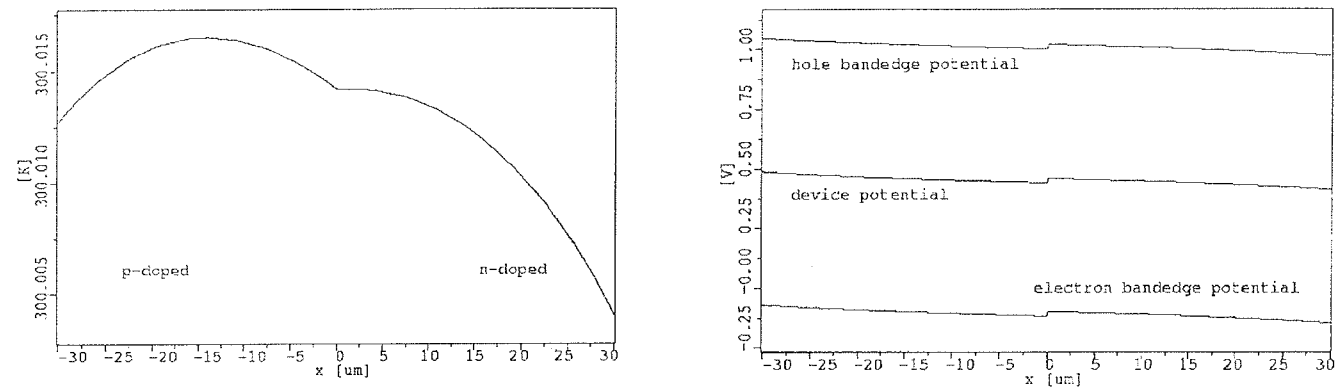

Fig. 4: Lattice temperature (left diagram) and band edge potentials (right diagram) of a diode in forward direction. The applied cathode voltage is 0.9V. The electrons move from the right to the left. The maximum lattice temperature is in the p-doped side. From this point the lattice heat flux flows to the anode contact and the heat sink of the p/n junction.

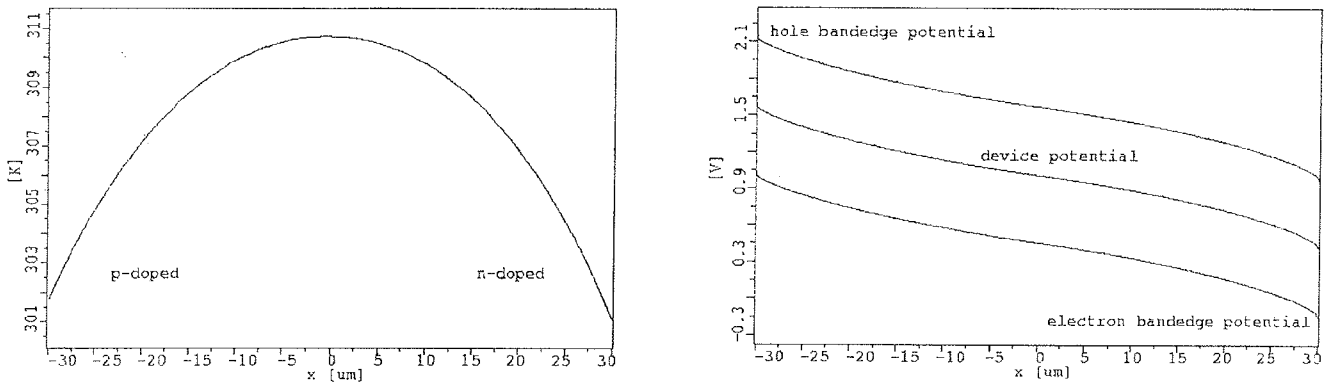

Fig. 5: Lattice temperature (left diagram) and band edge potentials (right diagram) of a diode in forward direction. The applied cathode voltage is 2.0V. The electrons move from the right to the left. The maximum of the lattice temperature is at the p/n junction. The device overheating is relatively high compared to the increase of the contact temperature. In a more realistic application the contact resistance would be higher so that the final lattice temperature would be also higher.

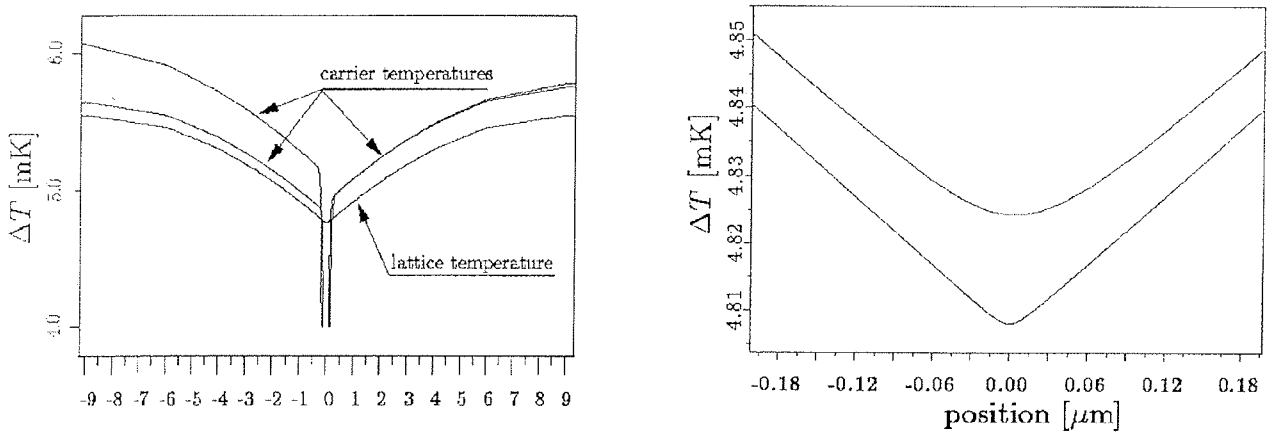

Fig. 6: Lattice temperature and carrier temperatures (in case of the HD simulation) of the diode with an applied voltage of 0.8V in the region of the p/n junction. A comparison between the DD and HD lattice temperature is given on the right side, which shows in more detail the lattice temperatures in the area of the p/n junction.

the electrons and holes. While the electrons move from the right to the left side, they have to overcome the cathode/n-doped semiconductor barrier. In the contact area they have to move against the electric field. This results in a lattice cooling because the energy gained by the carrier is needed to overcome the barrier. At least the net energy transfer from the carrier to the lattice is positive because the barrier for the holes, which leave the semiconductor at the cathode side, is much higher compared to the electron barrier.

One can see that the final lattice heating is highest at the anode contact of the device. This corresponds to a higher electron current, which finally results in a higher net heating of the anode contact. At the p/n junction a heat sink causes a strong lattice cooling. This sink is the remaining barrier of the Built-In potential drop where both carrier types have to overcome a potential barrier, which leads to the strong cooling effect. It should be noted that the net device heating is positive which means, that there is a lattice heat flow out of each contact. However this heat flow is not shown in the figure since only the silicon segment is calculated and not the heat flow inside the idealized contact. An indicator for a lattice heat flux out of the device is a raised contact temperature caused by the thermal contact resistance.

Fig. 3-6 show the increase of the lattice heating caused by the higher applied voltages. The Built-In potential nearly vanishes at high forward biases (and also the heat sink at the p/n junction), and the current is mainly caused by a drift current. At least the anode contact temperature is higher than the cathode temperature, which is the result of the higher electron current.

Fig. 6 shows the difference behaviour of the applied HD and DD equation set. The applied cathode voltage is

0.8V. In the figure the cooling of the p/n junction is shown. On the left side the temperatures of the lattice and of the carriers (in case of the HD simulation) are shown. At the junction the carriers are cooled down strongly because they have to overcome the Built-In barrier. This strong cooling is the result of the low carrier heat capacity. When the carrier temperature is below the lattice temperature the carriers are heated up by the lattice. The consequence is that the lattice looses thermal energy, which results in the lattice cooling at the p/n junction. The lattice cooling caused by the carriers is the result of the heat source term of the HD model (3) where the difference of the carrier and the lattice temperature becomes negative. The right side shows the shape of the lattice temperature in case of the HD (upper curve) and the DD simulation (lower curve). It should be noted that the carrier energy relaxation length l is the product of the saturation velocity v_{sat} = 10^5 m/s and the energy relaxation time τ_E =0.6 ps, which is about 0.06 μm. This value corresponds to the radius of the temperature distribution in the area of the junction.

B) The Hetero Bipolar Transistor

The last example shows the selfheating simulation results of a SiGe HBT with different specified boundary conditions. The simulated device consists of three segments, two silicon segments for the emitter and collector regions and a segment for the SiGe base. The two-dimensional device has a n-doped emitter (10e19cm^{-3}), a p-doped base (10e19cm^{-3}) and a low doped collector (2.0e17cm^{-3}). A buried layer, which starts below the low doped collector region gives a low device resistance. The base has a graded germanium fraction of 0%-20%. The germanium inside the base causes an accelerating field for the electrons which results in a fast transition time of the electrons trough the base.

To study the selfheating effects the applied voltages should enable high current densities. For this reason the base and collector voltage are about 1V, while the emitter is grounded. In this regime the base push out effect dominates the device characteristic, which causes a reduction of $\beta = I_C/I_B$ (β roll off). At this operating point the hole current supplied by the base is about a factor 13 lower than the collector current. To simulate more realistic conditions a thermal collector resistance of R_{th} =1.5e-4 [K cm^2/W] is specified. This condition assumes that the generated heat is transferred through the silicon bulk to the outside of the device. Because of the backend, the emitter and base contacts have a much lower ability to transfer the generated heat outside of the active area. In Fig. 7 the band edge and device potentials are shown.

The maximum potential drop is in the low doped collector region. The electrons move towards a positive potential and so the maximum power density in the collector region is at position x=-0.2, where the high doped buried layer starts. A second heat source is located in the SiGe base, where the electrons are accelerated by the drift field. The holes inside the base move towards a positive potential, which results in a lattice cooling. At least the fraction of the hole current is

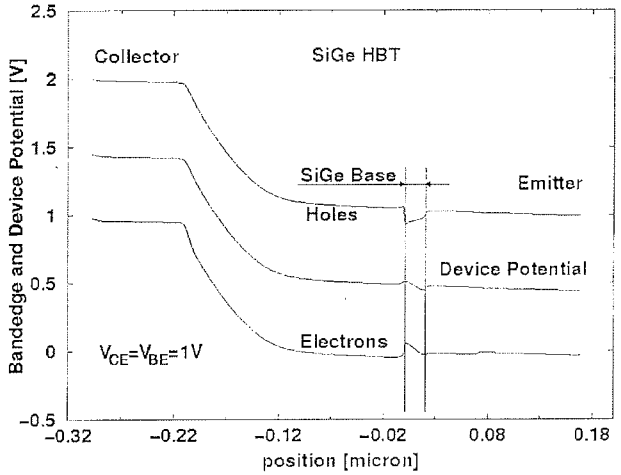

Fig. 7: Band edge potentials and device potential of the simulated SiGe HBT. The germanium fraction inside the base is graduated. The mole fraction is about 0% at the emitter/base interface and reaches the maximum value of 20% at the base/collector interface.

small compared to the electron current, so that the net energy transfer inside the base heats up the device. Fig. 8 shows the two dimensional temperature distribution of the heated device.

To estimate the sensitivity of the boundary conditions, the device heating is simulated with two different contact conditions. The sections of the two vertical temperature distributions is given in Fig. 9. The lower curve is the simulation result with a Neumann condition at the emitter contact, which means that there exists no heat transfer over the contact. This assumption is not realistic since a current crosses the contact. The specified Neumann condition neglects any contact heat and acts

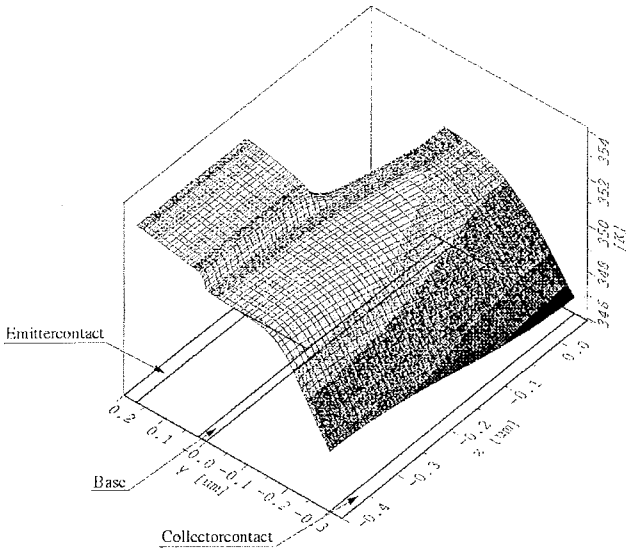

Fig. 8: Two-dimensional device heating with an applied electro/thermal contact model at the emitter contact which ensures energy conservation inside the device.

like a semiconductor/vacuum boundary. At least the thermal heat flow has a horizontal tangent towards the emitter contact.

In the second condition an electro/thermal contact with a very high thermal resistance is specified for the emitter contact (about 8 orders of magnitude higher than the collector contact). The simulation result is shown in the upper curve of Fig. 9 and ensures energy conservation. The contact heat, which leads to a lattice heating for both carrier types, causes a change in the slope of the lattice heat flux at the semiconductor/contact boundary. With these conditions nearly the complete generated heat leaves the device outside the collector contact. The final temperature distribution is higher compared to the Neumann condition, although in both simulations nearly no heat flux flows out of the emitter contact.

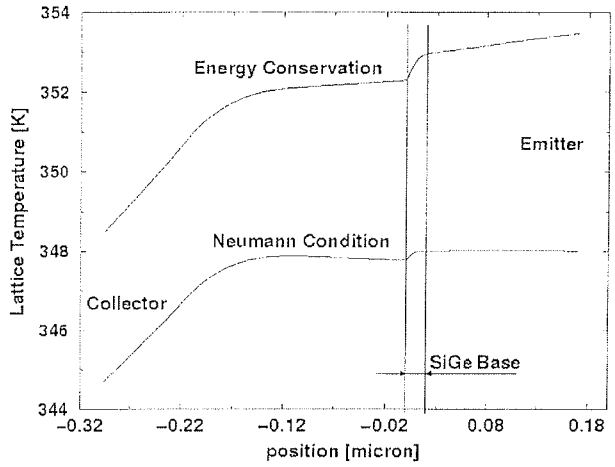

Fig. 9: Lattice temperatures of the two different emitter contact models. The vertical cross section of the device belongs to the position x=-0.4μm in Fig. 8.

A last a point has to be discussed to explain the lattice temperature distribution around the base area. Looking at Fig. 8 and Fig. 9 one would expect a heat sink near the base/collector junction. The sink exists because the electrons have to overcome the base/collector barrier. This barrier is the result of the decreased bandgap inside the base caused by the germanium fraction. But the second and much more dominant effect is the reduction of the thermal heat conductivity caused by the germanium atoms. At the maximum mole fraction of 20% the thermal heat conductivity is approximately reduced by a factor 10. The difference between a thermal heat sink and a variation in the heat conductivity is, that in the first case local minima in the lattice temperature distribution can appear. In the second case the sign of the slope of the lattice temperature does not change.

Acknowledgment

For the device simulations the generic device simulator MINIMOS-NT was used. MINIMOS-NT is a development of the Institute for Microelectronics, TU-Vienna. The author would like to thank the members of the institute for their fruitful discussions in the topic of self-heating.

References

/1/ W.S. Choi, J.G. Ahn, Y.J. Park, H.S. Min, C.G. Hwang. A Time Dependent Hydrodynamic Device Simulator SNU-2D With New Discretization Scheme and Algorithm, Trans. Computer-Aided Design,1994, Vol 13, No 7, p. 899-908

/2/ M. Knaipp. Modelling the Influence of Temperatures in Semiconductor Devices (written in German). PhD. Thesis. 1998, Institute for Microelectronics, TU-Vienna. http://www.iue.tuwien.ac.at/diss/knaipp/diss/diss.html

/3/ T. Simlinger. Simulation of Heterostructure Fieldeffect-transistors (written in German). PhD. Thesis,1996, Institute for Microelectronics, TU-Vienna. http://www. iue.tuwien.ac.at/diss/simlingerldiss/diss.htm 1

/4/ K. Kells. General Electrothermal Semiconductor Device Simulation PhD. Thesis, 1994, Hartung-Gorre 1994, ISBN:3-89191-787-2

/5/ S. Selberherr, Analysis and Simulation of Semiconductor Devices Springer 1984, ISBN:3-211-81800-6

Dr. Martin Knaipp
Process Engineer
Research & Development
Austria Mikro Systeme International AG
Schloss Premstätten
A-8141 Unterpremstätten
Austria
Fax.: ++43 (0) 3136 52501, 53650
Phone: ++43 (0) 3136 500-681
E-Mail: martin.knaipp@amsint.com

Franz Unterleitner
Austria Mikrosysteme International AG
Schloss Premstätten
A-8141 Unterpremstätten
Austria
Phone: ++43 (0) 3136 500-327
E-Mail: franz. unterleitner@amsint.com

Prispelo (Arrived): 25.04.00 *Sprejeto (Accepted): 17.05.00*

MODEL CALCULATION OF IONIZED CLUSTER BEAM INDUCED BIAS DEPENDENT INTERFACE CHARGE*

Dean Korošak and Bruno Cvikl
Faculty of Civil Engineering, University of Maribor, Maribor, Slovenia
and "J. Stefan Institute", Ljubljana, Slovenia

Keywords: insulator-semiconductor interfaces, metal-semiconductor interfaces, DIGS, Disorder Induced Gap States, DIG models, Schottky structures, ICB deposition, Ionized Cluster Beam deposition, interface charges, tight bindings, Green´s functions

Abstract: Within the framework of the simple one dimensional tight binding model of two coupled semiinfinite linear chains of atoms it is argued that the intrinsic interface charge induced at the interface between the two chains in principle depends on the applied bias. Approximate expressions in the limits of small and large applied bias are explicitly given and the necessity of self-consistent treatment of the induced interface charges is being discussed. In spite of the simplicity of the model, chosen as a first step towards investigation of the microscopic aspects of the interface physical properties, the findings seem to be in general agreement with our recent measurements of the reverse excess capacitance of the ionized cluster beam deposited Ag/p-Si(100) Schottky diode. Consequently, the findings might be relevant also to the theory of the disorder induced gap states, as the derived results imply that even at the given, lattice matched and undoped interface between the two (even identical) semiconductors, a strong, approximately bell shaped, bias dependent electric field is expected in general to appear, of which the consequence on the Fermi level pinning is presently unclear.

Modelski izračun odvisnosti induciranega naboja na vmesni plasti od zunanje napetosti v polprevodniških strukturah narejenih z metodo curka ioniziranih skupkov atomov

Ključne besede: vmesniki izolator-polprevodnik, vmesniki kovina-polprevodnik, DIGS stanja energijska nereda v reži energijski, DIGS modeli, SCHOTTKY strukture, ICB nanašanje s curkom skupkov ioniziranih, naboji električni vmesnika, povezave tesne, GREEN funkcije

Izvleček: V okviru enostavnega enodimenzionalnega modela stika med dvema linearnima verigama atomov je raziskana odvisnost induciranega naboja na stiku od zunanje napetosti. Podani so aproksimativni izrazi za odvisnost induciranega naboja pri velikih in majhnih vrednostih zunanje napetosti ter vpliv samousklajenosti pri računanju naboja na stiku. Čeprav izredno preprost, predstavlja podani model prvi korak k razumevanju mikroskopskih mehanizmov nastanka naboja na stiku odvisnega od zunanje napetosti in kaže, da so grobi rezultati v skladu z našimi ugotovitvami, ki temeljijo na izmerjenih karakteristikah kapacitete stikov Ag/p-Si(100) narejenih z metodo curka ioniziranih skupkov atomov. Predstavljeni rezultati lahko prav tako pomagajo osvetliti problem vpetja Fermijevega nivoja in z neredom induciranih stanj na stiku med različnimi materiali v okviru teorije DIGS.

1. Introduction

The unified model of disorder induced gap states (DIGS) for insulator-semiconductor and metal-semiconductor interfaces as proposed by Hasegawa /1/ seems to be able to explain the salient features of the metal-semiconductor interface formed either on the bare or oxide covered semiconductor /2/.According to DIGS model a deposition of either an insulator or a metal (or even semiconductor) on a given semiconductor effectively produces a thin disordered semiconductor interlayer, characterized by fluctuations of bond length and bond angles. The DIGS theory provides a formal understanding of the weak Fermi level pinning mechanism at semiconductor-metal junctions in terms of the microscopic morphology of the interface and is also, for a given metal-semiconductor junction, able to give a clue as to how and why seems to be possible to tailor Schottky barrier height /2/ over large interval, for which the manifestation of the induced interface dipoles might be most likely responsible /3/.

The problem of controlled variation of Schottky barrier height throughout its entire range, ranks as one among the important fundamental questions of semiconductor device physics remaining to be solved, notwithstanding also from the technological point of view. Although an old one /4/, it seems to be best amenable to the experimental investigation by utilizing the method of ionized cluster beam deposition ICB /5, 6/, the results of which seem to be strongly correlated to the basic assumption of DIGS theory of ref. /1, 2/. In particular, it has been found recently /7/ that the reverse excess capacitance of suitable ICB deposited Ag and Pb/Si(100) Schottky junctions could be understood in terms of the specific (modeled) biased voltage dependent excess interface charge density. Figure 1 shows the measured capacitance spectra of ICB deposited Ag/p-Si(100) Schottky structure (dots) and the calculated capacitance within the model incorporating the bias dependent interface charge density (full line). The details of the model and explicit expression for the interface charge are given elsewhere /7/. Although it is for the first time that such

In part presented at a poster section at the 18th European Conference on Surface Science, ECOSS-18, Wien, September, 1999

an explicit bias voltage dependent excess interface charge density has been introduced for the successful description of the measured low-frequency C-V data, its implicit existence seems to be introduced and in different context investigated by Darling /8/ and Gomila /9/.

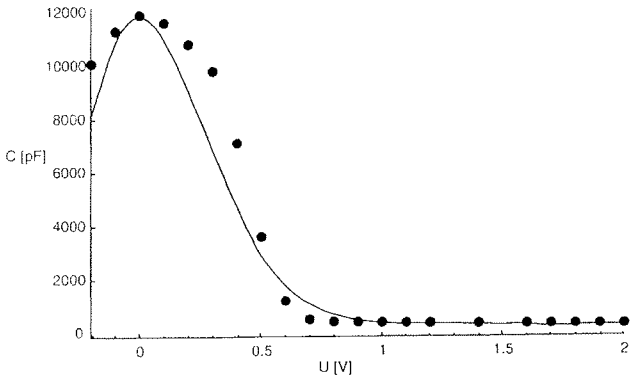

Fig. 1: Experimentaly determined low frequency capacitance of the ICB deposited Ag/p-Si(100) Schottky junction (dots) and calculated capacitance of the structure using the bias dependent interface charge model described in detail in /7/. As shown in /7/, the reasonable agreement with the measured spectra can only be achived by introducing bias dependent interface charge density.

Since the effect of the externally supplied bias voltage dependent interface charge density is expected strongly to correlate with the equilibrium as well as non-equilibrium transport properties of Schottky junctions it seems most appropriate to investigate its occurrence and its bias voltage functional dependence form the first principles, starting from the simple model of one dimensional chain of atoms.

In this paper we are tying to argue on the basis of a simple one dimensional model that the charge induced at the interface is in principle bias dependent (thus within certain interval of bias voltage always appearing at the junction, i.e. site of a broken periodicity of interatomic potential, even in cases of homojunctions, contrary to DIGS theory) and that special care should therefore be taken when modeling devices that incorporate the interface charge. We propose that the total interface charge in these models should be divided into intrinsic which is present even in most simplified and idealized models of homojunctions as shown below, and extrinsic which is a consequence of the possible disorder at the interface. In this note we are considering only the intrinsic interface charge. The study of both type of interface charges and possible effects of their interaction is the subject of the forthcoming paper.

2. One dimensional microscopic model of interface charge

Since we are interested in the charge localized near the ideal interface it is appropriate to consider the junction in the local description. We choose a very simple and highly idealized one dimensional model of the "device" in the tight binding approximation with N identical atoms on both sides with a single energy level E_0. We further postulate that the only effect of the explicit change of the applied bias ΔU in the "device" is a rigid shift of the atomic-state energies of N atoms on one side with respect to atomic-state energies of atoms E_0 on the other side of the interface. The problem is to determine the possible induced charge ΔZ on both sides of the interface when $\Delta U \neq 0$ and to study its dependence on the change of the applied bias. The calculation follows the approach used in obtaining heterojunction band offset /10, 11/.

The interface in our model is thought of as occurring on account of an infinitely thin, lattice matched, interface control layer /2/ imagined to be inserted at, say, at the middle of the linear chain of 2N identical atoms and consequently in the model it represents the region of the space where expected induced charge $\Delta Z \neq 0$. We start with the brief description of the "perfect" case when $\Delta U = 0$, when the solution is well known /12, 13/. The basis states are single localized atomic states centered at each site

$$|i> = c_i^+|0> \qquad \text{or} \qquad \Phi(x-x_i) = <x|c_i^+|0>$$

where c_i^+ is the creation operator. The tight binding Hamiltonian /13/ is:

$$H = \sum_i E_0 c_i^+ c_i + \sum_{i \neq j} W_{i,j} c_i^+ c_j \qquad (1)$$

and the solution of the Schrodinger equation is the linear combination of the basis states /14,13/:

$$\psi_k = \sum_i d_i(k)|i> \qquad (2)$$

which are assumed to form the complete orthonormal set. When only coupling $W_{i,j}=W$ between the nearest neighbors is considered the eigenvalues lie in the energy band of width $4W$ /14, 13/:

$$E(k) = E_0 + 2W \cos(ka) \qquad (3)$$

where $\vec{k}$ is the wave vector and a the distance between the neighboring atoms. As soon as the bias is applied to the "device" the periodicity of the problem is broken and the solution cannot be so easily found. One proceeds along the steps as for instance presented in /17, 18/.

The quantity of interest when calculating the induced charge at particular site m is the local density of states normalized to unity /17, 18/:

$$LDOS_m(E) = \sum d_m^*(k) d_m(k) \delta(E - E(k)) \qquad (4)$$

The perturbation induced by the applied bias changes the $LDOS_m(E)$ in the vicinity of the interface with respect to the unperturbed sites in the bulk. The occupied electron states localized at the interface are assumed to determine the induced interface charge ΔZ_m at the particular site m. Since the eigenvalues E of the localized energy states in one band model are found outside the band $|E-E_0|>2|W|$, we have to inspect the part of the perturbed local density of states which is extending over the band edges with respect to unperturbed ideal case. This is in accordance with /10/ where the interface charge in the vicinity of the heterojunction is defined as the difference between the local density of states in the neighborhood of the interface and the local density of states for an uniform (no interface) crystal summed over all occupied states. In our case in non-perturbed state ($\Delta U=0$) the local density of states is the same for every site and the sum over all band states serves as a reference value. Finally the sum of the induced charge ΔZ_m given with:

$$\Delta Z_m = \int_{|E-E_0|>2|W|} LDOS_m(E)dE \qquad (5)$$

at particular sites m, is performed. The number of atoms in the model N should be large enough to approximately ensure the bulk-like density of states sufficiently far from the interface on either side (m turns out ≈ 15). The approach we adopted here follows in some respect the model studied in /16/ where the charge transfer between two bands across the heterogap is considered in a perturbative manner. In contrast to /16/ we focus ourselves to a single (valence) band and specifically consider the diagonal heterocoupling of the states on opposite sides of the junction which was not investigated in /16/.

3. Numerical results and approximate solutions

In order to numerically obtain the bias induced interface charge in the described one dimensional model, we used exact diagonalization of the pertinent Hamiltonian matrix with N=40 and from orthonormal eigenstates calculate local density of states and induced charge at each site for different values of the applied bias. Since the in calculation of the induced interface charge involves only the coefficients $d_i(k)$ of the linear combination of the basis states (2) and the eigenvalues, the explicit set of basis states is not required. Because the change of all atomic-state energies by a constant value merely shifts the overall spectrum the only important parameter in the model is the hopping integral between the nearest neighbors W, which we take to be of the order of 1 eV as it is appropriate for semi-conducting materials /4/. Furthermore we assume that the change in the applied bias does not affect the coupling between nearest neighbors and that also the heterocoupling across the interface is of the same order as W /16/. In addition, we found from our computations that only the ratio of the applied bias and the hopping integral, or the "scaled" bias, determines the induced charge. Furthermore, since both sides of the interface are identical, apart for the rigid shift of atomic energies due to applied bias, the interface charge forms the induced interface dipole with equal amount of the total charge on both sides to comply to the overall charge neutrality of the problem as stated in /10/.

A further remark should be made considering the self-consistency of the calculated charges. In the first approximation the induced charge ΔZ_m at site m changes only the atomic-state energy of the atom by δV_m due to the intra-atomic or onsite interaction with energy J and inter-atomic coulomb interactions /19/:

$$\delta V_m = J\Delta Z_m + \frac{e^2}{4\pi\varepsilon_0}\sum_{n\neq m}\frac{\Delta Z_n}{b_{m,n}} \qquad (6)$$

where $b_{m,n}$ is the distance between the m-th and the n-th atomic site. On the other hand adding the δV_m to the atomic energies changes the Hamiltonian matrix, so the $LDOS_m(E)$ and consequently the induced charge are implicit function of the perturbation:

$$\Delta Z_m = \int LDOS_m(E,\delta V_m)dE \qquad (7)$$

In order to find the self-consistent charges the equations (6) and (7) ought to be simultaneously solved. The final self-consistent solution yields the applied potential as shown in fig. 2. The change of the potential near the interface extends only a few lattice sites far from the interface, suggesting the screening of the interface charge near the junction.

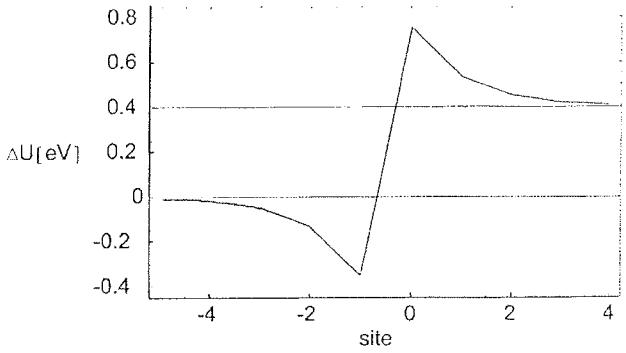

Fig. 2: Self-consistent applied potential in the vicinity of the interface for $\Delta U=0.4eV$. Sufficiently far from the interface ($m>5$) is the induced self-consistent potential difference practically equal to applied bias (dashed lines), suggesting that the the induced changes in the potential are effectively screened.

Total induced charge on one side of the junction, (at the junction m=0):

$$\Delta Z = \sum_{m=0}^{N}\Delta Z_m \qquad (8)$$

as a function of the change in the scaled applied bias $\Delta U/W$ is shown in fig. 3. It is evident that within this model the numerically obtained interface charge shows a distinct bias dependence with low values at low and high bias and a pronounced maximum between this two limits.

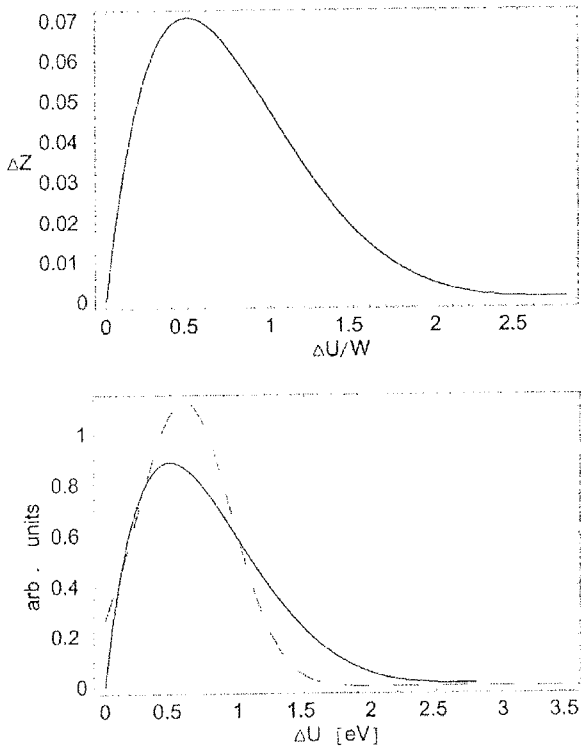

Fig. 3: Above - Total induced charge in one dimensional interface model on one side of the interface (at N=40) vs. "scaled bias" $\Delta U/W$. The interface is situated between N=40 identical atoms on each side and the bias is assumed to affect only the atomic-state energies. W is the hopping integral between nearest neighbors. Below - Total induced charge in one dimensional interface model (full line) and bias dependent interface charge function $\sigma(\Delta U)$ /7/ (dashed line) determined from measured excess capacitance in ICB deposited Ag/Si Schottky junctions, and given by $\sigma(\Delta U)=n_\sigma \exp(-(\Delta U/V_0 + K^2))$ /7/ (used in model for the capacitance shown in fig. 1), where n_σ, V_0, K are constants determined from fitting to the experimentally obtained capacitance spectrum. Both functions are for comparison normalized to 1.

The bias dependence in the very low and high bias regime can be qualitatively understood on the basis of the following arguments. In the limit of small bias $\Delta U/W<<1$ we assume that the perturbing constant potential at one side of the interface simply rigidly shifts the energy bands. The shift causes the part of the local density of states near the interface to extend over the non-perturbed band edges. The induced charge in this case can be approximated with the help of the expression for the local density of states in the infinite crystal /17, 18/:

$$\Delta Z_m = \int_{E_0-2W}^{E_0-2W+\Delta U} LDOS_m(E)dE \approx \frac{1}{\pi}\sqrt{\frac{\Delta U}{W}} \qquad (9)$$

The specific square root functional dependence of the induced charge on the bias is a consequence of the one dimensional model. In more detailed three dimensional models a linear dependence is expected /15/. The case $W/\Delta U<<1$ corresponds to the other limit of low values of induced charge and can be described in perturbative manner as shown /16/ for the case of two one dimensional bands, where now instead of the heterogap the applied bias is substituted in our model. In this limit the induced charge is given with the expression /16/:

$$\Delta Z = \left(\frac{W}{\Delta U}\right)^2 \qquad (10)$$

It is worth noting that the form (10) is equal to the expression one obtains in the one dimensional semi-infinite lattice when the atomic-state energy of the first atom is changed by $E_1=\Delta U$ with respect to others. It is well known (see for instance /17/) that if the difference is larger than the hopping integral between nearest neighbors $E_1>W$, the localized state outside the energy band exists with the energy $E_{loc} = E_1+W^2/E_1$. The weighting factor of this localized state $|d_j(E_{loc})|^2$ on the atoms at sites $j>1$ falls exponentially into the bulk /17/:

$$|d_j|^2 = \left(\frac{W}{E_1}\right)^{2(j-1)}\left(1-\frac{W^2}{E_1^2}\right) \qquad (11)$$

The sum over all atomic sites apart from the first is:

$$\sum_{j=2}^{\infty}|d_j|^2 = \sum_{j=1}^{\infty}|d_j|^2 - |d_1|^2 = 1-\left(1-\frac{W^2}{E_1^2}\right) = \left(\frac{W}{E_1}\right)^2 \qquad (12)$$

which is equal to (10).

4. Analytic expressions for the intrinsic induced interface charge in 1D model semiconductor junction

Our model semiconductor junction consists of two semi-infinite linear chains with identical atoms, which are held separately at different electrical potentials so that in each chain the thermal equilibrium is established. Let the two different potentials be $-\Delta U/2$ and $\Delta U/2$ respectively. The junction is formed when the beginnings of the two parts are brought into interatomic distance a so that the translational symmetry of the lattice is conserved. Let´s number the atoms in such a way that the $n \geq 1$ counts the atoms to the right and

$n \leq 0$ to the left of the interface. The one electron properties of the system are described in the tight binding approximation with the Hamiltonian given by (1). The most idealized conditions one can imagine occurs when all of the hopping integrals have the same value $W_{i,j}=W$ and when the formation of the system does not influence the atomic energies in the vicinity of the interface i.e. $E_n=-\Delta U/2$ for $n \geq 1$ and $E_n=\Delta U/2$ for $n \leq 0$. We have chosen $E_0=0$ for the origin from which all energies are measured.

The local density of states is found from the elements of the Green´s matrix or resolvent of the corresponding Hamiltonian (1):

$$G=\frac{I}{zI-H}\ , \tag{13}$$

where I is the identity matrix and $z=E+i\eta$. The diagonal element of the Green´s matrix is in this representation:

$$g(n,n)=\sum_k \frac{d_n^*(k)d_n(k)}{z-E(k)}\ , \tag{14}$$

where E(k) are the eigenvalues of the problem. Using the identity:

$$\lim_{\eta\to 0}\frac{1}{x+i\eta}=P\left(\frac{1}{x}\right)-i\pi\delta(x), \tag{15}$$

where P is the Cauchy principal value of the integral, it follows for the diagonal Green´s matrix element:

$$g(n,n)=P\left(\sum_k \frac{d_n^*(k)d_n(k)}{z-E(k)}\right)-i\pi\sum_k d_n^*(k)d_n(k)\delta(E-E(k)) \tag{16}$$

Knowing the definition of the local density of states at site n in the chain it follows immediately that the local density of states is given with the imaginary part of the diagonal element of the Green´s matrix. The explicit expression for the local density of states is therefore:

$$LDOS_n(E)=-\frac{1}{\pi}\mathrm{Im}\,g(n,n) \tag{17}$$

In writing the matrix element of the resolvent G as $g(m,n)=\langle m|G|n\rangle$ we always assume also the dependence upon the energy $E+i\eta$ and that the corresponding limit of $\eta\to 0$ is always understood.

In order to calculate the matrix elements of G we rewrite the equation for the resolvent as:

$$(H-zI)G=-I \tag{18}$$

First we calculate the bulk and surface Green´s functions for the one dimensional linear chain with no applied potential. Since the tight binding Hamiltonian in nearest neighbor approximation is a tridiagonal matrix, the following set of difference equations for the matrix elements g(m,n) is obtained /21, 22/:

$$-Eg(m,n)+W(g(m+1,n)+g(m-1,n))=-\delta_{m,n} \tag{19}$$

The general solution for the function g(m,n) can be written as:

$$g(m,n)=a_1p_1^{m-n}+a_2p_2^{m-n}\ . \tag{20}$$

The right-side Green´s function $g_>(m,n)$ for $m>n$ is matched to the left-side Green´s $g_<(m,n)$ for $m<n$ at $m=n$. p_1 and p_2 are the roots of the characteristic equation:

$$Wp^2-Ep+W=0 \tag{21}$$

and their explicit form is

$$p_{1,2}=\frac{E}{2W}\pm\sqrt{\left(\frac{E}{2W}\right)^2-1} \tag{22}$$

Characteristics roots obey the relation $p_1p_2=1$ so they can always be chosen such that $|p_1|<1$ and $|p_2|>1$.

Let´s consider the "bulk" matrix element far from both ends of the linear chain at some site n. Then g(m,n) should approach zero when m is near the end. Thus $g_>(m,n)=a_2p_2^{m-n}$ and $g_<(m,n)=a_1p_1^{m-n}$. Matching the solutions at $m=n$ yields:

$$g_>(m,n)=g(n,n)p_2^{m-n}\ \text{ and }\ g_<(m,n)=g(n,n)p_1^{m-n} \tag{23}$$

Substituting the above solutions into the equation for the diagonal matrix element:

$$-Eg(n,n)+W(g(n+1,n)+g(n-1,n))=-1 \tag{24}$$

yields the expression:

$$g(n,n)=\frac{1}{E-2Wp_2}\ . \tag{25}$$

With the site number $n=1$ the surface Green´s function is obtained:

$$-Eg(1,1)+Wg(2,1)=-1 \tag{26}$$

and

$$g(1,1)=\frac{1}{E-Wp_2} \tag{27}$$

To derive the interface Green´s function for the model semiconductor junction under applied bias we separate the total Hamiltonian H into two parts:

$$H = H_0 + V \tag{28}$$

H_0 describes the two linear chains separated at interatomic distance kept at different potentials (-ΔU/2, ΔU/2). V is the coupling between the two chains. When there is no applied potential i.e. ΔU=0, the perfect infinite linear chain is obtained and in this case the operator V is
$V = W(c_1^+c_0+c_0^+c_1) = W(|1><0|+|0><1$Times New Roman"Symbol"đ).
We consider the idealized case when in the presence of nonzero applied bias the coupling part of the Hamiltonian H (or more precisely the value of the hopping integral W) does not change. The perfect resolvent G_0 equals:

$$G_0 = \frac{1}{z - H_0} \tag{29}$$

and the total resolvent is

$$G = \frac{1}{z - H} = \frac{1}{z - H_0 - V} \tag{30}$$

From the above expression the Dyson´s equation is obtained connecting the two resolvents:

$$G = G_0 + G_0VG. \tag{31}$$

The interface Green´s function on the right-side of the connected linear chain is given by diagonal matrix element g(1,1) of G. Since G_0 represents the resolvent of the perfect semi-infinite linear chain it follows that its matrix elements $g_0(0,1)$ and $g_0(1,0)$ are zero by definition /23/ ($n \geq 1$ denotes the right-side of the coupled chain and $n \leq 0$ denotes the left-side). The matrix elements $g_0(1,1)$ and $g_0(0,1)$ are given by the equations:

$$g(1,1) = g_0(1,1) + Wg_0(1,1)g(0,1), \tag{32}$$

$$g(0,1) = Wg_0(0,0)g(1,1) \tag{33}$$

From the two equations the expression for the interface Green´s function follows:

$$g(1,1) = \frac{1}{g_0^{-1}(1,1) - W^2 g_0(0,0)} \tag{34}$$

Explicit expression suitable for practical calculations are obtained by inserting the appropriate surface Green´s functions (27) into the interface Green´s function. In the expressions for the surface Green´s function we now must transform E→E-ΔU/2 on the right-side and E→E+ΔU/2 on the left. Also let $p_{1,2}$ and $q_{1,2}$ denote the characteristics roots on the right and left respectively. Using this we derive the following expression for the interface Green´s function:

$$g(1,1) = \frac{1}{E - \Delta U/2 - W(p_2 + q_2)} \tag{35}$$

The interface density of states as a function of applied bias is:

$$LDOS_1(E, \Delta U/2) = IDOS(E, \Delta U/2) = -\frac{1}{\pi} \mathrm{Im} g(1,1). \tag{36}$$

The interface induced charge ΔZ is defined as the charge given by the localized electron states at the interface and is therefore given by the part of the local density of states extending over the corresponding "bulk" band edges. The important point one should notice is that depending on the value of the energy the characteristics roots are either real or complex. If the energy falls into the interval $E \in [-2W+\Delta U/2, 2W+\Delta U/2]$ the corresponding eigenstate is inside the "bulk" band and represents the extended Bloch state. The characteristic roots are in this case complex conjugated.

The interface density of states has two forms depending on the energy. If $\Delta U/2 \geq 2W$ then for $\forall E \in [-2W+\Delta U/2, 2W+\Delta U/2]$ the characteristic roots on the left side (p_2) are real and the interface density of states is:

$$IDOS(E,\Delta U/2) =$$

$$= \frac{1}{\pi} \frac{W\sqrt{1-\left(\frac{E-\Delta U/2}{2W}\right)^2}}{W^2\left(1-\left(\frac{E-\Delta U/2}{2W}\right)^2\right)^2 + \left(W\sqrt{\left(\frac{E+\Delta U/2}{2W}\right)^2 - 1} - \Delta U/2\right)^2} \tag{37}$$

If $\Delta U/2 < 2W$ then if for $\forall E \in [2W-\Delta U/2, 2W+\Delta U/2]$ the previous expression for the IDOS(E,ΔU/2) applies. If $E \in [-2W+\Delta U/2, 2W-\Delta U/2]$ then the correct expression for the interface density of states becomes:

$$IDOS(E, \Delta U/2) = \frac{1}{\pi} \frac{\varepsilon(E, \Delta U/2)}{(\Delta U/2)^2 + \varepsilon^2(E, \Delta U/2)}, \tag{38}$$

where

$$\varepsilon(E, \Delta U/2) = W\left(\sqrt{1-\left(\frac{E-\Delta U/2}{2W}\right)^2} + \sqrt{1-\left(\frac{E+\Delta U/2}{2W}\right)^2}\right)$$

In the limit ΔU→0 the interface density of states takes on the shape of the bulk density of states for the infinite one dimensional crystal:

$$IDOS(E, \Delta U/2 \to 0) = \frac{1}{\pi} \frac{1}{2W\sqrt{1-\left(\frac{E}{2W}\right)^2}} \tag{39}$$

When applied bias takes on large values $\Delta U/2>>W$ then the interface density of states has the form of the surface local density of states:

$$IDOS(E,\Delta U/2>>W)=\frac{1}{\pi W}\sqrt{1-\left(\frac{E}{2W}\right)^2} \tag{40}$$

The induced interface charge ΔZ given by the electron states with the energy lying outside the bulk band i.e. $|E-\Delta U/2|>2W$ is calculated as follows:

$$\Delta Z=1-\int_{-2W+\Delta U/2}^{2W+\Delta U/2} IDOS(E,\Delta U/2)dE \tag{41}$$

The calculated interface induced charge according to the previous expression is shown on figure 4.

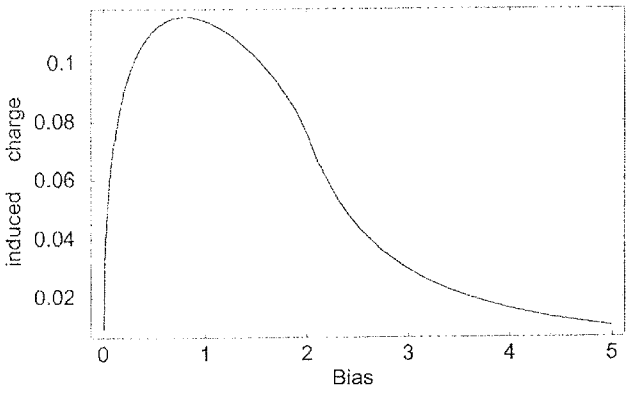

Fig. 4: Calculated induced interface charge from the analytic expression for the interface density of states.

As stated earlier, the complete interval of the applied bias should be divided into two parts depending on the ratio between the applied bias ($\Delta U/2$) and the hopping integral between nearest neighbors W. Let´s introduce non-dimensional variables $t=E/2W$ and $s=(\Delta U/2)/2W$. With these substitutions the integrals of the interface density of states i.e. $1-\Delta Z$) are cast into the following forms: for $s\geq 1$:

$$\frac{1}{2\pi s}\int_{-1+s}^{1+s} f_2(t,s)dt \tag{42}$$

and for $s<1$:

$$\frac{2}{\pi}\int_{-1+s}^{1-s} f_1(t,s)dt+\frac{1}{2\pi s}\int_{1-s}^{1+s} f_2(t,s)dt \quad . \tag{43}$$

Functions f_1 and f_2 are given with:

$$f_1(t,s)=\frac{\sqrt{1-(t-s)^2}+\sqrt{1-(t+s)^2}}{4s^2+\left(\sqrt{1-(t-s)^2}+\sqrt{1-(t+s)^2}\right)^2} \tag{44}$$

and

$$f_2(t,s)=\sqrt{1-(t-s)^2}(t+s)+\sqrt{\left((1+s)^2-t^2\right)\left(t^2-(1-s)^2\right)} \tag{45}$$

We are interested in the asymoptic behavior of the interface charge bias dependence for large values of applied bias, i.e. we seek the value of the above integral for $s>>1$. Since the induced interface charge monotically limits to zero for large values of applied bias, it is convenient to approximate the integrand with the power series up to the first non-vanishing order in $1/(\Delta U/2)$. Introducing the new variable $u=t-s$, the following expression needs to be evaluated for $s>>1$:

$$\Delta Z=\frac{2}{\pi}\int_{-\pi/2}^{\pi/2}\frac{\cos^2 u\ du}{\cos^2 u+\left(\sqrt{(\sin u+2s)^2-1}-2s\right)^2}. \tag{46}$$

The power series of the part of the integrand containing s is:

$$\sqrt{(\sin u+2s)^2-1}-2s=\sin u-k+2k^2\sin u \tag{47}$$

where $k=1/4s=W/\Delta U$. Expanding the whole integrand in power series to the second order in k and integrating the obtained series yields:

$$\frac{2u+\sin 2u}{2\pi}-\frac{3\cos u+\cos 3u}{3\pi}k-\frac{2u+\sin 2u}{2\pi}k^2 \tag{48}$$

Evaluation of the obtained asymptotic expression at the upper and lower integral boundary $[-\pi/2,\pi/2]$ yields:

$$\Delta Z=k^2=\left(\frac{W}{\Delta U}\right)^2. \tag{49}$$

For the very low values of applied bias, which equals the case when $s<<1$, the interface charge shows a square root dependence on the applied bias:

$$\Delta Z=\frac{4}{3\pi}\sqrt{s}=\frac{2}{3\pi}\sqrt{\frac{\Delta U}{W}}. \tag{50}$$

The asymptotic expressions for the bias dependence of the interface charge for small and large values of applied bias are in accordance with the ones previously presented in the numerical study of the induced interface charge. The forms (50) and (49) were previously obtained using simple yet plausible arguments of the rigid band shift in case of small bias, and considering the case of the seminfinite lattice with an adsorbed atom.

The origin of the maximum in the bias dependence of the interface charge reveals the structure of the expression (43) entering the calculation of the interface charge for $s<1$ which is a sum of a monotonically increasing and decreasing part. The sum of the two yields the curve exhibiting a maximum point in the interval $s\in[0,1]$. The situation is illustrated in fig. 5.

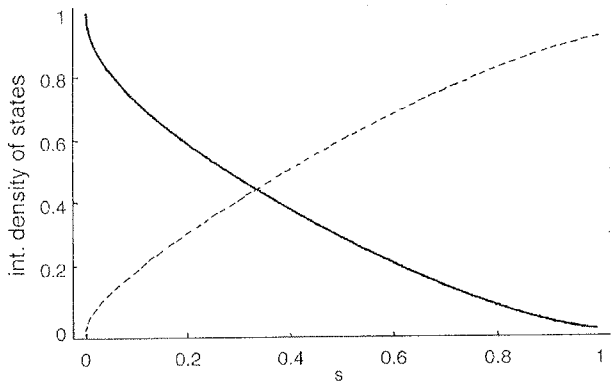

Fig. 5: Partial contributions to the total induced interface charge from the integrated density of states over the appropriate energy interval. The full curve shows the contribution of the states with the energy $E\in[-2W+\Delta U/2, 2W-\Delta U/2]$ whereas the dashed curve shows the integral over the states from the energy interval $E\in[2W-\Delta U/2, 2W+\Delta U/2]$.

5. Conclusions

Recently /7/ it has been realized that the measured capacitance spectra of the ICB deposited Ag/p-Si(100) can be suitable well described only if the charge model for the capacitance of the structure incorporated the bias dependent interface charge density. In this paper the first step towards the microscopic picture of the underlying physical processes is taken.

On the basis of the very simple model the bias dependence of the induced charge at the interface is calculated in tight binding approximation. The expressions for the limiting cases at small (9) and (50) and large (10) and (49) values of the applied bias are shown in the compact form. For the intermediate values between the limits the induced charge is expected to reach a maximum value. It is argued that the interface charge used in models of semiconductor devices should in general be divided into intrinsic, which is induced even in ideal heterojunctions and extrinsic, which is is a consequence of disorder present at the junction between dissimilar materials. In this study the effect of the disorder at the interface is not considered and only the applied bias dependent intrinsic induced interface charge is explored. As the preliminary investigations show, the presence of the disorder changes the bias dependence of the induced charge in accordance with the model of disorder and the details of the bonding so that the simple scaling of the bias does not apply, but still the pronounced maximum of the induced interface charge is to be expected. The detailed effects of the interface charges at the interface in the charge transport in semiconductor junctions is a subject of an ongoing research.

Note added in proof: Latest results show that the model function for the interface charge density of the form: $\sigma(\Delta U)=n_\sigma(a\Delta U+b)\exp(-(\Delta U/V_0+K)^2)$ included in the model for the capacitance /7/ gives a suitable description of the published measured capacitance data /23, 24, 25/ of the *ordinary* (i.e. *not* ICB deposited) Al/p-Si and Mo/p-Si Schottky structures. The parameters used to model the published data in *absolute scale* were:
for Al/p-Si: $n_\sigma=0.00710^{-5}$ As/cm^2, $V_0=0.19$V, $K=2.5$, $a=0.081V^{-1}$, $b=0.06$ and
for Mo/p-Si: $n_\sigma=0.000810^{-5}$ As/cm^2, $V_0=0.16$V, $K=1.6$, $a=0.01V^{-1}$, $b=0.51$. As it seems, the proposed model for the capacitance incorporating the bias dependent interface charge density could have a general validity for the metal/thin interlayer/semiconductor structures, and not only for the ICB samples. A detailed presentation of these findings is to be published.

6. References

/1/ H. Hasegawa, Jpn. J. Appl. Phys, 38. 1098 (1999).
/2/ K. Koyanagi, S. Kasai, H. Hasegawa, Jpn. J. Appl. Phys. 32, 502 (1993).
/3/ A. Ruini, R. Resta, S. Baroni, Phys. Rev. B 56, 14921 (1997).
/4/ Shannon, Appl. Phys. Lett. 25, 75 (1974).
/5/ T. Takagi, Ionized-Cluster Beam Deposition and Epitaxy (Noyes Publications, Park Ridge, New Jersey, 1988), see also T. Takagi, Vacuum 36, 27 (1986).
/6/ B. Cvikl, D. Korošak and J. Zs. Horvath, Vacuum 50, 385 (1998).
/7/ B. Cvikl, D. Korošak and M. Koželj Proceedings of 34th International Conference on Microelectronics, Devices and Materials, MIDEM´98, p. 107, September 23.-25. 1998. Rogaška Slatina, Slovenia. (MIDEM Society, Ljubljana, 1998).
/8/ R. B. Darling, IEEE Trans. Elec. Devices 43, 1153 (1996).
/9/ G. Gomila, J. Phys. D 32, 64 (1999).
/10/ F. Flores and C. Tejedor, J. Phys C 12, 230 (1979).
/11/ J. C. Duran, F. Flores, C. Tejedor and A. Munoz, Phys. Rev. B 36, 5920 (1987).
/12/ N. W. Ashcroft and D. N. Mermin, Solid State Physics, Chap. 10 (Saunders College Publishing, Orlando, 1976).
/13/ O. Madelung, Introduction to Solid-State Theory, Chap. 8 (Springer-Verlag, Berlin, 1978).
/14/ W. A. Harrison, Electronic Structure and the Properties of Solids (Freeman, San Francisco, 1980).
/15/ W. A. Harrison, J. E. Klepeis, Phys. Rev. B 37, 864 (1988).
/16/ E. O. Kane, Phys. Rev. B 33, 4428 (1986).
/17/ M. -C. Desjonqueres, D. Spanjaard, Concepts in Surface Physics 2nd ed., Chap. 5 (Springer, Berlin, 1996).
/18/ M. Lannoo and P. Friedel, Atomic and Electronic Structure of Surfaces (Springer-Verlag, Berlin, 1991).

/19/ W. A. Harrison, Phys. Rev. B 31, 2121 (1985).
/20/ A. -B. Chen, Y. M. Lai-Hsu and W. Chen, Phys. Rev. B 39, 932 (1989).
/21/ S. Krishnamurthy, A. -B. Chen and A. Sher, J. Appl. Phys 84, 5037 (1998).
/22/ D. Kalkstein and P. Soven, Surf. Sci. 26, 85 (1971).
/23/ H. Tseng and C. Wu, J. Appl. Phys. 61, 2966 (1987).
/24/ H. Tseng and C. Wu, J. Appl. Phys. 62, 302 (1987).
/25/ H. Tseng and C. Wu, Solid. State Elec. 30, 383 (1987).

mag. Dean Korošak
Fakulteta za gradbeništvo
Univerza v Mariboru
Smetanova 17
2000 Maribor
email: dean.korosak@uni-mb.si
tel.: +386 62 2294 313 in +386 61 1885 365
fax: +386 62 224-179 in +386 61 161 23 35

prof. dr. Bruno Cvikl
Fakulteta za gradbeništvo
Univerza v Mariboru
Smetanova 17
2000 Maribor
in
Inštitut "Jožef Stefan"
Jamova 39
1000 Ljubljana
email: bruno.cvikl@ijs.si
tel.: +386 62 2294 362 in +386 61 1885 239
fax: +386 62 224-179 in +386 61 161 23 35

Prispelo (Arrived): 15.03.00 *Sprejeto (Accepted): 25.04.00*

BATTERY CHARGER BASED ON DOUBLE-BUCK AND BOOST CONVERTER

Miro Milanovič, Andrej Roškarič and Milan Auda
Faculty of Electrical and Computer Engineering, Maribor, Slovenia

Key words: electrical accumulators, battery charger, electric converters, voltage converters, buck converters, boost converters, nonlinear current controllers, experimental results

Abstract: The paper describes a double-buck and boost converter structure suitable for battery charger in electrical vehicle application. It is very convenient to use inverter elements for battery charging task. Different DC to DC converter structures can be organized from the inverter semiconductor elements. In the case of the induction motor electrical drive application, the required inductors could be established from the motor windings. Such combined converter should satisfy the unity power factor operation as well. By using the double-buck circuit the current high harmonic distortion will be either avoided or significantly reduced. The boost converter established from the inverter elements enables the energy transfer from the mains to the load during the whole mains voltage half period. Such combined converter does not need any additional semiconductor or inductor elements except the diode bridge.

Polnilnik baterij zasnovan na dvojnem pretvorniku navzdol in pretvorniku navzgor

Ključne besede: akumulatorji električni, polnilniki akumulatorjev, pretvorniki električni, pretvorniki napetosti, pretvorniki navzdol, pretvorniki navzgor, regulatorji toka nelinearni, rezultati eksperimentalni

Povzetek: V prispevku je predstavljena kombinacija vezij osnovnih DC/DC pretvornikov z namenom uporabe v polnilniku akumulatorskih baterij. Novo vezje je ocenjeno iz zahtev bremena (napetostna regulacija) in vpliva na obliko vhodnega toka (tokovna regulacija). Z ozirom na delne rezultate je podrobneje razčlenjeno sinhronizirano delovanje vzporedne vezave dveh pretvornikov navzdol in pretvornika navzgor. Na osnovi dinamične karakteristike sestavljenega pretvornika, ki je bila ocenjena z avtoregresivno metodo za identifikacijo sistemov, je bil določen regulator. Na sestavljenem pretvorniku so bile izvedene meritve vhodnih in izhodnih veličin. Rezultati so komentirani glede zahtev bremena in zahtev standarda IEC 1000-3-2.

1 Introduction

Power conversion system is sometimes constructed by paralleling converters in order to improve performance or reliability, or attain a high system rating. The parallel converters operation is a usual operation mode in the telephone-exchange power supply systems.

Some authors put their atention in the study of the current sharing techniques depending on the load requirements /1/, /2/, /3/. All of them considered the buck converter parallel operation as an autonomous system. The current reference values have been provided to the buck converters from the central control unit and the DC to DC converters do not operate under the synchronous mode /1/. The parallel operation of boost converter is an attractive operation mode as well. In /5/ authors discuss current ripple cancellation by simultaneous operation of two boost converters.

The inverters in electric vehicle consist of six transistors and diodes. It is simple to establish the battery charger circuit from this set of elements. It is possible to establish the different battery charger structures by using the inverter elements. Same converter circuits are going to be describe here. From the set of the converter circuits, the double buck and single boost have been chosen. By using this structure, it is possible to avoid the high current distortion when the single buck converter operates. This property could be reached if the double-buck structure is operated in synchronous mode. The voltage control and current inner loop control will be also presented.

The objectives for such operation mode is to reach the unity power factor operation with less current distortion than that of ordinary buck converter /4/. Such battery charger structure is also appropriate for the telephone-exchange power supply system.

2 Circuit proposals

In electrical vehicle applications and in telephone-exchange power supply systems, the battery charger circuits require an output voltage which is usualy less than the input voltage.

In Fig. 1(a) the inverter circuit is shown. This is a voltage source inverter and it is supplied from the battery (U_0). With dashed line the diode bridge is shown as well. The diode bridge will operate only when the battery charging function will be required. To transform the inverter circuit function into converters behaviour, suitable for battery charging tasks, some of the connections in inverter circuits should be disconected.

The first circuit of the stage is the simple buck circuit which is shown in Fig. 1(b). By using this configuration, the battery task function has been solved on an appropriate way, but regarding the mains this circuit have a poor power factor. As could be concluded from the input current waveform in Fig. 2(a), the power factor is poor because of two reasons:

- the input current is discontinuous;
- there is no energy transfer during the whole half period (only when $U_d > U_0$).

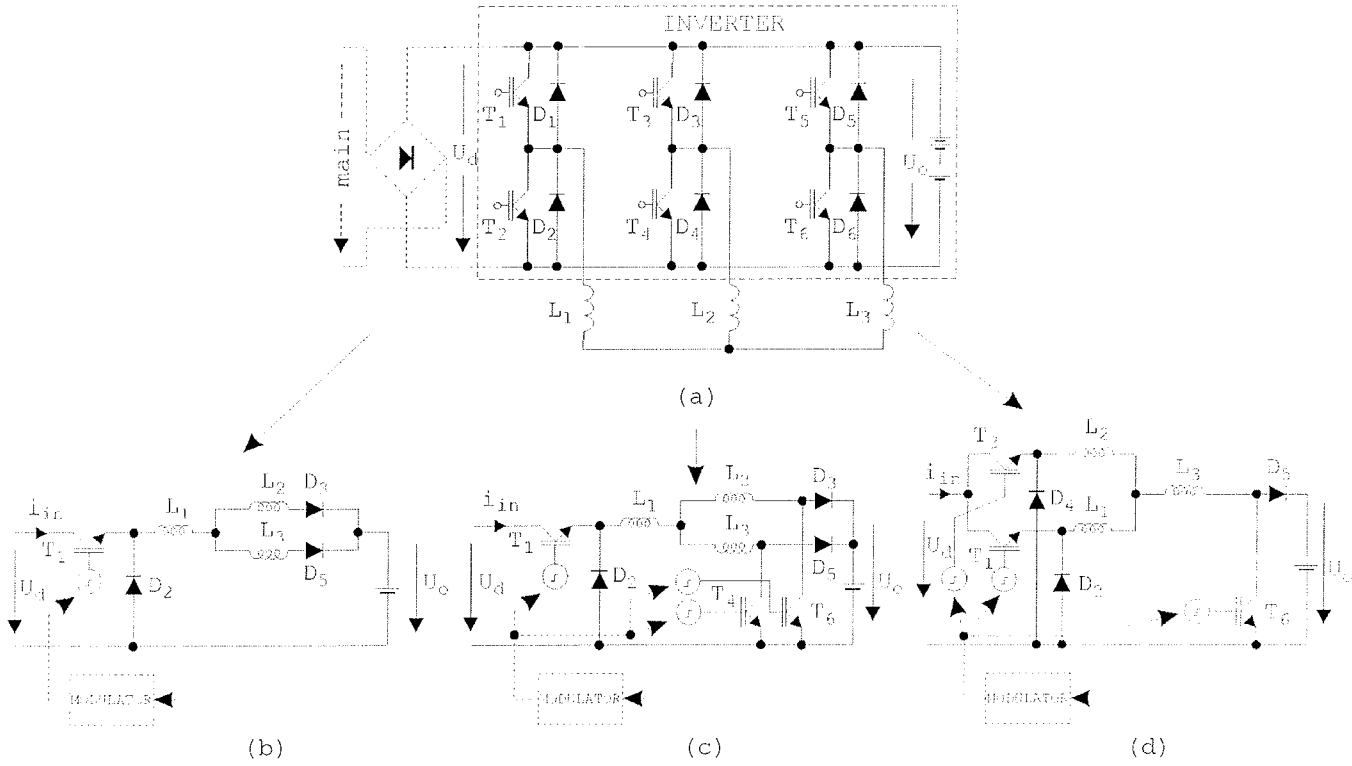

Fig. 1: Inverter to DC-DC converters transformation: (a) Electrical vehicle inverter, (b) Buck converter, (c) Boost and buck converter, (d) Double-buck and boost converter.

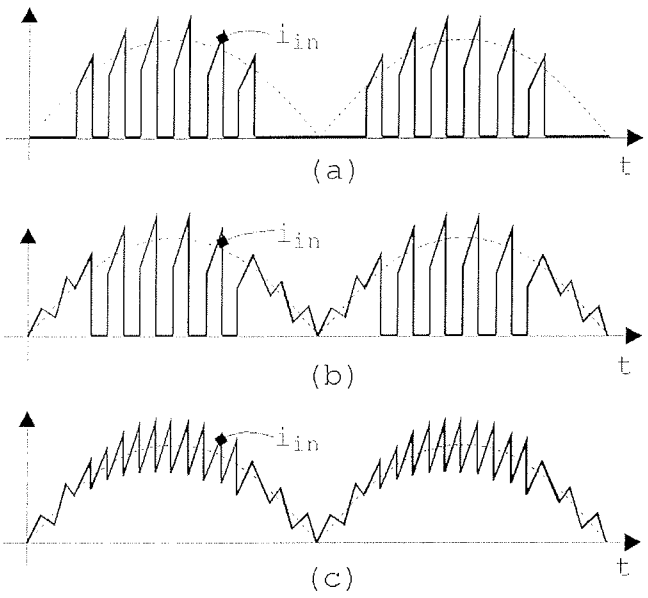

Fig. 2: Input current shapes: (a) Input current for single buck converter only; (b) Input current for single buck and boost converter; (c) Input current for double-buck and boost converter.

The circuit shown in Fig. 1(c) has an advantage regarding the converter shown in Fig. 1(b). This circuit enables the energy transfer from the mains, even if the instantaneous input voltage is lower than the DC output voltage. This advantage has been provided by two boost converters. These two converters could work in simultaneous mode or in synchronous mode as was proposed in /5/. Regarding the current waveform shown in Fig. 2(b), the power factor of this circuit is better than in the previous case but there is still discontinuous current when buck converter operates.

To avoid this disadvantage from the inverter circuit, the converter shown in Fig. 1(d) also proposed. This is a double-buck and boost converter circuit. By using the two buck converters, it is possible to avoid the discontinuous current, which appears in the previous proposed converters, as shown in Fig. 2(c). The boost converter provides the energy to the load when the instantaneous input voltage is lower than the output voltage. By using this structure, the previous mentioned disadvantages disappear. The circuit advantages can be summarized as follows:

- the input current is continuous;
- there is energy transfer during the whole half period.

For the further investigation the double-buck and boost converter has been chosen.

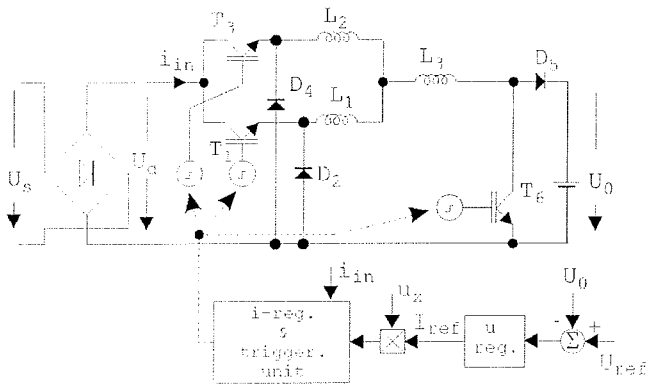

Fig. 3: The double-buck and boost converter complete control scheme.

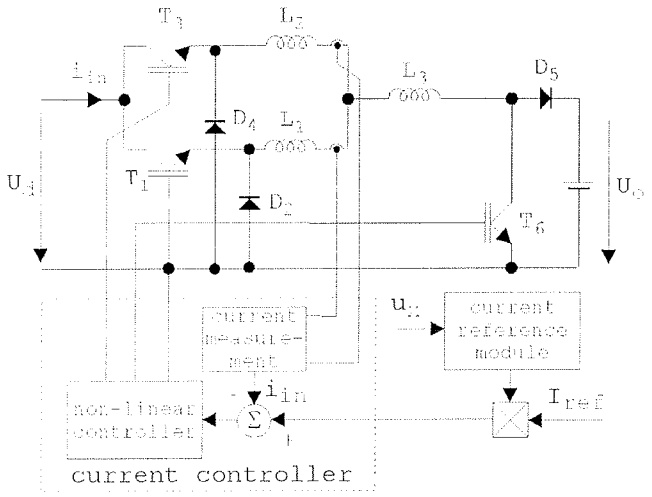

Fig. 4: The current control scheme.

3 Double-buck and boost converter control

For the double-buck and boost rectifier, the control requirements are defined regarding the load. There are two operating modes required by the bateries. The rectifier should operate as:

- a current source;
- a voltage source.

Regarding the battery condition, the converter will work as a current source or as a voltage source. The unity power factor requirements cause that the rectifier input current on the main side should follow the sinusoidal reference waveshape. This means, that when the rectifier works as a voltage source, a current loop control as an inner loop should be included in the control algorithm. In this case, the current reference will be produced by a voltage controller. The sinusoidal current

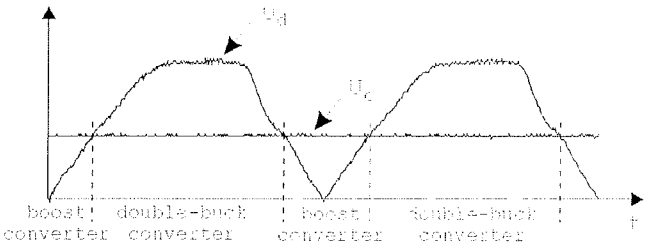

Fig. 5: Intervals where the converter changes its sturucture depending of input-output voltage conditions.

reference will be established by multiplication of the current reference produced by the voltage controller with the "sinusoidal" signal (u_x) of the input voltage normalized to a unity magnitude amplitude as follows:

$$u_x = \hat{U}_s \frac{1}{\hat{U}_s} |\sin(\omega t)|, \qquad (1)$$

where $\hat{U}_s$ represents the magnitude of the input voltage.

In Fig. 3 the complete control scheme is shown.

3.1 Current controller and triggering unit

The combined operation of two different converter structures requires a non-linear approach to control the system. In Fig. 4, a current control loop is shown. During the mains voltage half period the converter changes the structure as depicted in Fig. 5.

The boost converter operates only when the input voltage is lower than the DC output voltage ($U_d < U_0$) and the double-buck converter operates when the input voltage is higher than the DC output voltage ($U_d > U_0$). Each of those two modes requires a special atention regarding inner current references. Regardless what happens with the sinusoidal reference value (if it changes the magnitude), the input current average value in boost converter and the input current average value in the double-buck converter must follow the sinusoidal current reference.

3.1.1 The boost converter operation

Regarding Fig. 5 the boost mode of the converter operation is mandatory when the instantaneous input voltage is lower than output voltage value.The hysteresis-controlled principle of operation in the boost mode has been used. To avoid the discontinuous current mode operation from the current reference module, two current references are needed as shown in Fig. 6. From the timing sequences in Fig 6, the hysteresis controller is designed as shown Fig 7.

3.1.2 The double-buck converter operation

For double-buck converter operations, the intervals when the instantaneous input voltage is higher than the output voltage are obligatory. Otherwise there will be no energy transfer from source to load. In Fig. 8, the two buck converters synchronous operation is indicated.

UDK 621.3:(53+54+621+66)(05)(497.1)=00 ISSN 0352-9045

INFORMACIJE MIDEM 2 ◦2000

Strokovno društvo za mikroelektroniko elektronske sestavne dele in materiale

Strokovna revija za mikroelektroniko, elektronske sestavne dele in materiale
Journal of Microelectronics, Electronic Components and Materials

INFORMACIJE MIDEM, LETNIK 30, ŠT. 2(94), LJUBLJANA, junij 2000

UDK 621.3:(53+54+621+66)(05)(497.1)=00 ISSN 0352-9045

INFORMACIJE MIDEM 2 ◦ 2000

INFORMACIJE MIDEM LETNIK 30, ŠT. 2(94), LJUBLJANA, JUNIJ 2000
INFORMACIJE MIDEM VOLUME 30, NO. 2(94), LJUBLJANA, JUNE 2000

Revija izhaja trimesečno (marec, junij, september, december). Izdaja strokovno društvo za mikroelektroniko, elektronske sestavne dele in materiale - MIDEM.
Published quarterly (march, june, september, december) by Society for Microelectronics, Electronic Components and Materials - MIDEM.

Naslov uredništva
Headquarters
Uredništvo Informacije MIDEM
Elektrotehniška zveza Slovenije
Dunajska 10, 1000 Ljubljana, Slovenija
tel.: +386 (0)1 5112 221
fax: +386 (0)1 5112 217
Iztok.Sorli@guest.arnes.si
http://paris.fe.uni-lj.si/midem/journal.htm

Letna naročnina znaša 12.000,00 SIT, cena posamezne številke je 3000,00 SIT. Člani in sponzorji MIDEM prejemajo Informacije MIDEM brezplačno.
Annual subscription rate is DEM 200, separate issue is DEM 50. MIDEM members and Society sponsors receive Informacije MIDEM for free.

Znanstveni svet za tehnične vede I je podal pozitivno mnenje o reviji kot znanstveno strokovni reviji za mikroelektroniko, elektronske sestavne dele in materiale. Izdajo revije sofinanci rajo Ministrstvo za znanost in tehnologijo in sponzorji društva.
Scientific Council for Technical Sciences of Slovene Ministry of Science and Technology has recognized Informacije MIDEM as scientific Journal for microelectronics, electronic components and materials.
Publishing of the Journal is financed by Slovene Ministry of Science and Technology and by Society sponsors.

Znanstveno strokovne prispevke objavljene v Informacijah MIDEM zajemamo v podatkovne baze COBISS in INSPEC.

Prispevke iz revije zajema ISI ® v naslednje svoje produkte: Sci Search® , Research Alert® in Materials Science Citation Index™

Scientific and professional papers published in Informacije MIDEM are assessed into COBISS and INSPEC databases.

The Journal is indexed by ISI® for Sci Search®, Research Alert® and Material Science Citation Index™

Po mnenju Ministrstva za informiranje št.23/300-92 šteje glasilo Informacije MIDEM med proizvode informativnega značaja, za katere se plačuje davek od prometa proizvodov po stopnji 5 %.

Grafična priprava in tisk
Printed by
BIRO M, Ljubljana

Naklada
Circulation
1000 izvodov
1000 issues

Poštnina plačana pri pošti 1102 Ljubljana
Slovenia Taxe Percue

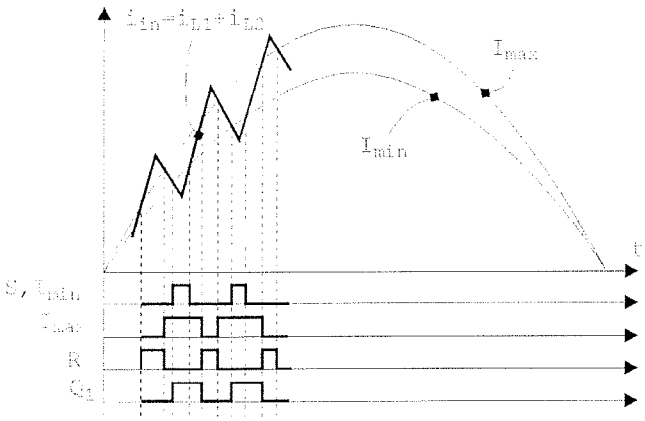

Fig. 6: The boost mode hysteresis control.

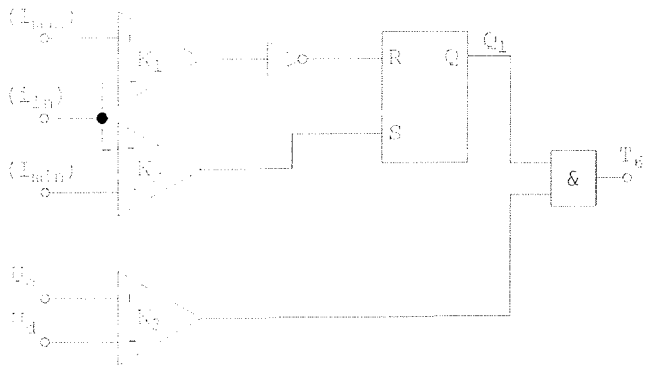

Fig. 7: The boost mode hysteresis controller.

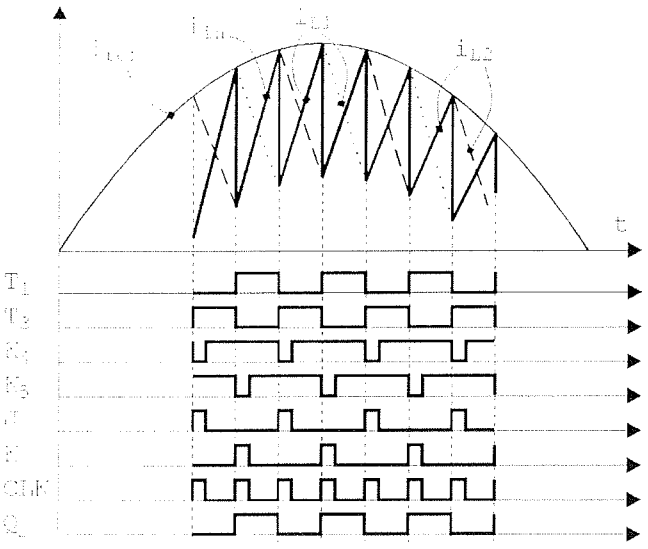

Fig. 8: The double-buck mode hysteresis control.

From Figs. 4 and 8, the double-buck converter operation can be described. When the current from the first converter, composed of transistor T_3 and inductance L_2 reaches the sinusoidal current reference value, then this transistor switches OFF and the transistor T_1 from the second converter switches ON. The current through T_3 is instantly zero and the current through inductance L_2 and diode D_4 is decreasing. At the same time, the current through transistor T_1 is increasing and when the current reaches the sinusoidal current reference, transistor T_1 switches OFF and the whole procedure is repeated. The above description can be summarized in the timing diagrams, of Fig. 8.

This time sequences help us to design the double-buck hysteresis controller (Fig. 9).

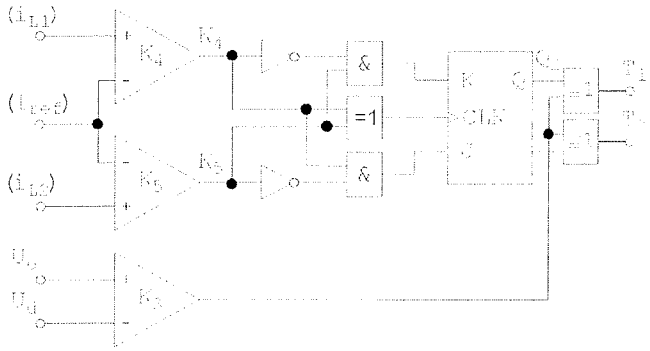

Fig. 9: The double-buck hysteresis controller.

As derived from the above description, when the converter is operated in double-buck mode, the input current i_{in} does not reach a zero value. This means that in the double-buck converter structure the continuous input current operation mode has been achieved. Actually there are some commutation problems when current goes from transistor T_1 to transistor T_3 but, appropriate snubber circuit design will make this problems negligeable.

3.1.3 The current reference module

As follows from the above description, the current controller needs three current reference values. Two of them are needed by the boost part of the converter and the third one is required by the double-buck converter part.

The current reference module provides to the current controllers the apropriate current references. At the output U_d the circuit provides the information to the comparator K_3 which will decide which converter will operate. Regarding the circuit in Figs. 7 and 9, the references $U(I_{max})$ and $U(I_{min})$ will be active when the boost structure has been chosen and the reference $U(I_{ref})$ will be active when the double-buck structure has been chosen.

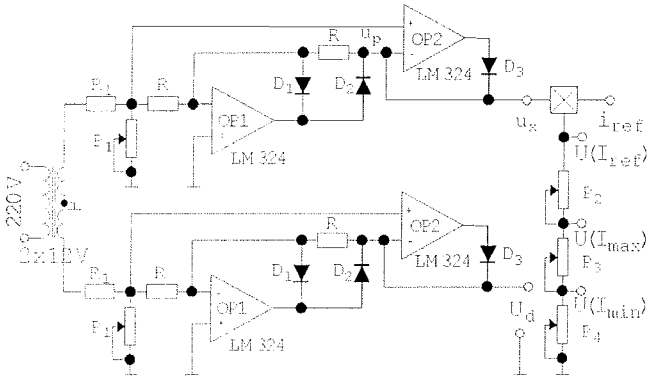

Fig. 10: The current reference module.

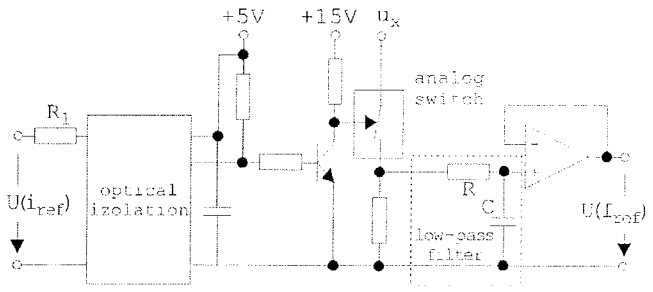

Fig. 11: The PWM multiplier.

3.1.4 The multiplier

As it has been shown in Fig. 10, for generating appropriate "sinusoidal" current references the multiplier function should be organized. At the voltage controller output, the PWM signal of i_{ref} is available in its voltage form $U(i_{ref})$. This signal should be multiplied by a voltage "wave-shape" signal u_x. The multiplier function can be realized by using the circuit shown in Fig. 11.

The circuit consist of an analog switch which is controlled by a PWM signal from the digital voltage controller, and a lowpas filter. The signal $u_x U(i_{ref}) = U(I_{ref})$ shown in Fig. 12 can be described by Fourier series, as follows:

$$U(I_{ref}) = \frac{a_0}{2} + \sum_{k=1}^{\infty} a_k \cos k\omega t + \sum_{k=1}^{\infty} b_k \sin k\omega t \qquad (2)$$

The coefficients a_0, a_k and b_k, can be evaluated in the usual way:

$$a_0 = \frac{2}{T}\int_0^T U(I_{ref})dt$$

$$a_k = \frac{2}{T}\int_0^T U(I_{ref})\cos k\omega_0 dt \qquad (3)$$

$$b_k = \frac{2}{T}\int_0^T U(I_{ref})\sin k\omega_0 t\, dt$$

where $\omega_0 = 1/T$.

The low-pass filter in Fig. 11 causes that the spectrum higher harmonics will be rejected because its cut-off frequency is much higher than the frequency of u_x which can be described as follows:

$$u_x = \hat{U}_x \sin \omega t\,, \qquad (4)$$

where $\omega = 2\pi f = 314.159$ rad/s. Because of that, only coefficients a_0 will be identified. Regardig the time diagrams in Fig. 12 for a_0 coefficients yields:

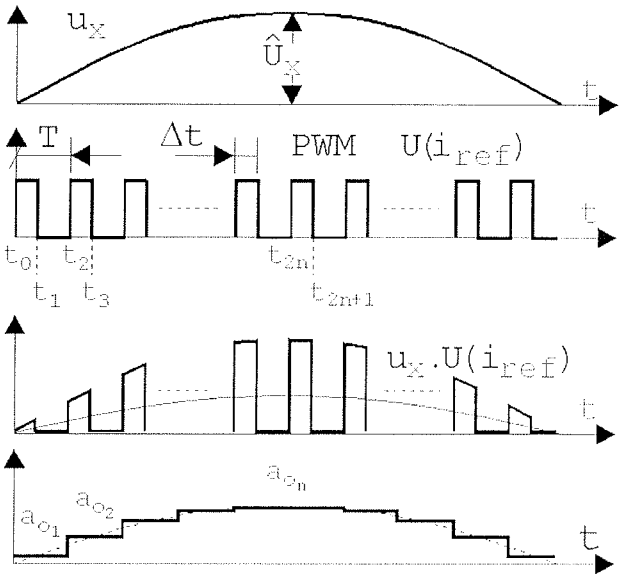

Fig. 12:The PWM multiplier timing diagrams.

$$a_{0_1} = \frac{2}{T}\int_{t_0}^{t_1} \hat{U}_x \sin \omega t\, dt$$

$$a_{0_2} = \frac{2}{T}\int_{t_2}^{t_3} \hat{U}_x \sin \omega t\, dt \qquad (5)$$

$$a_{0_n} = \frac{2}{T}\int_{t_{2n}}^{t_{2n+1}} \hat{U}_x \sin \omega t\, dt\,.$$

For coefficients a_{0n}, the next equation will be taken into consideration:

$$a_{0_n} = \frac{2}{T}\int_{t_{2n}}^{t_{2n+1}} \hat{U}_x \sin \omega t\, dt = \frac{2}{T}\int_{t_{2n}}^{t_{2n+\Delta t}} \hat{U}_x \sin \omega t\, dt\,. \qquad (6)$$

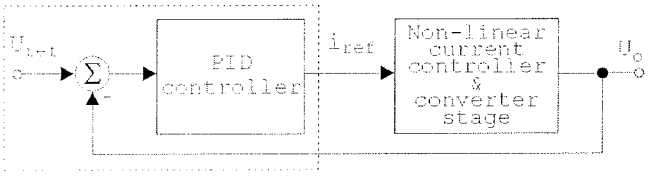

Fig. 13: The voltage control loop.

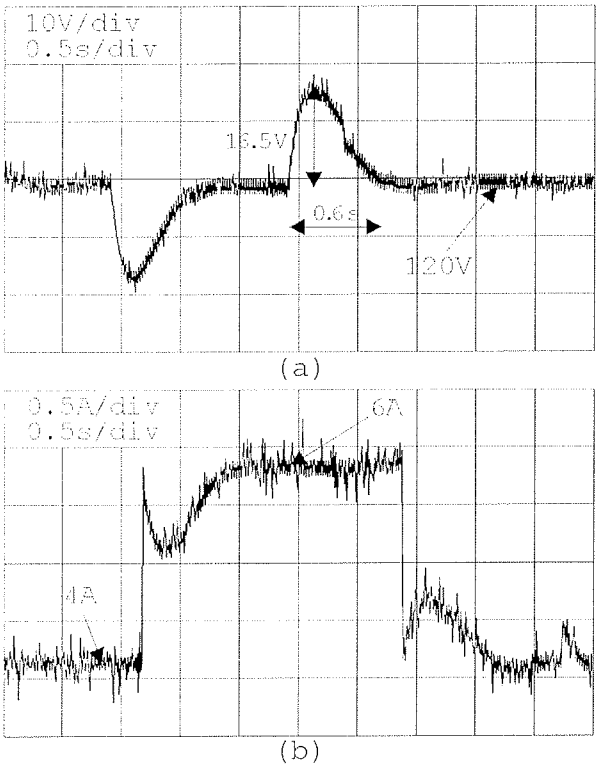

Fig. 14: Dynamic response to a resistive load change: (a) Voltage response; (b) Current response.

After soloving (6), it follows:

$$a_{0_n} = \frac{2\hat{U}_x}{\omega T} A \sin(\omega t_{2n} + \varphi), \qquad (7)$$

where:

$$A = \sqrt{2}\sqrt{1-\cos(\omega\Delta t)}, \quad \tan\varphi = \frac{\cos(\omega t\Delta t)-1}{\sin(\omega t\Delta t)}.$$

Because Δt is a small quantity tan φ approaches to zero and coefficient a_{0n} has a maximum value when sin (ω t_{2n}) is the unity. Then, (7) becomes:

$$a_{0_n} = \frac{2\hat{U}_x}{\omega T}\sqrt{2}\sqrt{1-\cos(\omega\Delta t)}. \qquad (8)$$

After first order Taylor expansion of the expression under the square root, it follows:

$$a_{0_n} = \frac{2}{T}\hat{U}_x\Delta t. \qquad (9)$$

The result is the product of signals u_x andΔt multiplied by factor 2/T. Signal Δt is proportional to i_{ref} ($\Delta t = K\, i_{ref}$).

3.2 The voltage control

The voltage control function has been realized by using digital signal processing. The risc microcontroller unit SH7032 has been used. The block diagram of the voltage control loop is shown in Fig. 13.

The non-linearity in the inner current loop causes that the clasical modeling methods as injected-absorbed current method or state space averaging method are not appropriate for modeling the double-buck and boost converter. Because of that, the auto-regressive identification method (AR-method) has been used /6/. The AR-method was based on the measured results. The output voltage to input reference current transfer function was estimated in the different operating points. For the controller design the worst case dynamic response has been taking into consideration. In Fig. 14(a) and (b) the dynamic response when the resistive load was changed from 30 Ω to 20 Ω and to 30 Ω afterwards is shown. The dynamic response to a step voltage reference change is shown in Fig. 15.

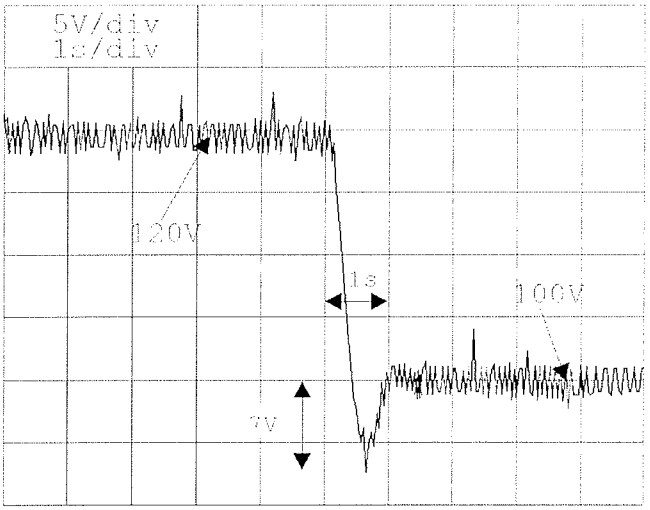

Fig. 15: Dynamic response to a step reference voltage change.

4 Unity power factor rectification - experimental results

The double buck and boost converter has been built with the aim of getting a good unity power factor of rectifier operation. Such control approach of this converter structure enables the converter operation with PF close to unity.

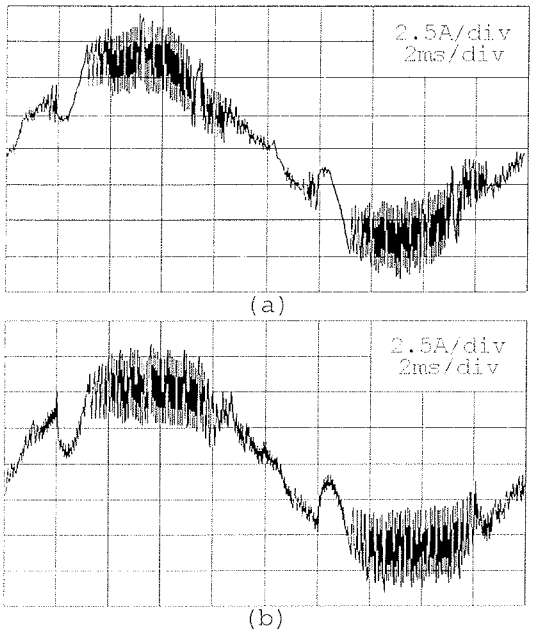

Fig. 16: The double-buck and boost rectifier input current: (a) Supplied by laboratory voltage source 220 V_{rms}; (b) Supplied by mains 220 V_{rms}.

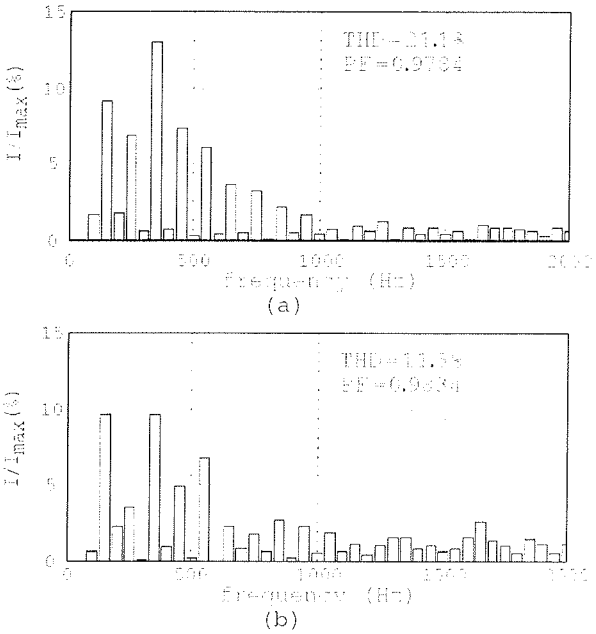

Fig. 17: The double-buck and boost rectifier input current spectrum: (a) Supplied by laboratory voltage source 220 V_{rms}; (b) Supplied by mains 220 V_{rms}.

In Figs. 16(a) and 16(b) the input current waveforms are shown when the double-buck and boost rectifier has been supplied by the laboratory voltage source and mains voltage source repectively. The current "drop" which appears, when the converter changes the operation mode from the boost to the buck mode, is consequence of the fact that, during the boost operation mode, the currents through inductances L_1 and L_2 are half of the current of inductor L_3 which, in term as the starting current of the buck converter.

The spectrum of the currents in both cases are shown in Figs. 17(a) and (b). The THD factors could be improved by the filter in the input line. The power factor meets the IEC standard requirements.

5 Conclusion

The experimental results show that it is possible to explote the double-buck and boost rectifier circuit to improve the unity power factor rectification. From the control point of view, this structure is a non-linear plant and the current controller solves this non-linearity problem. The experimental results have also demonstrated that this converter can operate in the required mode. Such converter is appropriate for telephone exchange power supply units where the current-sharing technique are required.

References

/1/ D.J.Perreault,R.L.Selders,J.G.Kassakian,"Frequency - Based Current-Sharing Technique for Paralleled Power Converters", Conference Record of the 28th IEEE PESC´96, Baveno-Italy, pp. 1073-1079, Jun. 1996.

/2/ J.Chen, C.Chu, "Combination Voltage-Controlled and Current-Controlled PWM Inverters for UPS Parallel operation", IEEE Transaction on Power Electronics, Vol. 10, No. 5, Sept. 1992.

/3/ J.G.Kassakian, "High Frequency Switching and Distributed Conversion in Power Electronic System", Proceedings of the 6th PEMC´90, Budapest 1990.

/4/ J.G.Kassakian, M.F.Schlecht, G.C.Verghese, "Principle of Power Electronics", Addison-Wesley, 1991.

/5/ J.Kolar, F.C.Zach, N.Mohan, C.R.Kamath, "Self-adjusting Input Current Ripple Cancellation of Coupled Parellel Connected Hysteresis-Controled Boost Power Factor Corrector", Conference Record of the 27th IEEE PESC´95, Atlanta-USA, Jun. 1995.

/6/ J.G.Proakis, D.G.Manolakis, "Introduction to Digital Signal Processing", Macmillan Publishing Company, New York 1988.

dr. Miro Milanovič, univ.dipl.inž.
Andrej Roškarič, univ.dipl.inž.

Univerza v Mariboru
Fakulteta za elektrotehniko,
računalništvo in informatiko
Smetanova 17, 2000-SI Maribor
Slovenija

mag. Milan Auda, univ.dipl.inž.
Srednja elektro računalniška šola Maribor
Smetanova 6, 2000-SI Maribor
Slovenija

Prispelo (Arrived): 05.03.00 *Sprejeto (Accepted): 25.04.00*

TEHNOLOŠKO PREDVIDEVANJE: INSTRUMENT NABORA DRUŽBENO IN GOSPODARSKO RELEVANTNIH VSEBIN RAZISKOVANJA

Miloš Komac
Ministrstvo za znanost in tehnologijo RS,
Ljubljana, Slovenija

Ključne besede: tehnološko predvidevanje, ključne tehnologije, Delfi metoda, scenariji, paneli, megatrendi

Povzetek: Vse več držav se pri snovanju raziskovalne politike, poleg zagotavljanja svobode izbire vsebine raziskovanja, odloča tudi za tim. s strani države usmerjano raziskovanje. V obeh primerih pa se pri izboru projektov in programov vse bolj uveljavlja sistem raziskovalnih prioritet. Ne gre le za družbeno relevantne teme kot so npr. okolje, zdravje, izobraževanje itd., temveč tudi za teme, ki so osnova tehnološkega razvoja. V ta namen se vlade pogosto odločajo za spodbujanje procesa tehnološkega predvidevanja, ki skuša izluščiti iz dolgoročnih napovedi tehnološkega razvoja na globalnem nivoju tiste tehnologije, ki bodo zagotavljale konkurenčno sposobnost domače industrije. V članku so predstavljene običajno uporabljane tehnike predvidevanja s primeri ter tudi bistveni kritični pogledi.

Technology Foresight: a Convenient Tool for the Prioritization of Scientific Research

Key words: technology foresight, key technologies, Delphi method, scenario writing, expert panels, megatrends

Abstract: Technology foresight process is usually undertaken by national authorities in order to stimulate the inclusion of forward looking approach into the science and technology policy planning toolbox. For small countries such as Slovenia, outcomes of the foresight exercise could present a convenient tool in determining research priorities. In the present article the most important methodologies which could be employed in foresight exercise are described and illustrated by examples. In addition, some reasons for the possible failure of the foresight exercise are also mentioned.

1. Uvod

Tehnološko predvidevanje (Technology Foresight) je po definiciji, ki se je izoblikovala zlasti v obdobju zadnjih desetih let, postopek, s pomočjo katerega se skuša izluščiti najbolj verjetne smeri dolgoročnega tehnološkega razvoja, upoštevaje predvsem globalne trende razvoja znanosti in tehnologije, seveda pa tudi lokalno specifiko. Na nivoju države lahko izsledki tehnološkega predvidevanja usmerjajo izobraževalno, znanstveno, tehnološko in industrijsko politiko ter s tem posledično predstavljajo temeljna izhodišča bodočega družbenega in gospodarskega razvoja.

Tehnološko predvidevanje ne more napovedati bodočnosti, lahko pa nas opozarja na izzive bodočnosti, pomaga nam odkrivati naše prednosti in slabosti, usmerja naše akcije danes, da bi lahko izzive in priložnosti bodočnosti znali izrabiti v svojo korist.

S stališča oblikovalcev znanstvene politike je seveda tehnološko predvidevanje (TP) zelo prikladen pripomoček za določanje prednostnih usmeritev, še posebej, ker temeljijo rezultati TP na konsenzu precej širokega spektra sodelujočih. Kljub temu akademska raziskovalna sfera, vsaj tako kažejo izkušnje iz drugih držav, na TP praviloma ne gleda z naklonjenostjo, ker na nek način pač omejuje svobodo raziskovanja, kar je v bistvu v nasprotju s temeljnim poslanstvom znanosti. Še posebej se to opaža v državah v tranziciji, saj tehnološke prioritete dodatno vse preveč spominjajo na plansko gospodarstvo in je zato TP tudi v gospodarskih krogih v glavnem, vsaj dokler se zadeve ne razčistijo, sprejeman z rezervo. Zato je že na začetku tega prispevka potrebno ugotoviti, da sta obe dilemi odveč. Svoboda znanstvenega raziskovanja ostaja neokrnjena, država si pač jemlje pravico, da bo vlagala več v bolj uporabno usmerjene cilje temeljnega raziskovanja (tim. anglo-saksonska paradigma znanstvene politike), gospodarstvo pa se mora tudi zavedati, da so določene tehnologije bolj, druge pa manj primerne za Slovenijo. Za ministrstvo, ki je pristojno za tehnološki razvoj, je torej samoumevno, da se prvenstveno spodbujajo tehnologije, ki so npr. ekološko in energetsko sprejemljive, da o obetu visoke dodane vrednosti sploh ne govorimo.

Na vsak način pa se ne da izogniti občutku, da postaja TP neke vrste modna zadeva, da se ga iz tega razloga (dejansko pa na pobudo EU) lotevamo tudi v Sloveniji in bo rezultat dokument, v katerega bo sicer vloženega veliko dela, bo pa, kot mnogo drugih, končal v predalu. Mnenje avtorja tega prispevka je, da bo odločilnega pomena, poleg seveda politične odločitve za TP, podpora podjetniške sfere in pa tistega dela raziskovalcev, ki razumejo in sprejemajo zgoraj omenjeno anglo-saksonsko paradigmo znanstvene politike.

2. Tehnike predvidevanja

Kljub skeptičnim ugotovitvam, da gre lahko za modno zadevo pa ima tehnološko predvidevanje za sabo že kar nekaj zgodovine in temu primerno so se razvile tudi različne tehnike TP. Na nivoju predvidevanja, ki ga namerava izvesti Ministrstvo za znanost in tehnologijo RS si velja pobližje ogledati naslednje metodologije:

- Ključne tehnologije
- Delfi metoda

- Metoda scenarijev
- Ekspertni paneli

2.a. Ključne tehnologije

Metoda korenini v ZDA, kjer različne institucije (npr. The Rand Corporation, Battelle, Department of Defence) razmeroma redno objavljajo spisek tehnologij, ki bodo ključnega pomena čez 10-20 let. Za Slovenijo je morda zanimiv neke vrste mini TP, ki ga je po tej metodi v letih 1994-1996 izvedla privatna raziskovalna ustanova Fondazione Rosselli na pobudo (zlasti velikih) gospodarskih družb in pripravila nabor tehnologij pomembnih za razvoj in dvig konkurenčne sposobosti italijanske industrije /1/. Tehnološka področja so bila razdeljena na tim. družine, le te pa ocenjene glede na »privlačnost« (npr. nova delovna mesta, vpliv na okolje, prodor na nove trge) in izvedljivost (npr. znanstvena in tehnološka infrastruktura). Ugotovljeno je bilo, da je aktualnih sedem tehnoloških področij - novi materiali, mikroelektronika, informacijske tehnologije, mikrosistemi, software, biotehnologija, proizvodne tehnologije – ter da se cca 25 % znanja nahaja še v fazi temeljnega raziskovanja, enakega obsega pa naj bi bila tudi ekonomska eksploatacija v letu 2004.

Na področju novih materialov so bile kot ključne identificirane sledeče družine:
- kovine, keramika in kompoziti za konstrukcijske aplikacije,
- polimeri in polimerni kompoziti,
- magnetni materiali,
- optoelektronski materiali,
- biokompatibilni materiali,
- materiali za embalažo,
- tehnologije za recikliranje materialov.

Na področju mikrolektronike so bile kot ključne identificirane sledeče družine:
- VLSI proizvodni procesi,
- VLSI načrtovalni procesi,
- VLSI arhitekture,
- mikroelektronski močnostni sistemi,
- visokofrekvenčne heterostrukture,
- kvantne in nanostrukture,
- visokotemperaturni superprevodniki.

Tudi v Sloveniji beležimo poizkus nabora ključnih tehnologij, ki ga je leta 1995 na pobudo MZT izvedel M. Kos s sodelavci /2/, pri čemer je služila kot izhodišče študija o ključnih tehnologijah, ki jo je izdelal Fraunhofer Institut fuer Innovations- und Systemforschung /3/. Ocenjevalci so izbrali 18 meril, od katerih jih je 7 ocenjevalo okvirne pogoje, 11 pa prispevek tehnologije k gospodarskim, socialnim, strateškim in tržnim rešitvam. Poleg nabora tehnologij, se da iz sklepov povzeti pravzaprav pričakovano dejstvo, da se slovensko gospodarstvo, pa tudi država premalo zavedata, da raziskave in razvoj odločujoče krojijo usodo gospodarstva in končno naroda v celoti in da bi bilo treba bistveno odločneje usmerjati sredstva v tiste vsebine raziskovanja, ki so podlaga razvoju novih tehnologij in bodo s tem vplivale na konkurenčni položaj slovenskega gospodarstva v začetku 21. stoletja. Čeprav je bilo predvideno, da projekt ne bi bila enkratna akcija ampak ponavljajoč proces, se to na žalost ni zgodilo, ker vsaj po mnenju avtorja tega prispevka ni bilo ustrezne politične podpore.

Kritiki metode ključnih tehnologij predvsem izpostavljajo, da preveč poudarja pomen tehnologije, premalo pa upošteva širše družbeno-ekonomske vidike razvoja.

2.b. Delfi metoda

Metoda /4/ temelji na vprašalnikih, ki jih za posamezno področje sestavijo ekspertne skupine, na njih pa se odgovarja v več »rundah«, s ciljem priti do odgovorov, temelječih na vnaprej domenjeni stopnji konsenza udeležencev. Torej gre za neke vrste virtualno interakcijo, pri čemer je anonimnost udeležencev zajamčena. Osnovna filozofija podpore tej metodi je, da je s konsenzom doseženo mnenje določene skupine ekspertov bolj zanesljivo kot pa nabor individualnih mnenj. Rezultati te metodologije so običajno: predvideni časovni okviri realizacije določene tehnologije, bistvene ovire za realizacijo, pomembnost za državo itd.

Kot kritične pripombe na Delfi metodologijo se največkrat omenjajo:

- gre za delovno zelo intenzivno in časovno razmeroma dolgotrajno proceduro,
- s številom rund zanimanje za sodelovanje močno upada,
- težnja k konvergenci mnenj gre v glavnem na škodo neupoštevanja manjšinskih, vendar zanimivih mnenj.

Delfi metoda zahteva razpoložljivost izredno številnega strokovnega kadra, zato jo v glavnem uporabljajo velike države (npr. Japonska, Nemčija, Velika Britanija), veliko redkeje manjše (npr. Avstrija, Madžarska), ki pa se zato poslužujejo svoji specifičnosti prirejenih že obstoječih vprašalnikov. Tudi pri izvedbi prve Delfi študije v Nemčiji se je uporabilo japonske vprašalnike.

Za ilustracijo v nadaljevanju navajam primere vprašanj s področja materialov iz zadnje nemške Delfi študije. Odgovoriti je bilo potrebno na naslednja vprašanja (v oklepaju so navedeni tudi razpoložljivi odgovori):
- osebna ocena poznavanja ožje stroke (dobro, srednje, slabo),
- ocena pomembnosti teme za: splošno širitev znanja; gospodarski razvoj; družbeni razvoj; reševanje okoljevarstvenih problemov; zaposlovanje; na sploh nepomembno,
- predviden časovni okvir realizacije, vključujoč tudi možnost, da je zadeva neizvedljiva,
- država z najbolj razvitim RR potencialom na tem konkretnem področju (ZDA, Japonska, Nemčija, druga država iz EU, druga država izven EU),
- potrebni ukrepi (boljše izobraževanje, pospeševanje sodelovanja gospodarstva z akademsko raziskovalno sfero, pospeševanje mednarodnega sodelovanja, izboljšava RR infrastrukture, vključevanje

večjega števila finančnih akterjev, sprememba zakonodaje, drugo),
- kje so učinki lahko tudi problematični (okolje, državna varnost, družbeni aspekti, drugo).

Primeri vprašanj (v oklepaju je navedeno najbolj verjetno leto do katerega naj bi bila zadeva realizirana):
- razviti bodo organski superprevodniki s temperaturo prehoda 77K (2017),
- ogljikov nitrid s trdoto višjo od trdote diamanta se bo začel uporabljati kot visoko zmogljiv visokotemperaturni polprevodnik (2013),
- razviti bodo magnetni materiali z nasičeno magnetizacijo višjo od 3T (2009),
- v praksi se bodo pričeli uporabljati organski feromagnetni materiali (2016),
- v praksi se bodo pričeli uporabljati polimerni materiali z enako električno prevodnostjo pri sobni temperaturi kot jo ima baker (2015),
- razviti bodo samoregenerirajoči polimeri (2022),
- rešeni bodo tehnični problemi v zvezi s proizvodnjo elektronskih komponent na osnovi Si-Ga-As tehnologije (2008),
- razvite bodo mikrosistemske tehnike, ki bodo omogočale izdelavo struktur z dimenzijami do 10 nm (2010),
- razvit bo superprevodni material s temperaturo prehoda pri sobni temperaturi (2022),
- razvita bo tehnika, ki bo neodvisno od vrste materiala omogočala heteroepitaksijo na silicijevih rezinah (2010),
- na razpolago bodo večplastne sončne celice z izkoristkom pretvorbe energije nad 50% (2020),

Izbrane so bile predvsem take teme, ki so zanimive za bralce časopisa INFORMACIJE MIDEM. V celoti je poglavje »Materiali« obsegalo 104 teme. Več o pričujoči študiji je dosegljivega tudi preko interneta /5/.

2.c. Metoda scenarijev

Metodo še najbolje predstavlja definicija, da gre v bistvu za organizacijo lahko tudi nasprotujočih si informacij o možnem razvoju dogodkov v bodočnosti, s tem pa so avtorji potisnjeni v izdelavo alternativnih vizij, oziroma stalno je potrebno imeti pred očmi neke vrste samoumevnost nepredvidljivih dogodkov. Po drugi strani pa se metodi očita, da obstaja nevarnost, da predvidi samo en možen razvoj dogodkov, da ostaja na pretežno generalnem nivoju in zato ni posebej operativna. Po mnenju avtorja je bila v Sloveniji metoda scenarijev uporabljena pri izvedbi študije Slovensko kmetijstvo in Evropska unija/6/.

2.d. Metoda ekspertnih panelov

Vključevanje ekspertnih panelov, ki so vsebinsko strukturirani po tehnološkem in/ali sektorskem ključu je običajno za praktično vse do sedaj izvedene TP, pa tudi tiste, ki še tečejo. Pravzaprav ne gre za samostojno metodologijo, temveč za neke vrste podporo ostalim tehnikam. Res pa je, da vse bolj prevladuje mnenje, da je TP preko panelov (seveda z ustrezno informacijsko in analitsko podporo), primerno zlasti za majhne sisteme (kot je npr. Slovenija), ker za delovanje zadostuje tudi manjše število strokovnjakov. Še posebej pa delo v panelih močno spodbuja dialog širokega spektra članov panelnih skupin, posledično so na ta način izsledki dela dostopni razmeroma široki publiki, delo v panelih z neposrednimi konfrontacijami različno mislečih spodbuja toleranco in kreativno razmišljanje ter je močno orodje mrežnega povezovanja. Pasti pa sta v glavnem dve. Možna je prevlada mnenj močnih osebnosti ali pa obratno, da so člani panelne skupine preveč uglašeni in se s tem poruši načelo nepristranosti. Zato je sestavljanje panelnih skupin izredno zahtevna naloga. Izkušnje kažejo, da vsekakor ne gre izključevati tako ali drugače spornih oseb, pod pogojem seveda, da zadoščajo kriterijem strokovnosti. Kot pozitivna izkušnja iz dela panelov TP v Veliki Britaniji pa se omenja posledično bistveno večja stopnja sposobnosti dialoga in povezovanja na relaciji akademska raziskovalna sfera – industrijski razvoj. Ker se bomo v slovenskem TP najverjetneje odločili za sistem panelov, navajam kot primer strukturiranje panelov švedskega TP:
- Medicina in javno zdravstvo,
- Biološki naravni viri,
  - kmetijstvo in gozdarstvo
  - voda
  - hrana
  - papir in celuloza
  - lesni proizvodi
  - surovine za bio-maso
- Komunalna infrastruktura,
  - stanovanje
  - urbanizem
  - transport in logistika
  - oskrba
  - regionalni razvoj
- Proizvodne tehnologije in sistemi,
  - Informacijski in komunikacijski sistemi,
  - Materiali in procesi,
  - funkcijski in konstrukcijski materiali
  - procesna tehnika
  - recikliranje
  - kemijsko inženirstvo
- Storitve,
  - mediji
  - trgovina
  - finance
  - zavarovalništvo
  - prosti čas
- Izobraževanje.

V Sloveniji bomo seveda morali najti strukturo panelov, ki bodo odsevali naše karakteristike. Opozoriti pa velja, da praktično pri vseh TP opažamo odstopanje od čisto tehnoloških tem ter da stopajo v ospredje tudi družbeno relevantne teme. Posledično se tudi TP vse pogosteje naslavlja samo kot »Predvidevanje«.

3. Megatrendi

Nekatere države, npr. Avstrija, Nemčija in Nova Zelandija so pri izvedbi svojih TP izhajale iz predvidevanja širših družbenih in ekonomskih gibanj, ki presegajo okvire držav samih, se bodo pa seveda odslikavali na lokalnem nivoju. V Avstriji npr. se večina vprašanih strinja, da bo upravljanje s prometom najkasneje v 15 letih bolj pomembno kot same tehnične rešitve; enako kot Nemci pa se strinjajo, da bodo visoko industrializirane države trajno soočane z visoko stopnjo brezposelnosti, prav tako pa se oboji tudi strinjajo, da bodo naraščajoči okoljski problemi vse bolj vplivali na zdravje prebivalstva.

V Novi Zelandiji so identificirali sedem globalno relevantnih tem in iz njih izluščili megatrende za nacionalno TP diskusijo. Tako predvidevajo:

- znatne spremembe v sistemih ustvarjanja novega znanja in njegovega razširjanja,
- informacijske tehnologije, genetika, biotehnologija, energetika ter materiali in procesi bodo tista področja, kjer bodo tehnološki preboji največji in tudi najpomembnejši,
- vse večjo relevanco okoljskih problemov (biodiverziteta, voda, odpadki, klimatske spremembe, ozonska luknja),
- naraščajoče družbene probleme (staranje prebivalstva, socialna izključenost, organiziran kriminal in terorizem, bolezni in epidemije).

Skozi te megatrende se predvidevanje vse bolj dviguje na nadnacionalni nivo. V primeru EU je potrebno omeniti dve študiji. Prva, Scenarios Europe 2010 /7/, pri njej je sodelovalo 15 direktoratov, predstavlja več možnih makro scenarijev razvoja EU, vključno z vplivom možnega razvoja dogodkov na proces širjenja. Druga študija, ki je tik pred zaključkom, je Projekt FUTURES /8/ (uporabljena je bila metoda panelov), katerega cilj je definiran kot »identifikacija problemov, izzivov in priložnosti, s katerimi se bo srečala Evropa v prihodnjih desetih letih«; kajti, kot je dejal J.M.Cadiou, direktor Joint Research Centre inštituta, ki je koordinator projekta, »bo po vsej verjetnosti naslednjih deset let obdobje največjih sprememb v zgodovini Evrope v mirnem času«. Osnovne teme Projekta FUTURES so tehnološka konkurenčnost Evrope, problem zaposlovanja oz. odpiranja novih delovnih mest, starajoče prebivalstvo, mobilnost na segmentih dodiplomskega in podiplomskega študija in podoktorske specializacije, širitev EU, zagotavljanje virov za pokrivanje stroškov delovanja socialne družbe. S stališča TP sta zanimivi predvsem tehnološka konkurenčnost in mobilnost. Evropa v povprečju tehnološko zaostaja za ZDA na praktično vseh razvojno pomembnih tehnologijah, medtem ko je z Japonsko trenutno še primerljiva; res pa je, da na določenih segmentih kot so npr. mobilne komunikacije, razvoj zdravil, senzorji/aktuatorji, izkazuje izrazite prednosti, drugje, kot npr. fotovoltaika, umetna inteligenca, keramični materiali pa slabosti. Glede mobilnosti študija z žalostjo ugotavlja, da je nizka, precej mladih talentov se odloča za zaposlitev v ZDA, medtem ko je obratni tok zanemarljiv, kar pomeni, da bo potrebno evropsko RR sceno narediti bolj privlačno za mlade strokovnjake iz prekomorskih dežel.

4. Kritični pogledi na TP

Podobno kot ima TP mnogo zagovornikov ne manjka tudi kritičnih pogledov, ki se jih da povzeti v sedmih točkah /9/:

TP pogosto izhaja iz predpostavke da bodo nove tehnologije popolnoma zamenjale stare, in to v razmeroma kratkem času. V resnici pa tekmujoče tehnologije koeksistirajo tudi skozi daljša obdobja.

Pogosto je prisotno prepričanje, da bodo nove tehnologije rešile stare probleme oziroma izpopolnile obstoječe tehnološke sisteme. V resnici pa nove tehnologije pretežno vodijo do popolnoma novih tehničnih rešitev.

TP obravnava tehnološki razvoj zelo ozko segmentirano. Praksa pa kaže, da največje razvojne možnosti običajno nudijo kombinacije različnih tehnologij in znanj.

Izvajalci TP so pogosto »ujeti« v svoj čas, kar posledično vodi do zmotnega prepričanja, da bodo velike teme sedanjosti tudi velike teme prihodnosti.

Za večino TP je značilno, da se preveč poudarja pomen tehnologije, zanemarjajo pa se ekonomski pokazatelji. Na kratko, pogreša se cost/benefit analiza.

Poleg ekonomike so seveda tudi drugi vrednostni sistemi, ki vplivajo na sprejemljivost novih tehnologij in ki jih TP običajno tudi ne upošteva.

Podlaga mnogih TP študij so lahko tudi pomanjkljive informacije. Ne sme se pozabiti, da veliko znanstvenih raziskovanj in tehnološkega razvoja poteka pod oznako »strogo zaupno« (npr. vojaške raziskave).

5. Zaključek

Glede na število držav, ki so se odločile, da iz določenega razloga pristopijo k TP, vse pogosteje pa kar k integralnemu predvidevanju, seveda vsaka s svojimi specifičnimi izhodišči, cilji in nameni, lahko ugotovimo, da vendarle ne gre za modni pojav, ampak za enostavno nujo, saj smo se znašli v času, ko se turbulentno spreminjajo pravila igre na vrsti vitalnih segmentov določene družbe. Mnogi strokovnjaki zagovarjajo stališče, da bo kontinuiteta sprememb neke vrste permanenten pojav v celotnem 21. stoletju. Pa tudi če temu ne bo tako, se ne da napovedati kako dolgo bodo te turbulence trajale, preden se bo – če se seveda sploh bo – situacija umirila in se bo ustalil določen ekonomski in družbeni red, ki bo zagotavljal dolgoročno preglednost. Proces predvidevanja tako »pod nujno« usmerja našo pozornost na prihodnost in nas seveda tudi, kot majhen gospodarski sistem, opozarja na pomen sposobnosti fleksibilnega odzivanja. Poudarjam pa, ne na osnovi ad hoc odločitev, katerih podlaga bi bila trenutno aktualna politika, temveč tudi na osnovi TP, ali pa kar integralnega predvidevanja, ki z variantami s konsenzom sprejetih scenarijev omogoča zadosti široko strokovno oporo nosilcem odločanja.

Te vrste razmišljanje je vodilo Ministrstvo za znanost in tehnologijo, da v predlog programa Vlade RS podpore gospodarskim družbam pri razvoju novih tehnologij in

vzpostavljanju in delovanju njihovih razvojnih enot v obdobju 2000 – 2003 vključi tudi izvedbo TP. Rezultati TP se bodo morali, če bo le zadosti politične volje, odražati v sistemu financiranja temeljnega in aplikativnega raziskovanja, konkretno v dajanju prednosti raziskavam, ki so osnova propulzivnih, za Slovenijo relevantnih tehnologij bodočnosti.

6. Literatura

/1/ C. Roveda, Technology Foresight in Italy, Rosselli Foundation Report, 1996.

/2/ M. Kos, Tehnologije za 21. stoletje, Gospodarski vestnik, št.13, 1997.

/3/ H. Grupp, Technologie am Beginn des 21. Jahrhunderts, Physica Verlag, Heidelberg, 1993.

/4/ H. A. Linstone, M. Turoff, Eds., The Delphi Method: Techniques and Applications, Addison Wesley, London, 1975.

/5/ www.futur.de

/6/ E. Erjavec, M. Rednak, T. Volk, uredniki, Slovensko kmetijstvo in Evropska unija, ČZD Kmečki glas, Ljubljana, 1997.

/7/ G. Bertrand, A. Michalski, L. Pench, Eds., Scenarios Europe 2010, EC, Forward Studies Unit, 1999.

/8/ www.futures.jrc.es

/9/ L. Olson, Technology Foresights Need to Look Backwards, The IPTS Report, No 43, April 2000.

Dr. Miloš Komac
Ministrstvo za znanost in tehnologijo
Trg OF 13
1000 Ljubljana

Tel: 386 (0)61 178 4600
Fax: 386 (0)61 178 4719
Email: milos.komac@mzt.si

Prispelo (Arrived): 15.05.00 *Sprejeto (Arrived): 25.05.00*

A STUDY OF PLANARIZING PROPERTIES OF THIN BPSG FILMS

R. Osredkar, Faculty of Computer Sciences and Faculty of Electrical Eng., University of Ljubljana, Slovenia,
and
B. Gspan, Repro MS, Ljubljana, Slovenia

Keywords: IC integrated circuits, microelectronic technologies, planarization processes, topography planarization, BPSG Boro-Phospho-Silicate Glasses, reliability

Abstract: In order to develop a reflow process for planarization of the IC device topography, the reflow angles and structural stability under the influence of humidity of BPSG films have been studied. It has been determined that for planarization purposes the optimal composition of a BPSG film is 3 weight % of boron and 4 weight % of phosphorus. At this composition the transition angles are not minimal, however, structural stability of such films is greatest.

Študija planarizacijskih lastnosti tankih BPSG plasti

Ključne besede: IC vezja integrirana, tehnologije mikroelektronske, procesi planarizacije površine, planarizacija topografije, BPSG stekla boro-fosfo-silikatna, zanesljivost

Povzetek: Z namenom, da bi za idelavo integriranih vezji razvili planarizacijski postopek na osnovi toka plasti borofosfosilikatnega stekla (BPSG) pri visoki temperaturi, smo proučevali nagnjenost nanešene plasti nad stopnico in njeno strukturno stabilnost pod vplivom vlage. Ugotovili smo, da je za planarizacijske namene najprimernejše steklo takšno, ki vsebuje 3 utežne odstotke bora in 4 utežne odstotke fosforja. Pri tej sestavi kot nad stopnico ni najmanjši, toda stabilnost filma je največja.

Introduction

Device planarization, i.e. reduction of distances between topography extremes in the direction normal to the wafer plane and reduction of the side wall slopes in order to facilitate subsequent processing steps, came to the technology forefront as lateral dimensions of ICs began to shrink. Planarization is most critical during the final steps of fabrication, when several metallization and dielectric layers are deposited, and is used primarily to enhance step coverage of these layers. Also, is considerably easier to image fine line geometries on nearly planar surfaces and to etch lithographic patterns into a flat film /1,2/.

There are several planarization techniques used in IC processing /3/. Physical methods include polishing, which is applied where perfect planarization is required, and also different techniques where planarization of existing dielectric layers is attempted by film reflow, etch–back of sacrificial layers etc. Fluidic planarization techniques utilize low viscosity of certain materials, e.g. photoresists, polyimides and spin on glasses, which can fill the trenches in wafer topography. These methods usually require low processing temperatures (below 400 °C) which is frequently advantageous. However, due to poor compatibility of the fluidic materials with the standard dielectric materials in ICs, the application of these methods frequently results in poor device reliability. Therefore, when high processing temperatures are not a consideration, deposition and reflow of doped glasses is still an attractive alternative. In this contribution results of a detailed study, concerning the degree of planarization and defect density, of such a planarization process for a 1.2 μm IC fabrication process is presented.

Experimental

Boron and phosphorus doped glass films (BPSG) were deposited on wafers in a PECVD reactor, Novellus Concept One PECVD System. During the deposition wafers are processed individually in a 6 step process which guarantees physical uniformity of the deposited layers. Silicon source in the process is silane (SiH_4), boron source diborane (B_2H_6), and phosphorus source phosphine (PH_3). Densification and reflow of the deposited films were performed in a Thermco diffusion furnace, according to standard procedures. The composition of resulting films was analyzed by Auger spectroscopy by Balzas Analytical Laboratory, Ca. USA, according to their laboratory specifications.

Transition angles between topography levels were measured directly by electron microscopy; a Hitachi, model 450, SEM was used for taking the micrographs. The number of defects in the deposited films was measured with a Tencor SurfScan, model 4500, surface analyzer.

Results and discussion

It is well known /1,4/ that the composition of the BPSG films critically determines their utilizable properties: addition of boron to phosphorus doped glass film (PSG) reduces the temperature required for the reflow of the film, on the other hand, boron doped glass films (BSG), which possess a conveniently low reflow temperature, are highly susceptible to damage by moisture, resulting in poor reliability of fabricated ICs. Optimization of a planarization process involving BPSG requires a careful balancing of these two tendencies. An optimal composition of the planarization film was sought in the range

of 2 – 4 weight percent of boron, and 3 – 5 weight percent of phosphorus in the film. In a preliminary study we have determined that a 650 nm thick BPSG film is sufficient for planarization of surfaces where topography extremes do not exceed 700 nm, and in our study films of this thickness have been used throughout. Deposition parameters and resulting film compositions, as determined by Auger spectroscopy, after a densification (30 min at 920 °C in H_2O vapor atmosphere) and reflow (30 min at 950 °C in oxygen atmosphere) are given in Table 1. All films were deposited at temperature 400 °C, pressure 293.3 Pa and RF power of 1 kW.

Table 1. Deposition parameters and film composition of BPSG films, deposited at temperature 400 °C, pressure 293.3 Pa and RF power of 1 kW, after densification (30 min at 920 °C in H2O vapor atmosphere) and reflow (30 min at 950 °C in oxygen atmosphere).

sample #	w. % B	w. % P	B_2H_6 (lpm)	PH_3 (lpm)	SiH_4 (lpm)
1.	3.1	4.5	0.51	0.49	0.20
2.			0.60	0.47	0.20
3.	2.4	5.4	0.40	0.61	0.20
4.			0.46	0.58	0.20
5.	2.5	3.2	0.40	0.37	0.20
6.			0.46	0.33	0.20
7.			0.32	0.47	0.20
8.	1.6	4.6	0.26	0.49	0.20
9.	2.8	4.4	0.40	0.49	0.20
10.	3.0	4.2	0.40	0.49	0.20

SEM cross-sections samples of planarized structures were treated by a short dip in the Hammond etchant /5/ to increase the contrast. The influence of humidity on the deposited films was determined by exposing films that have not been densified and reflowed to atmospheres of different relative humidity (RH) for different periods of time. The atmospheres were dry nitrogen gas, standard atmosphere in IC fabrication facilities (50 % RH at 21 °C), and atmosphere almost saturated with water vapor (90 % RH at 21 °C).

The degree of planarization, given by the transition angle measured between the normal to the wafer and normal to the sloped side wall of the transition region, was determined on two different test structures. The so called single stack structure is an array of 600 nm thick and 1,2 μm wide parallel aluminum lines formed on a flat, oxidized wafer; in the double stack structure the metal lines are formed on top of oxide lines of the same dimensions, resulting in a 1,2 μm step in topography. Both types of structures were prepared at two different separations of the lines, 1 μm and 2,5 μm (i.e. at spatial frequencies of 2,2 μm and 3,7 μm). The transition angle between the topography levels before the planarization has in all cases been close to 90 deg. The results are given in Table 2. Each number represents the average of measurements on 3 parallel samples and estimated error is around 7 %.

Effects of humidity on the number of defects of different sizes on a 6" wafer is given in Table 3. There is some ambiguity regarding the number of defects, as defects and particulate contamination can not be completely differentiated. An attempt has been made to determine particulate contamination by counting particles under an optical microscope in correspondingly correct the defect count. Complete differentiation could not be achieved, however, our results are in general agreement with published results /1/. From our results a trend regarding the distributions of the defect size with increasing exposure to humidity is apparent: with increasing exposure time the typical defect size is shifted to higher dimensions, implying, that the sizes of individual defects increase due to humidity. After densification and reflow the sensitivity of the film to the humidity is appreciably reduced and is of no further concern. Similar observations have been published elsewhere /6,7/.

On the basis of these results, the optimal composition of a planarization BPSG film has been determined, consisting of 3 weight % of boron and 4 weight % of phosphorus (corresponding to Sample no. 10). At this composition the transition angle between the levels in both kinds of structures is not minimal, however, structural stability of such films under the influence of humidity seems to be greatest. The densification and the reflow times of films prepared for our study are relatively long, which conceivably could be a consideration in their application in a standard production environment.

Table 2. Transition angles in single and double stack structures, after BPSG densification and reflow, at different film compositions.

sample #	w. % B	w. % P	transition angle (deg.)				average angle (deg.)
			line separation 1 μm		line separation 2.5 μm		
			double s.	single s.	double s.	single s.	
1	3.1	4.5	22.7	22.0	19.7	19.0	20.9
3	2.4	5.4	24.6	23.2	23.1	16.4	21.8
5	2.5	3.2	30.8	30.9	33.0	33.5	32.1
8	1.6	4.6	40.0	35.9	36.9	34.3	36.8
9	2.8	4.4	29.8	21.3	30.5	22.2	26

Table 3. Effects of humidity on the number of defects on a 6" wafer at different exposure times.

RH (%)	t (hours)	number of defects of size (in μm)			cumulative
		0.30 - 1.00	1.00 - 2.00	2.00 - 3.00	
90	0	1453	442	109	2004
90	0	2628	904	245	3777
50	0	4716	1324	412	6452
dry N_2	0	2738	823	267	3828
90	2	13627	3623	1569	18819
90	2	3630	687	302	4619
50	2	4627	934	337	5898
dry N_2	2	1138	379	164	1681
90	17	282	528	495	1305
90	17	2020	1415	1310	4745
50	17	1648	2743	1453	5844
dry N_2	17	286	880	710	1876

Conclusion

A detailed knowledge of the processing parameters of the planarization process and planarizing film properties is required in order to develop a successful planarization process. In particular, degree of planarization and influence of environmental humidity on planarizing films should be considered. By a detailed study of both requirements, which by themselves are contradictory, a useful planarization process by reflowing BPSG has been established.

Acknowledgements

The authors gratefully acknowledge the use of IMP, San Jose, Ca., USA, facilities. Special thanks are due to Mr. A. Belič of IMP for illuminating discussions regarding the utility of the developed process. The study has been supported by a grant from the Ministry of Science and Technology of the Republic of Slovenia.

References

/1/ S. Wolf, Silicon Processing for the VLSI Era, Vol. 2 – Process integration, Lattice Press, Sunset Beach, Ca. USA, 1990

/2/ P. B. Johnson and P. Sethna, Semiconductor Int., Oct. 1997, p. 80

/3/ B. Gspan, Ph.D. Thesis, Faculty of Electrical Eng., University of Ljubljana, 1995

/4/ C. Dornfest, Borophosphosilicate Glass Film Properties and Process Repeatability, p. 122, 1989

/5/ S. K. Gupta, Spin-on-glass for Dielectric Planarization, Microelectron. Manuf. Test., Vol. 12, No. 5, p. 10, April 1989

/6/ Pramanik D., CVD Dielectric Films for VLSI, Semiconductor Int., Oct. 1987, p. 94

/7/ Gralenski N. Advanced APCVD: BPSG Film Quality and Production Reliability Report, Watkins-Johnson Co. report, 1992

Prof.dr.Radko Osredkar
FRI in FE Univerze v Ljubljani
Laboratorij za mikroelektroniko
Tržaška 25
SI 1000, Ljubljana
Slovenia
e-mail: radko.osredkar@fri.uni-lj.si

Dr.Boštjan Gspan
Repro MS
Šmartinska 106
SI 1000, Ljubljana
Slovenia
e-mail: bostjan.gspan@reproms.si

Prispelo (Arrived): 29.05.2000 *Sprejeto (Accepted): 10.06.2000*

KONFERENCE, POSVETOVANJA, SEMINARJI, POROČILA
CONFERENCES, COLLOQUYUMS, SEMINARS, REPORT

Tridesetletnica Laboratorija za mikroelektroniko na Fakulteti za elektrotehniko v Ljubljani

V teh dneh Laboratorij za mikroelektroniko na Fakulteti za elektrotehniko v Ljubljani praznuje tridesetletnico ustanovitve. Ves čas svojega obstoja laboratorij usmerja svojo dejavnost na tri področja:

- V raziskovalnem delu največ pozornosti posveča metodologiji načrtovanja integriranih vezij in mikrosistemov z mešanimi analogno digitalnimi signali. S tega področja lahko zabeležimo vrsto vabljenih predavanj sodelavcev Laboratorija za mikroelektroniko na najeminentnejših ustanovah v ZDA, Evropi in Aziji. Založba McGraw Hill Book Co. je avtorjema iz Laboratorija za mikroelektroniko na Fakulteti za elektrotehniko v Ljubljani objavila knjigo iz tega področja, ki je bila zelo lepo sprejeta v načrtovalski srenji. Med zapažene uspehe s tega področja tudi uvodni članek v ugledni reviji IEEE Solid State Circuit.
- V raziskovalno razvojnem področju je Laboratorij za mikroelektroniko ves čas znan po svoji tesni povezanosti z industrijo. Več sto uspešno realiziranih projektov integriranih vezij, zasnovanih in izdelanih tako na osnovi tankoplastne hibridne tehnologije kot monolitnih tehnologij vse do razsežnosti 0.35 μm, nakazuje njegovo usmeritev. Ti uspehi potrjujejo njegovo usmeritev v službi za okolje. To pa ga je po drugi strani tudi izdatno podpiralo.
- Tretji segment dejavnosti Laboratorija je na pedagoškem področju. Študentje v laboratoriju v okviru vaj načrtajo vezja in spremljajo njihov nastanek ter analizirajo dobljene rezultate. V Laboratoriju za mikroelektroniko na Fakulteti za elektrotehniko potekajo poleg rednih študentskih vaj tudi zaključna dela iz vseh treh ravni študija.

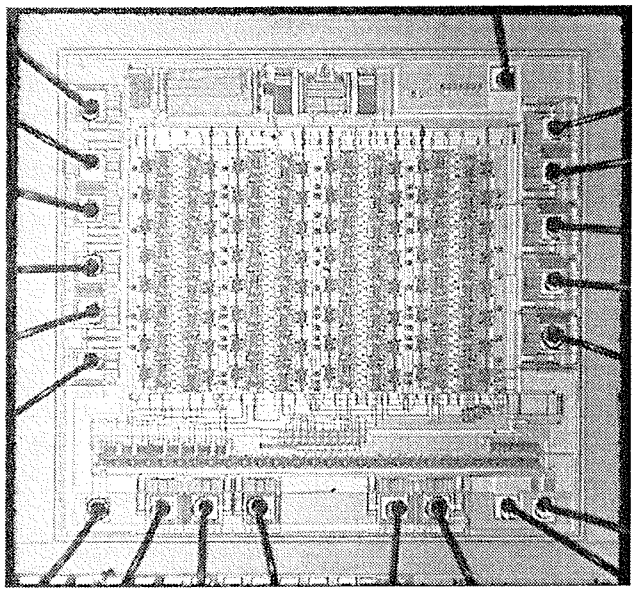

BLISK - *Študentski projekt za leto 1999/2000:*
6-bitni A/D pretvornik
Lastnosti:
čas pretvorbe: 50ns
Maksimalna frekvenca pretvorbe: 100 MHz
Tehnologija: 0.8 μm CMOS

Iz izkaznice Laboratorija lahko razberemo, da v njem deluje 15 doktorjev znanosti različnih profilov in 10 visoko usposobljenih inženirjev in tehnikov. Laboratorij ima približno 400m^2 čistih prostorov razreda 10 do 100. Instalirana oprema omogoča realizacijo pilotnih serij vezij CMOS vse do submikronskih razsežnosti. Približno 1000m^2 ostalega prostora služi za tehnološko podporo ter za testno in načrtovalsko dejavnost.

V zadnjem obdobju se laboratorij vse bolj usmerja v tehnologijo mikrosistemov (MEMS, MOEMS). Kot zgled usmeritve lahko služi magnetni mikrosistem za precizno merjenje linearnega pomika.

S svojo živahno dejavnostjo na vseh omenjenih področjih in izbrano tehnološko nišo, ki se zaradi pomembnosti vse bolj uvaja tudi v drugih deželah, Laboratorij za mikroelektroniko na Fakulteti za elektrotehniko zanika govorice, da njegovo življenje ugaša in da njegov obstoj nima več smisla. Realnost kaže povsem drugo sliko!

Lojze Trontelj

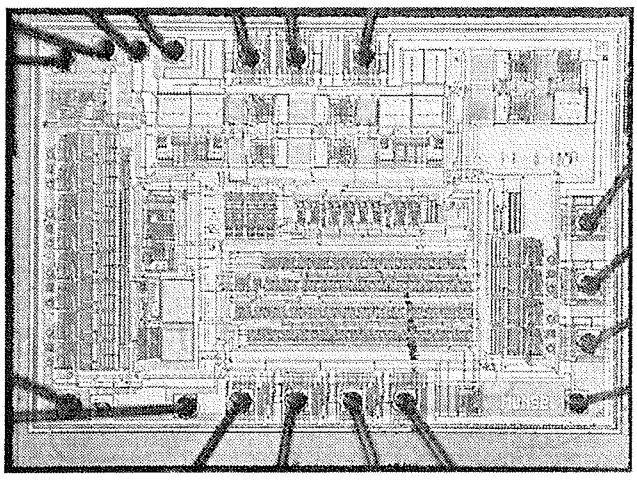

MUNS - *Magnetni mikrosistem za precizno merjenje linearnega pomika*
Lastnosti:
Ločljivost: 5μm
Maksimalna hitrost: 10m/sek
Tehnologija: : 0.8 μm CMOS

Sixth Grove Fuel Cell Symposium

Udeležil sem se šestega Grove-ovega simpozija o gorivnih celicah, ki je bil od 13. do 16. septembra v Queen Elizabeth II Conference Centre v Londonu. Simpozij, ki poteka vsako drugo leto, se imenuje po Sir William Grove-u, ki je naredil prvo gorivno celico leta 1839. Oziroma, bolj natančno rečeno, Grove je odkril princip gorivne celice oziroma v njegovem primeru "obrnjeno" elektrolize vode. Pri njegovem eksperimentu je bil reducent vodik, oksidant kisik, oba pod rahlim nadpritiskom, elektrolit pa je bil razredčena žveplena kislina. Pod temi pogoji je na platinastih elektrodah dobil električno napetost.

Na simpoziju je bilo registriranih preko 400 udeležencev iz 34 držav, skoraj polovica jih je bila izven Evrope. Vabljeni referati, ki so podajali ekonomske ali tehnološke preglede problematike gorivnih celic (transport in energetika, promet, ekonomika, varstvo okolja, ...), so imeli 20 min. časa za predstavitev in 5 minut za zelo kratko diskusijo, na koncu vsake sekcije pa je bilo na voljo še okrog pol ure za bolj splošno diskusijo. Bolj tehnični prispevki so bili predstavljeni kot posterji. Teh je bilo čez 120, dvakrat več kot na prejšnji konferenci leta 1997. Posterji so bili postavljeni ves čas simpozija, eno dopoldne pa je bilo namenjeno za ogled in diskusijo.

Najprej ponovimo nekaj definicij oziroma kratic, ki se bodo ponavljale skozi poročilo. Gorivna celica je element, sestavljen iz dveh elektrod, anode (gorivo) in katode (oksidant, večinoma zrak), med katerima je elektrolit. Po sestavi elektrolita jih delimo na:

- gorivne celice s trdnim oksidnim elektrolitom (**SOFC** - solid oxide fuel cell). Elektrolit je običajno z itrijevim oksidom stabiliziran kubični ZrO_2 (YSZ), anoda je na osnovi kovinskega niklja in YSZ, katoda pa na osnovi polprevodnih perovskitov. Gorivo je lahko H_2, zmes H_2 in CO ali pa naravni plin. Temperatura delovanja je okrog 1000°C. Ta tip gorivne celice ima teoretično najboljše karakteristike, vendar so zaradi zahtevne konstrukcije, pogojene z visoko temperaturo delovanja, zaenkrat še najdlje od komercializacije.
- gorivne celice s staljenimi karbonati (**MCFC** - molten carbonate fuel cell). Elektrolit je $(Li,K)CO_3$, anoda je na osnovi poroznega niklja, katoda pa zmes NiO in Li_2O. Gorivo je lahko H_2, zmes H_2 in CO ali pa naravni plin. Temperatura delovanja je nad 600°C.
- gorivne celice s trdnim protonskim prevodnikom v obliki polimerne membrane (**SPFC** - solid proton conductor fuel cell ali **PEMFC** - proton exchange membrane fuel cell). Anoda in katoda sta grafitni s platinskim katalizatorjem. Gorivo je vodik, temperatura delovanja pa do 100°C.
- gorivne celice s fosforno kislino (**PAFC** - phosphoric acid fuel cell). Elektrolit je fosforna kislina H_3PO_4, anoda in katoda sta grafitni s platinskim katalizatorjem. Tudi tu je gorivo vodik, temperatura delovanja pa okrog 200°C.

Omenil bom še najstarejše gorivne celice oziroma celice, ki so jih prve razvili do te mere, da so bile uporabne. To so gorivne celice z alkalnim elektrolitom (**AFC – alacaline fuel cell**), ki so zaradi dolgega časa, odkar so v uporabi, verjetno tehnološko najbolj "dodelan" tip gorivnih celic. Veljalo je, da se te celice ne razvijajo več za komercialne namene, ker so preveč "občutljive" na CO_2, ki je lahko prisoten tako v gorivu kot v zraku. Z elektrolitom, na primer KOH, nastajajo karbonati, ki degradirajo delovanje celice. Zato se mora uporabljati zelo čist vodik za gorivo in zelo čist zrak ali kisik za oksidant, kar preveč podraži uporabo. Zaradi svoje "zrelosti" in zanesljivosti pa se uporabljajo v aplikacijah, kjer cena ni tako zelo pomembna, na primer na vesoljskih plovilih. Zanimivo pa je, da je na tem simpoziju eden od referatov predstavil AFC gorivno celico, pri kateri se vsak dan elektrolit preciklira in prečisti, tako da lahko kot oksidant uporablja zrak.

V poročilu bom na kratko opisal vsebino nekaterih zanimivejših prispevkov. Na razpolago pa je zbornik razširjenih povzetkov, kjer so objavljeni vsi povzetki tako vabljenih predavanj kot posterjev.

Pred simpozijem je bila delavnica z naslovom "Gorivne celice – nove dimenzije za pretvorbo energije?". V okviru delavnice je imel H. J. Koch (International Energy Agency) uvodno predavanje z naslovom "Challenges of implementing new technologies for sustainable energy". Trije vabljeni predavatelji so predstavili svoje poglede na tehnologijo in bodočnost gorivnih celic. B. McNutt (Department of Energey) je predstavil stališča vlade Združenih držav Amerike in M. Tallantyre (British Gas Technologies) poglede angleške plinske družbe. Član parlamenta J. Gummer pa je problem tako gorivnih celic kot širše obnovljivih virov energije ocenjeval s stališča politike. V glavnem so se vsi strinjali, da so gorivne celice krasna stvar, kar se tiče izkoristka pretvorbe kemične v električno energijo in s tem povezanega zmanjšanega onesnaževanja. Še vedno pa niso dosegle tiste stopnje oziroma cene, da bi se povprečnemu uporabniku oziroma potrošniku splačalo, da jih uporablja. Po drugi strani pa so tako Koch kot še nekaj drugih predavateljev opozorilo, da poraba nafte narašča okrog 2% na leto. Čez eno ali dve desetletji bo naraščajoča poraba dosegla optimalno možno proizvodnjo, nato pa bodo cene nafte začele hitro rasti. To bo posledica tako naraščajočega povpraševanja kot tudi izčrpanja virov, ki se jih lahko razmeroma poceni izkorišča. Nekateri ocenjujejo, da bo moralo biti čez 50 let že 50% energije iz obnovljivih virov.

Tule bi še napisal nekaj tem oziroma "prepirov", ki so se pojavljale v več diskusijah med simpozijem. Kot je v diskusiji nekdo komentiral; razviti so že vsi mogoči tipi celic, narejenih je tudi nekaj prototipov osebnih avtomobilov. Vendar, če bi kdo hotel zgraditi naselje in recimo sto ali dvesto hiš opremiti z gorivnimi celicami namesto s klasično centralno kurjavo, teh celic nima kje kupiti. Več diskutantov je trdilo, da je jedrska energija, vsaj kar se tiče onesnaževanja okolja s CO_2, ki povzročajo učinek tople grede, najboljša. Opozorili so, da precej držav, med njimi med industrijskimi posebej izstopata Francija s 76% in Belgija s 55%, dobivajo pomemben delež električne energije iz nukleark. Če bi centrale zaprli in energijo dobivali iz, na primer, nafte ali plina, bi se močno povečal izpust CO_2, kar je v nasprotju s sprejetimi dokumenti (Kyoto Global Climate

Conference, december 1997). Nasprotni argumenti so seveda opozarjali na probleme shranjevanja jedrskih odpadkov in razprave o tem, koliko energije, dobljene iz fosilnih goriv, je potrebno za postavitev nuklearnih elektrarn. Obnovljivi viri so zaenkrat, z izjemo hidroelektrarn, razen za posebne namene, predragi. Za biomaso kot alternativni energetski vir je bilo povedano, da danes še ni realistična rešitev. Konkurenčna bi postala, če bi cena nafte narasla na dva ali trikratno današnjo vrednost, to je na okrog ali nad 60 dolarjev za sodček. Nekaj diskutantov je tudi opozorilo na staro dilemo; na zemljišču, kjer lahko rastejo rastline, ki se jih da potem pokuriti za pridobivanje energije, v precej primerih lahko raste tudi "hrana", na primer žitnice ali riž. Ta pa je vsaj danes bolj pomembna in ima višjo ceno kot, na primer, celulozna masa.

Osebni avtomobili z električnimi motorji, ki bi dobivali energijo z gorivnimi celicami, so bili tema nekaj referatov in precej razprav (avto je pač nekaj, kar nas vse zanima). Avtomobili naj bi imeli PEM gorivne celice, ki pa uporabljajo ali čisti vodik ali pa rabijo reformer, ki neko drugo gorivo spremeni v gorivo, bogato na vodiku. Vse skupaj, to je rezervoar goriva in reformer, gorivna celica in električni motor, je treba spraviti v "ohišje" povprečnega avtomobila. Ker gorivna celica ne reagira takoj na "pritisk na plin", rabi avto še akumulator za pospeške. Razviti so bili prototipi, vendar kaže, da bolj v reklamne namene. V diskusijah izražena mnenja so bila večinoma, da v bližnji prihodnosti osebni avto z gorivnimi celicami nima prave komercialne perspektive. Problem bo predvsem gorivo. V rafinerije nafte na eni strani in bencinske črpalke na drugi je bilo samo v Združenih državah Amerike vloženo nekaj deset ali celo sto milijard dolarjev. Ta hip ni videti investitorja, ki bi bil pripravljen investirati podobno vsoto za sistem proizvodnje in distribucije goriv za vozila z gorivnimi celicami, na primer metanola ali celo vodika. Poleg tega avtomobilska industrija daje na trg nove in nove tipe osebnih avtomobilov z manjšo porabo goriva in čistejšim "izpuhom", kar spet spodmika tla enemu glavnih argumentov, da bi bil avto z gorivnimi celicami bolj ekonomičen in da bi manj onesnaževal okolje. Upajo pa, da bodo večje investicije proizvajalcev avtomobilov in naftne industrije v gorivne celice znižale ceno prevsem PEM gorivnih celic, tako da bodo bolj dostopne. S tem bi se lahko prekinil začaran krog. Dokler se gorivne celice, ne glede na tip, ne bodo serijsko izdelovale, bodo namreč predrage. Dokler bodo predrage, pa jih možni uporabniki ne bodo kupovali, zato ne more priti do serijske proizvodnje. M. A. B. Nurdin (World Fuel Cells Council) je na primer v prispevku z naslovom "Market actors – promoting the benefits and application of fuel cells" ocenil, da mora cena sistema z gorivnimi celicami pasti pod 60 $/kW za avtomobile in pod 1500 $/kW za elektrarne.

Na začetku je udeležence simpozija pozdravil G. Acres (Johnson Matthey), ki je bil tudi predsedujoči celega simpozija. Grove-jeva nagrada (Sir William Grove Memorial Medal) za dolgoletno delo na področju gorivnih celic je bila podeljena B. Bakerju, vodji firme Fuel Cell Energy Inc. (prej, do leta 1997, Energy Research Corporation). Baker-jev glavni doprinos je bil predvsem na področju gorivnih celic s staljenimi karbonati, baterij in hibridnih sistemov.

Referat, delo več avtorjev, z naslovom "The CAPRI project, a hybrid vehicle concept with autothermal methanol reformer and fuel cell" je prikazal sodelovanje več partnerjev (Volkswagen iz Nemčije, ECN iz Nizozemske, Johnson Matthey iz Anglije in Volvo iz Švedske) na projektu CAPRI (Car Authotermal Process Reactor Iniciative). Projekt je sofinanciran od Evropske skupnosti v okviru programa Joule. Hibridni pogon osebnega avtomobila sestavljajo reformer, gorivna celica, električni motor in akumulator, v katerem je "zaloga" energije za pospeševanje. Akumulator je potreben zato, ker moč, ki jo proizvaja gorivna celica, ne sledi dovolj hitro zahtevam. Na vprašanje med diskusijo, kdaj bo tak avto mogoče kupiti za sprejemljivo ceno, pa ni bilo jasnega odgovora. J. M. Seisler, direktor ENGVA (European Natural Gas Vehicle Association) pa je v svojem referatu "Fuel cell vehicles? Not so fast" na primeru avtomobilov, ki za gorivo uporabljajo naravni plin in so precej bolj ekološko prijazni kot avtomobili na bencin, opozoril na vse težave, ki čakajo vozila z gorivnimi celicami z novim gorivom. Avtomobili z motorji s plinskim gorivom (NGV – Natural Gas Vehicle) so že dolgo časa okrog, vendar se ENGVA trudi, ne preveč uspešno, da bi za njih vzpostavili mednarodne in nacionalne standarde. V precej državah lastniki ne smejo, na primer, parkirati vozila s plinskim pogonom niti v javnih pokritih parkirišči niti v zasebnih garažah, ampak samo na prostem. Vozila, ki bodo uporabljala vodik, ki ga večina ljudi dojema kot izjemno nevaren in eksploziven plin, bodo še teže sprejemljiva. Nekoliko pesimistično je ocenil, da pred letom 2020 na cestah razen reklamnih prototipov ne bo omembe vrednega števila osebnih avtomobili z gorivnimi celicami.

Dva referata sta predstavila načrt uvajanja gorivnih celic za pogon vozil z dvemi ali tremi kolesi (motorji, skuterji, tricikli...) na Daljnem vzhodu. Tam jih uporablja veliko več ljudi kot v zahodnih državah in ta vozila, posebno z dvotaktnim pogonom, močno onesnažujejo zrak. Na Tajvanu na primer država sicer propagira električne motorje, ki jih tudi sofinancira, če ne bi bili 50 do 100 % dražji kot običajni. Vendar pa zaradi baterij tehtajo tudi do 70 % več kot "navadni", čas polnjenja baterij pa je nekaj ur.

Več referatov je bilo posvečenih "vojaški" uporabi gorivnih celic. M. J. Binder in sodelavci so v referatu z naslovom" From Florida to Alaska; results of thirty demonstrations of 200 kW phosphoric acid fuel cells" predstavili rezultate šestletne študije, dobljene s tridesetimi postajami s PAFC gorivnimi celicami, ki jih je vojska namestila v vseh klimatskih pogojih, kot je rečeno v naslovu, od na pol tropske Floride do mrzle Aljaske. R. J. Nowak (DARPA – United States Defense Advanced Research Project Agency) je v referatu "Portable power for military and civilian applications" prikazal razvoj in aplikacijo PEM gorivnih celic za "prenosne" aplikacije. Specifična "vsebnost" energije na enoto teže je pri gorivu, na primer bencinu ali kurilnem olju, okrog 100 krat večja kot v najboljšem akumulatorju. Ocenjujejo, da tehta gorivna celica hkrati z rezervoarjem vodika štirikrat manj kot baterije. Moderen vojak bo imel čez nekaj let že toliko osebne opreme, ki porablja električno energijo, da bodo akumulatorji preprosto pretežki. Kot primeri so bili navedeni telekomunikacijska oprema, naprave za nočno gledanje, laserski namerilniki, "klimatizirana" obleka za delovanje v ekstremnih, vročih ali

mrzlih pogojih in tako dalje. Vodik za pogon celice je zaenkrat shranjen v steklenih mikro kapsulah, v katerih je 4 utežne procente vodika. To je precej več kot v kovinskih steklenicah, kjer je pri pritisku 140 barov samo 1 utežni % vodika. Razvijajo pa shranjevanje vodika v ogljikovih nano vlaknih, s čemer bodo dosegli kar 48 utežnih procentov.

Pri firmi Ingenieurkontor Lubeck – IKL – v Nemčiji proučujejo uporabo gorivnih celic za vojne ladje, predvsem podmornice. Gorivne celice bodo proizvajale energijo za plovbo pod morjem, za kar se navadno uporablja elektrika iz akumulatorjev. Sistem imenujejo "Air Independent Propulsion". Kisik je tekoči kisik, gorivo pa vodik, spravljen v hidridih. Ker je rezultat reakcije v gorivni celici voda, jo lahko izpuščajo v morje. Pogon je neslišen, podmornice pa lahko ostanejo pod vodo do pet krat dalj kot konvencionalne podmornice na baterije. G. Sattler (IKL) je v referatu z naslovim "Fuel cells – going on board" predstavil razvoj ladijskega pogona na osnovi gorivnih celic. Ocenjujejo, da za ladje, predvsem civilne, zaenkrat še ni primeren. Gradijo pa šest podmornic s PEM celicami za nemško mornarico in dve za italjansko. Za prihodnost načrtujejo študij možnosti uporabe visokotemperaturnih celic.

Q. A. Velev (AeroVironment) je s sodelavci predstavil prototip propelerskega letala brez pilota, ki bo letel v višini med 17 in 23 kilometri. Razvili so ga za ameriško vojsko. Služilo bo kot nadomestek satelita za telekomunikacije in opazovanje. Letalo bo ostalo v zraku neprekinjeno vsaj 6 mesecev. Letalo, ki so ga praktično sama krila, ima razpon 80 metrov. Na površini kril so sončne celice, ki proizvajajo električno energijo, ki se uporablja za pogon propelerjev. Za 12 ur nočnega letenja pa je potrebno spraviti okrog 120 kWh. Teža sistema za spravljanje energije ne sme biti večja kot 200 kilogramov in dovolj zmogljivi akumulatorji so preprosto pretežki. Zato so uporabili PEM gorivne celice. Te čez dan z viškom električne energije iz sončnih celic delujejo v "obratni smeri" in elektrolizirajo vodo v vodik in kisik. Vodik, spravljen pod pritiskom nekaj barov, služi ponoči kot gorivo. Ocenjujejo, da je učinkovitost te pretvorbe energije iz električne v vodik in spet nazaj v električno okrog 50%.

Tudi W. Smith (Proton Energy Systems) je v referatu z naslovom "Oportunities for fuel cells in energy storage" opisal PEM gorivne celice, ki z viški električne energije elektrolizirajo vodo. Omeniti pa je treba, da to ni tekoča voda, ampak zrak, nasičen z vodno paro pri temperaturi med 80°C in pod 100°C. Te celice nato po potrebi, recimo, če zmanjka elektrike ali pa v času, ko je elektrika dražja, spet pridobivajo električno energijo. Pri 3 voltih napetost pri elektrolizi je tlak vodika, spravljenega v rezervarjih, do 10 barov, pri nekaj večji napetosti pa tudi nekaj deset barov. Cilj pa je spravljanje vodika tako, da bo predstavljal več kot 5% teže "kontejnerja". To lahko dosežejo v tankih z vodikom pod pritiskom nad 200 barov, vendar so za to potrebne črpalke. Druge možnosti, ki jih ocenjujejo, so spravljanje vodika v kovinske hidride, ogljikova nano vlakna ali fulerene.

Na Japonskem, kjer jim kronično primanjkuje naravnih virov in uvažajo preko 95% goriv, država financira raziskave in razvoj na področju gorivnih celic v višini 100% in izdelavo prototipov delujočih celic ter postavljanje demonstracijskih postaj s 50%. V tem pogledu Japonska daleč vodi pri vlaganju v razvoj gorivnih celic. T. Ishikawa (MCFC Research Association) je predstavil postavitev in zagon električne centrale z močjo 1 MW z gorivnimi celicami s staljenim karbonatom (MCFC), ki je vsaj sedaj največja na svetu. Sistem je modularno sestavljen iz štirih 250 kW podsistemov in zaenkrat doseže izkoristek 45%.

R. B. Godfrey (Ceramic Fuel Cells Ltd., Avstralija) in N. M. Sammers (University of Waikato, Nova Zelandija), oba s sodelavci, sta predstavila v dveh prispevkih možnost uporabe manjših sistemov z gorivnimi celicami na redko naseljenih področjih, kot sta na primer Avstralija in Nova Zelandija. Za evaluacijo so na razpolago tako 200 kW PAFC, ki so primerne za podjetja ali manjša naselja, kot PEM gorivne celice z močmi od 10 kW do 100 kW tako za individualne hiše kot za transport, na primer avtobuse. Prototipe planarnih SOFC gorivnih celic od 1,5 kW do nekaj 10 kW bo avstrijska družba ponudila v sredini leta 2000, komercialno dostopne enote pa naj bi ponudili trgu leta 2001 ali 2002.

V nadaljevanju bom opisal nekaj zanimivejših prispevkov na "našem" področju, to so SOFC - visokotemperaturne gorivne celice s keramičnim elektrolitom. Kot sem že omenil, je trdni elektrolit običajno YSZ, anoda kovinski nikelj v matrici YSZ, katoda pa je na osnovi električno prevodnih perovskitov, navadno $(La,Sr)MnO_3$. Temperatura delovanja je okrog 1000°C. Večina delujočih prototipov SOFC je realiziranih s temi materiali. Visoka temperatura delovanja omogoča "notranji reforming", to je reakcijo med vodno paro in ogljikovodiki, tako da dobimo vodik in CO v sami celici, medtem ko nizko temperaturne gorivne celice, predvsem PEM in PAFC, potrebujejo poseben reformer, da dobijo dovolj čist vodik. Zadnja leta obširno preiskujejo materiale za SOFC-e s temperaturami delovanja okrog 800°C ali niže, vendar pri teh temperaturah ohmska upornost YSZ naraste za velikostni razred ali več. Alternativna trdna elektrolita z višjo ionsko prevodnostjo za SOFC z nižjo temperaturo delovanja sta predvsem s trovalentnimi ioni dopiran CeO_2 in z dvovalentnimi ioni dopiran $LaGaO_3$.

R. A. George (Siemens Westinghouse Power Corp.) je v referatu z naslovom "Status of tubular SOFC field unit demonstration" opisal njihovo testiranje velike SOFC enote z nominalno močjo 100 kW, za katero kot gorivo uporabljajo naravni plin. Gorivna celica je cevaste izvedbe s 1150 cevkami, povezanimi v svežnje. Skozi cevi teče zrak, v prostoru med cevmi pa gorivo. Sistem obratuje že preko 4000 ur in proizvaja 127 kW enosmernega toka z ocenjenim izkoristkom 53%. Vroči plini poleg tega grejejo vodo, ki se lahko uporablja za segrevanje prostorov, tako da je skupen izkoristeh kemične energije goriva še večji. Dokončujejo tudi kombinacijo SOFC gorivne celice in mikro turbine. Pri tej vroči plini iz SOFC poganjajo turbino, ta pa komprimira plin in zrak, ki vstopata v SOFC. Enota ima moč 220 kW, od tega prispeva SOFC 170 kW in plinska turbina 50 kW. Pri nadpritisku 3 bare je izkoristek ocenjen na 60%. H. E. Vollmar z več sodelavci (Siemens AG) in A. L. Dicks s sodelavci (British gas Technol.) pa so opisali relativno nov pristop, kako kombinirati SOFC kot visoko temperaturno gorivno celico in PEM gorivno celico, ki dela pri temperaturah pod 100°C. SOFC, kot je bilo že omenjeno, je zaradi visoke temperature delovanja tudi re-

former; ogljikovodiki z dodatkom vodne pare reagirajo, tako da nastane zmes H_2, CO in CO_2. SOFC v tem primeru deluje tako, da samo del kemične energije pretvori v električno. Plini na izhodu, bogati z vodikom, so nato uporabljeni kot gorivo za PEM celico ali kot sintetični plin (Syngas) za kemično industrijo. Vroč plin, ki izhaja iz SOFC, se ohladi tako, da preda toploto vstopajočemu gorivu in zraku. Ocenjeni izkoristki so preko 60%.

F. J. Gardner (Rolls-Royce Research Centre) je predstavil razvoj druge generacije planarnih SOFC, ki so jih imenovali integrirane planarne SOFC ali s kratico IP-SOFC. Na poroznem keramičnem nosilcu zaporedno vezane celice. Na nosilcu je anoda, preko katere sega trdni elektrolit debeline samo okrog 10 μm, na elektrolitu pa je plast katode. Gorivo priteka skozi porozno keramiko, zrak pa na zgornji strani. Kot zanimivo anekdoto naj povem, kako se je v diskusiji po referatu pokazalo, da lahko predavatelj, če nečesa noče razkriti, odgovarja, ne da bi kaj povedal. Na vprašanje, če je vmesnik keramičen ali kovinski (vmesnik – interconnect – povezuje posamezne celice in mora biti dober elektronski prevodnik, ne sme pa biti ionski prevodnik) je odgovoril, da so vse možnosti odprte. Naslednje vprašanje je bilo, kako so plasti narejene. S tem je diskutant hotel seveda vprašati, s kakšno tehniko so bile plasti izdelane; debeloplastno s sitotiskom, tankoplastno s katero od metod vakuumskega nanašanja, z naprševanjem suspenzij itd. Odgovor je bil preprost. Komponente celic so bile narejene z metodo zaporednega nanašanja?!

G. A. Tompsett in sodelavci (University of Waikito, Nova Zelandija in Keele University, Anglija) so predstavili zanimivo možnost uporabe mikrocevaste izvedbe SOFC. Cevke so iz YSZ in imajo premer samo 2,4 mm. Anoda je na notranji strani, katoda pa na zunanji. V izvedbi plinskega gorilnika, namenjenega tabornikom, butan zgoreva na platinskem katalizatorju. Pri tem se razvija toplota za kuhanje, ki pa tudi segreva snop mikrocevk, ki dajejo električno energijo. Butan kot gorivo teče skozi cevke, zrak pa med cevkami.

N. Hart in sodelavci (Brunel University, Anglija) so proučevali stroške proizvodnje elektrod na ploščicah YSZ. Pri tem so primerjali ceno oziroma porabo energije za 6 različnih postopkov. To so bili nalivanje keramičnih folij, sitotisk, naprševanje suspenzije, kalandriranje, elektromehanična depozicija iz parne faze in fizična depozicija iz parne faze. Ugotovili so, da je sitotisk nacenejši način.

Kot smo že omenili, se v SOFC kot anoda običajno uporablja material na osnovi zmesi kovinskega niklja in keramične vezivne faze. Nikelj zelo dobro katalizira oksidacijo vodika. Če pa se kot gorivo uporabljajo ogljikovodiki, se pri njihovem razpadu lahko izloča ogljik, ki pokrije površino niklja in zmanjša izkoriste. G. Pudmich in sodelavci (Intitute for Materials and Processes in Energy Systems, Nemčija) so študirali prevodne perovskitne materiale, ki bi lahko imeli boljše katalitične lastnost. Perovskiti so na osnovi $LaCrO_3$ in na "B" mestih dopirani $sTiO_2$, Fe_2O_3, Nb_2O_5 ali V_2O_5. V reducirajoči atmosferi na anodni strani imajo nizke upornosti, do 10 mohm.cm ter temperaturni razteznostni koeficient blizu razteznostnemu koeficientu trdnega elektrolita.

Eden od problemov pri delovanju SOFC z YSZ trdnim elektrolitom je reakcija med lantanovimi perovskiti, ki se uporabljajo za katodo, in ZrO_2 iz YSZ. Vsi lantanovi perovskiti reagirajo z YSZ in tvorijo piroklor $La_2Zr_2O_7$. Ta faza, ki nastaja po staranju pri povišanih temperaturah med katodno plastjo in YSZ, ima visoko specifično upornost in zniža izkoristek celice. D. Gutierrez in sodelavci (Instituto de Ceramica y Vidrio, Španija) so poročali o preiskavah alternativnega katodnega materiala na osnovi trdne raztopine $Y(Mn,Ni)O_3$, ki je kompatibilen z YSZ. Sa, $YmnO_3$ je feroelektrik in izolator, trdne raztopine pa so polprevodniki z nizko upornostjo in so uporabne kot elektrode.

Več prispevkov se je ukvarjalo s kemičnimi sintezami materialov za SOFC. M. Marinšek in sodelavci (Univerza v Ljubljani) so predstavili kemično sintezo anodnega materiala. S precipitacijo gelov so pripravili zmes YSZ in NiO, ki so jo sintrali do visoke gostote pri 1300°C. NiO so nato reducirali v kovinski nikelj. M. Mori in sodelavci (Research Institute of Electric Power Industry in University of Waikato, Nova Zelandija) so predstavili sintezo katodnih materialov na osnovi $(La,Sr)MnO_3$ in $(La,Ca)MnO_3$ s koprecipitacijo in žganjem pri 1100°C, kar je razmeroma nizka temperatura sinteze. K. Zupan in sodelavci (Univerza v Ljubljani) so z zgorevalno sintezo iz nitratov in citratov predstavili material na osnovi $(La,Ca)CrO_3$ za vmesnik, ki povezuje posamezne SOFC celice. Tako dobljen prah je imel veliko specifično površino (7 do 11 m^2/g) in se je pričel zgoščevati že pri 900°C.

Pri Netherlands Energy Research Foundation so postali pred pilotsko linijo za izdelavo komponent za ploščate SOFC. Trdni elektrolit izdelajo z nalivanjem folij in sintranjem, na sintrane plošče pa s sitotiskom nanašajo elektrodi. Ocenjujejo, da bodo lahko na leto izdelali 15 tisoč celic velikosti 10x10 cm^2.

V. Dusastre in sodelavci (Imperial College, Anglija) so študirali kompatibilnost med nizkotemperaturnim trdnim elektrolitom za SOFC s temperaturo delovanja med 500 in 700°C na osnovi $Ce_{0,9}Gd_{0,1}O_{2-y}$ in prevodnimi perovskiti $(La,Sr)(Fe,Co)O_3$, $Sr_4Fe_{6-x}Co_xO_{13}$ ter $La_{2-x}Sr_xNiO_4$ ter vpliv omenjenih katodnih materialov na električne karakteristike. Lantanov ferit je imel najboljše karakteristike, ki pa so jih še izboljšali z uporabo "mešanih" katod, narejenih iz zmesi $Ce_{0,9}Gd_{0,1}O_{2-y}$ in perovskita. S. J. A. Livermore in sodelavci (Keele University, Anglija) so proučevali notranji reforming v SOFC z elektrolitom na osnovi dopiranega CeO_2 s temperaturo delovanja prav tako med 500°C in 700°C. Proučevali so vpliv temperature, sestave anode (razmerje med kovinskim Ni in dopiranim CeO_2) ter razmerje vodna para / metan na izkoristek pretvorbe v H_2 in CO. S. Ohara in sodelavci so proučevali vpliv sestave anode (Ni in dopiran CeO_2) in temperature sintranja na električni izkoristek celice s trdnim elektrolitom na osnovi CeO_2.

T. Inagaki in sodelavci so poročali o preiskavah materialov za katode SOFC gorivnih celic s trdnim elektrolitom na osnovi dopiranega $LaGaO_3$. Izbrali so s SrO dopiran $LaCoO_3$ in ugotovili, da dobijo najboljše rezultate, to je najnižje polarizacijske izgube, če sintrajo plast katode na predsintrani ploščici trdnega elektrolita pri 1000°C. Na vprašanje, kakšna je adhezija med lan-

tanovim kobaltitom in gosto zasintranim galatom pri tej, razmeroma nizki temperaturi, nismo dobili pravega odgovora.

Kot poster je bil na simpoziju predstavljen tudi naš prispevek z naslovom "Characterisation of $(La_{1-x}Sr_x)RuO_3$ as a possible low temperature SOFC cathodes" (M. Hrovat, A. Benčan, J. Holc, Z. Samardžija, M. Kosec). Poročali smo o rezultatih evaluacije $LaRuO_3$ in s SrO dopiranega lantanovega rutenata kot možne elektrode za SOFC s trdnim elektrolitom na osnovi $LaGaO_3$. Študirali smo odvisnost upornosti $(La_{1-x}Sr_x)RuO_3$ od vsebnosti stroncijevega iona ter kompatibilnost z $LaGaO_3$ ali z $(La,Sr)(Ga,Mg)O_3$. S SrO in MgO dopiran $LaGaO_3$ je namreč v literaturi predstavljen kot eden najboljših trdnih elektrolitov za SOFC.

Marko Hrovat
Institut Jožef Stefan
Jamova 39
1000 Ljubljana

Konferenca MicroTechnologies 2000, London, 24. do 25. januar 2000

V dneh od 24. do 25. januarja 2000 je bila v Londonu konferenca "MicroTechnologies 2000" s "podnaslovom" Mikrotehnologije za novo tisočletje. Konferenca je bila formalno sestavljena iz dveh delov, "The Sixth European Conference on MultiChip Modules" in "Microsystem Packaging 2000", čeprav so se teme obeh prepletale. Organizirala jo je angleška sekcija IMAPS (International Microelectronics and Packaging Society). Ob konferenci je bila tudi razstava proizvajalcev opreme in materialov za hibridno mikroelektroniko. Pripomba; v tekstu bo za Multi Chip Module večinoma uporabljana okrajšava MCM.

Multi Chip Moduli (MCM) so komponente, podsistemi ali sistemi z zelo visokim številom funkcij. Narejeni so na večplastnih substratih, na katerih so pritrjene ali gole polprevodne tabletke ali pa tabletke v Chip Sized Package (CSP), ki so samo okrog 20% večje kot gole tabletke. V večplastnem substratu in na njegovi površini so prevodne linije. Vezje je navadno hermetično zaprto. V glavnem ločijo tri tipe MCM, ki so izdelani v različnih tehnologijah, to je tankoplastni, debeloplastni (keramika) in v tehnologiji tiskanih vezij. Oznake so MCM-L (laminate - tiskana vezja), MCM-C (ceramics - keramika) in MCM-D (deposited - tanki filmi). MCM-C so "keramični" hibridi visoke gostote, navadno večplastni keramični substrati ali pa kompleksna debeloplastna večplastna vezja. MCM-D imajo nanešene tankoplastne večplastne kovinske povezave, ločene predvsem s polimernim ali včasih napršenim tankoplastnim dielektrikom. Kot substrat za MCM-D se običajno uporablja Al_2O_3 ali silicij. MCM-L so zahtevna večplastna tiskana vezja z linijami čim manjše širine. Ta tip MCM je najcenejši. Prevodnik je baker, dielektrik pa polimer. Glaven problem pri MCM-L je neujemanje temperaturnih razteznostnih koeficientov med silicijevimi tabletkami in organskim substratom.

V poročilu je na kratko opisana vsebina nekaterih zanimivejših predavanj, na razpolago pa je zbornik referatov na Odseku za keramiko na Institutu Jožef Stefan.

Konferenca "MicroTechnologies 2000", na kateri je bilo registriranih okrog 80 delegatov, je potekala v sledečih sekcijah:

- Tehnologija
- Izboljšanje izkoristka in zanesljivosti
- Design in aplikacije
- Materiali, procesiranje in modeliranje
- "Izzivalne" aplikacije (Challenging Applications)
- Načrtovanje, prototipi in proizvodnja

C. E. Baier (TechLead Corp., Colorado) je v referatu z naslovom "Leading edge MCM technologies" predstavil trende in razvoj na področju MCM. Gonilna sila razvoja na področju MCM-ov so bile prej predvsem zahteve vojaške elektronike, nekje v sredini devetdesetih let pa je postala gonilo razvoja komercializacija. Predavatelj meni, da pri multi chip modilih ni niti tako pomembno, da bi bili boljši od drugih izvedb, ampak predvsem to, da so majhni. To zahteva razvoj telekomunikacij, na primer prenosnih telefonov, modemov, daljinskih upravljalcev itd. Skratka, elektronskih naprav, ki združujejo vedno več funkcij, še vedno pa morajo biti tako majhne, da se jih lahko drži v roki. Avtor meni, da bo predvsem na področju potrošne elektronike (throw away products) prevladali MCM-L, v glavnem zaradi nižje cene. Poleg tega razvijajo nove materiale, ki bodo imeli temperaturne razteznostne koeficiente (TEC) blizu TEC siliciejevih tabletk.

V MCM je vedno pogostejša kombinacija tabletk (chipov), ki se bondirajo z žičko in flip chipov. Flip-chip so tabletke, ki se pritrdijo "z obrazom navzdol". Na površini so kroglice spajke, ki se s pretaljevanjem pritrdijo na substrat. Prednost bondiranih tabletk je zrela tehnologija in dobavljivost, prednost flip chipov pa, da v vezju zasedejo manj prostora. Ker je dodatna opracija pri izdelavi flip chipov izdelava spajkalnih kroglic, je ta tip tabletk tudi dražji. Pri izdelavi MCM z obema tipoma tabletk je prva operacija spajkanje flip chipov, druga pa bondiranje. Med spajkanjem so kontakti za bondiranje, zlati na tiskanem vezju in aluminijasti na tabletkah, zaščiteni z organskim film, ki se nato izpere z vodo. Nečistoče, ki jih je treba odstraniti pred bondiranjem, so organske (ogljikovodiki), kisik (oksidirane aluminijaste blazinice), halogeni itd. L. Lombardi in sodelavci (IBM Italy) so v referatu "Nitrogen/hydrogen plasma cleaning on MCM-L: a new study how to improve bondability in hybrid applications" predstavili problene pri čiščenju vezij s plazmo. Učinkovitost

čiščenja s plazmo je odvisna od vrste plazme. Pri dušikovi plazmi ioni samo mehansko odstranjujejo atome ali mulekule nečistoč in težko "pridejo do živega" organskim nečistočam in oksidom. Vodikova plazma poleg mehanskega čiščenja tudi kemijsko reagira s kisikom ali ogljikom, ki sta odstranjena kot H_2O ali CH_4. Vendar pa lahko s spajko tvori SnH_3 radikale, ki reagirajo z bondirnimi blazinice in na površini puščajo kositer. Zato so uporabili za plazmo mešanico vodika in dušika, kar je dalo dobre rezultate. Tudi referat R. Nickerson-a (Advanced Surface Technology) z naslovom "Pre-wire bond and BGA cleaning for maximum yield" je obravnaval problem čiščenja pred bondiranjem. Čiščenje z vodnimi topili odlično odstrani vodotopne anorganke spojine, na primer soli. Ni pa zelo učinkovito pri odstranjevanju organskih nečistoč. Plazemsko čiščenje s kisikovo plazmo učinkovito odstrani na primer ogljikovodike (oksidirajo se v H_2O in CO_2), je pa nevarnost, da se oksidirajo aluminijaste bondirne bla-zinice. Čiščenje z razmeroma nevtralnimi plini (dušik) ali pa plemenitimi plini (argon) pa več ali manj samo fizično odstranjujejejo nezaželjene nečistoče in ni prav učinkovito pri odstranjevanju anorganskih soli. Naj-boljše rezultate so dobili s kombiniranim čiščenjem; najprej mokro čiščenje, nato pa čiščenje v plazmi.

M. S. Aftanasar is sodelavci (University of Surrey, Anglija) so v referatu z naslovom "Feasibility study of materials for novel millimetre-wave multi-chip modules" prikazali rezultate evaluacije različnih materialov za izdelavo MCM za mikrovalovne (75 GHz do 300 GHz) aplikacije. Zaradi karakteristik mikrovalovnih vezij mora biti dielektrik razmeroma debel. Testirali so MCM-D, kjer so na substrate s "spiniranjem" nanašali SiO_2 kot dielektrik (in seveda kot izolator za ločevanje prevodnih plasti) in MCM-C, to je keramične folije z nizko temperaturo žganja (LTTC – Low Temperature Cofired Ceramics) in debeloplastni tehnologijo. Primerjalni rezultati so pokazali sledeče: pri tankoplastnem MCM-D je potrebno SiO_2 v več zaporednih korakih nanašati in žgati, da dobimo primerno debelino. Pri tem film pogosto razpoka. LTCC tehnologija je zelo primerna za MCM-C za vezja, ki delujejo pri nižjih frekvenca, pri zahtevanih frekvencah nad 75 GHz pa so izgubni koti keramičnega materiala previsoki. V bližnji prihodnjosti (predavatelj ni definiral, kaj pomeni bližnja prihodnjost) proizvajalci LTCC folij obljubljajo izboljšane dielektrične karakteristike keramike z nizko temperaturo žganja. Najboljše rezultate so dobili z uporabo debeloplastne tehnologije za izdelavo večplastnih vezij. Uporabili so paste s fotoobčutljivim organskim materialom (photoimaginable; mogoče bi bil boljši izraz optičnega oblikovanje). Moj vtis je bil, da so uporabili sistem dielektričnih in prevodnih past firme Du Pont, čeprav tega niso povedati. Fotoobčutljive debeloplastne paste po tiskanju in sušenju osvetlijo skozi maske z ultravijolično svetlobo, ki sproži polimerizacijo v organskem materialu. Nepolimerizirane dele natiskane plasti nato sperejo z vodo. Nadaljni postopki so isti kot pri izdelavi debeloplastnih hibridnih vezij. To je tehnologija, ki uspešno kombinira zrel način debeloplastne tehnologije z natančnostjo fotolitografije. Dosegljive ločljivosti tako odprtin za povezovanje (vias) kot širine prevodnih linij so nekaj deset mikrometrov. Dodatna investicija za fotolitografijo, ki jo avtorji ocenjujo na 100 do 200 tisoč dolarjev, po njihovem mnenju omogoča izdelavo MCM-C, ki so po karakteristikah primerljivi z MCM-D, vsaj za njihove potrebe mikrovalovnih vezij - substratov.

Dva referata ("Materials issues for microsystems packaging" in "3D wafer level packaging") sta prikazala trodimenzionalno "zlaganje" in enkapsuliranje. Prvi je obravnaval predvsem enkapsulacijo mikro mehanskih naprav in senzorjev na nivoju tabletk, ki zaradi občutljivosti zahtevajo skrben izbor materialov. Spajkanje je na primer zelo primerna metoda povezovanja, vendar lahko ostanki fluksov poškodujejo aktivne površine. Za optoelektronsko industrijo so razvili posebne nizko taljive spajke brez fluksov, ki se sedaj prenašajo tudi na področje pritrjevanja mikro sistemov. Pomembna je tudi izbira materiala za zaščito tabletk. Tabletke se običajno zaščiti s kapljo trdega epoksija, čeprav ta zaradi večjega TEC povzroča napetosti. Če pa je na tabletki tanka izjedkana membrana, na primer pri senzorjih tlaka ali mikro črpalkah, priporočajo mehkejši, "glob top" enkapsulant, čeprav ne ščiti tako dobro pred mehanskimi poškodbami. Tu pripomnimo, da sta dve zahtevi za kvalitetno plastično zaščito nasprotni; zaščita naj bi bila "trda", da dobro ščiti pred zunanjimi vplivi in "mehka", da ne povzroča mehanskih stresov. Trde zaščite so epoksiji, ki imajo temperaturo prehoda Tg (glass transition temperature) okrog 150°C, mehke pa silikoni s Tg okrog –50°C. Drugi referat je obravnaval tematiko tridimenzionalnega povezovanja golih tabletk in tanjšanje tabletk, oziroma, kot je predavatelj to imenoval, vertikalno miniaturizacijo. Danes so trendi po čim tanjših tabletakah, na primer za vgrajevanje v pametne kartice. Tanki chipi imajo tudi nižjo toplotno upornost in so bolj "upogljivi" kot debelejši, kar je pomembno za vezja na fleksibilnih substratih. Po drugo strani pa so silicijeve rezine (wafer-ji) vedno večje; sedaj prehajajo na premer 300 mm. Večje rezine pa morajo imeti zaradi rokovanja večjo mehansko trdnost in morajo zato biti debelejše. Po izdelavi integriranih vezij na rezinah se te lahko tanjšajo na različne načine. Mehansko brušenje in poliranje je razmeroma poceni in hitro, vnaša pa napetosti in razpoke v silicijev monokristal. Drug našin je jedkanje s CF_4 plazmo, ki odtranjuje Si kot hlapen SiF_4. CF_4 plazma jedka Si desetkrat bolje kot SiO_2 in dvajset krat bolje kot Al prevodne plasti na siliciju. Zato se da na ta način tudi tridimenzionalno oblikovati tabletke. Kot enega primerov je navedel izdelavo prevodnikov skozi telo tabletke namesto ob robovih, kar zelo poveča gostoto povezav pri zloženih chipih. Na aktivni strani, kjer je izdelano integrirano vezje, najprej zjedkajo "jamice" v silicij. Luknjice napolnijo s prevodnikom - aluminijem, nato drugo stran stran tanjšajo s plazmo, dokler prevodni čepek ne "pogleda ven". Minimalna debelina, ki so jo dosegli, je 30 um; seveda pa je težko rokovati s tako tankimi in fleksibilnimi ploščicami. Samo da se spomnimo, debelina lasu pa je okrog 50 um, tabletke pa so lahko centimeterskih dimenzij. Referat "Modelling of MST packages" (MST – Micro Systems Technologies) pa je obravnaval predvsem problematiko enkapsulacije tri dimenzionalnih struktur. Predavateljica (G. Kelly, National Microelectrinics, Irska) je povedala, da je groba ocena, da dvig temperature za 10 K nad dovoljeno temperaturo, na primer 125°C, prepolovi življensko dobo naprave. Medtem ko se pri dvodimenzionalnih strukturah, recimo tabletke na substratu, lahko poveča odvajanje

toplote z dovolj velikim hladilnim telesom za vsako tabletko, pa je odvajanje pri 3 D strukturah odvisno predvsem od izbire materialov, ki morajo odvesti toploto iz notranjosti. Obravnavala je tudi računalniško modeliranje različnih struktur, ki olajšajo pravilno izbiro ohišij in materialov.

Več referatov je obravnavalo problem enkapsulacije vezij in naprav. Z izrazom "enkapsulacija" sem poskusil prevesti angleški "packaging", vendar ima ta precej širši pomen. Cena enkapsulacije lahko doseže tretjino cene izdelka. Vsi so poudarjali, da je pri izbiri primernih materialov in metod seveda pomembno, da enkapsulacija omogoča nemoteno delovanje pod zahtevanimi pogoji. Prav tako pa je pomembno, da enkapsulacija ni "predobra"; eden predavateljev je uporabil izraz "over-engineered solutions", kar je bilo včasih potrebno za vojaške aplikacije, ker to zmanjša dobiček proizvajalcu. Zelo poenostavljeno povedano, dražje hermetično keramično ali kovinsko ohišje ni potrebno, če zadošča zapiranje v plastiko. Prav tako je pomembno, da se že pri začetku razvoja prototipov odloči, kako bodo enkapsulirani. To so ilustrirali z nekaj zanimivimi anekdotami o tem, kako so prototipi vezij ali senzorjev v laboratoriju imeli vse zahtevane karakteistike, ko pa so jih enkapsulirali ali kam vgradili, so pa odpovedali, na primer zaradi neujemanja TEC, pregrevanja ali kaj podobnega.

C. G. J. Schabmüller in sodelavci (University of Southampton) so v referatu z naslovom "Packaging of closed chamber PRC-chips for DNA amplification) predstavili chipe, namenjene pomnoževanju DNA molekul. Pomnoževanje sledov DNA je pomembno na velikem številu področij, na primer pri kriminalistiki ali detekciji "nosilcev" različnih bolezni, kjer so vzorci premajhni za neposredno analizo. PRC je kratica za "Polymerase Chain Reaction". To je metoda za pomnoževanje identičnih DNA molekul. V raztopini so osnovne mulekule, potrebne za tvorbo DNA molekul, to so štiri deoksinukleotidne baze (adenin, citosin, guanin in thimin) in mulekule, ki bodo tvorile sladkorno – fosforno "oporo" (backbone). Poleg tega je dodan encim, ki omogoča kopiranje DNA. Ta encim, ki ga izolirajo iz bakterij, ki živijo v vročih vrelcih pri okrog 90°C, zdrži visoke temperature, ki so potrebne pri pomnoževanju DNA. V raztopino dodajo majhno količino, lahko bi rekli sledove, DNA. Raztopina se segreje na 95°C, da se razplete dvojna vijačnica. Nato se ohladi na okrog 70°. Pri tej temperaturi encim ob vsaki enojni verigi sintetizira kompatibilno verigo in število DNA se s tem podvoji. Po 30 ciklih naraste število DNA mulekul za okrog miljardkrat. Razvili so chip, v katerm poteka ta reakcija. Chip je za enkratno uporabo predvem zaradi tega, ker se pri tem lahko pomnožijo tudi ostanki DNA iz prejšnjih analiz in je preprosteje vzeti nov chip kot pa s težavo dezinficirati ozke kanale, ki so v siliciju narejeni z mikro oblikovanjem (tako sem prevedel izraz "micro machining"). Tabletke izdelajo tako, da v silicij najprej zjedkajo mikro kanale, ki jih nato pokrijejo s stekleno ploščico, ki jo z anodnim bondiranje neprodušno pritrdijo na silicij. Na hrbtni strani tabletke s tanko plastno tehnologijo izdelajo Pt grelec in Pt senzor temperature. Anodno bondiranje je postopek, pri kateren na silicij pritrdijo steklo z TEC blizu TEC silicija. Sendvič segrejejo na nekaj 100 stopinj Celzija, da prične steklo nekoliko ionsko prevajati. Pod vplivom električne napetosti difundirajo kisikovi ioni proti siliciju in ga oksidirajo. Tvori se močna vez Si/SiO_2/ steklo, ki je močnejša od mehanske trdnosti stekla.

D. J. Hitchings in solelavci (Technology for Industry, Wilburton, Anglija) so v referatu "Medical applications for MST" predstavili stanje mikro oblikovanih chipov (senzorjev, črpalk, injeciranje brez igel, srčni vzbujevalci itd.) na področju medicine. Predavatelj je na začetku povedal, da mikroelektronika zelo hitro napreduje, kar je ilustriral s primerom, da stane na primer kalkulator toliko kot nekaj štruc kruha. Že leta obljubljajo, da bodo imele mikro naprave (microengineered systems) velik pomen za medicino. Vendar se na tem področju stvari premikajo precej počasneje, kot so mislili. Eden razlogov je, da morajo vsako stvar, najsi bo to novo zdravilo ali naprava, preiskusiti in odobriti "odgovorna telesa". Navadno to traja pet ali več let. Precejšen čas se porabi tudi za klinične teste, ki morajo potrditi, da so predlagane mikro naprave neškodljive in kompatibilne z zahtevami medicine. Po odobritvi pa je navadno problem prepričati uporabnike, to je zdravnike, da pričnejo uporabljati nove sisteme ali metode, ki jih večkrat niti ne razumejo dobro. Pri tem je predavatelj poudaril, da morajo naprave delovati zanesljivo. Zdravnik se ne spozna na principe, recimo invazivnega merjenja krvnega tlaka ali mikroanalizatorja glukoze v krvi, zato mora verjeti odčitanim vrednostim. Dva primera, senzor za invazivno merjenje krvnega tlaka in merilnik pospeška pri srčnem spodbujevalcu, je navedel kot izjemi, ki sta prišli v proizvodnjo in uporabo že po dveh letih. To se je zgodilo zato, ker sta bila oba senzorja že razvita za potrebe avtomobilske industrije in jih je bilo treba samo prenesti na področje medicine.

V našem referatu z naslovom "Thick film resistors and multilayer diffusion patterning technology" (avtorji D. Belavič in M. Pavlin, HIPOT, Šentjernej in M. Hrovat, Institut Jožef Stefan, Ljubljana) smo predstavili materiale (izolacijske-dielektrik, prevodne, in uporovne) za izdelavo MCM s tehnologijo difuzijskega oblikovanja. Difuzijsko oblikovanje je način izdelave večplastnih debeloplastnih vezij, ki omogoča doseganje večje gostote vezij z obstoječo tehnologijo sitotiska in žganja. Večplastno vezje, narejeno s to tehnologijo, je pri isti kompleksnosti 20% do 40% manjše od "navadnega" debeloplastnega večplastnega vezja. Načrtali smo testna vezja, s katerimi smo določili tolerance izdelave ozkih odprtin v dielektriku večplastnih vezij. Prikazali smo rezultate preiskav karakteristik debeloplastnih uporov, žganih na plasti dielektrika in v dielektrični strukturi.

Naslednje leto bo konferenca o Multi Chip Modulih del konference MicroTech 2001 – Microelectronics and Packaging Conference, ki bo od 5. do 7. februarja 2001 v Londonu.

Marko Hrovat
Institut Jožef Stefan
Jamova 39
1000 Ljubljana

Kdor pride pozno, dobi kosti

(razmišljanje ob ugotovitvah delovne skupine št.55 združenja EIRMA z naslovom »Technology monitoring for business success« – Nadzorovanje tehnološkega razvoja za poslovni uspeh – publikacija poročila EIRME, 34,rue de Bassano, 75008 Paris; 1999)

Spremembe so neizprosna stvarnost, so pa hkrati tudi priložnosti. Najpomembneje je, spremembe pravočasno predvidevati in tako pridobiti čas za pravočasno prilagoditev.

Premalo je le slediti tehnični in tehnološki razvoj na ožjem strokovnem področju. Slediti in predvidevati je treba tudi razvoj na socio-ekonomskem, kulturnem političnem področju in področju zaščite okolja. Vse to vpliva na porajanje novih potreb in novih proizvodov in poznavanje tega nam olajša napoved sprememb.

Poznano je, da se poslovno okolje stalno in vse hitreje spreminja in tako narašča pritisk za zmanjšanje časa od ideje do tržljivega proizvoda. Življenjski cikli proizvodov se krajšajo.**Tako je pravočasno inoviranje ponudbe in proizvodnega procesa nujno. Kdor zamudi, izpade iz igre, oziroma pobere le še drobtinice** (kosti) in pokrivanje stroškov razvoja in ostalih vložkov je vprašljivo. Nadaljnja konkurenčnost na trgu upade, s tem pa donosnost podjetja.

Potrebno je torej pravočasno predvidevanje razvoja potreb trga in novih znanj, ki omogoča vzdrževanje konkurenčnih prednosti s primernimi proizvodi in tehnologijami izdelave.

Strateški management mora biti osrednja dejavnost vodstva, ki redno pregleduje položaj podjetja in njegovih proizvodov v konkurenčnem okolju in vzdržuje najtesnejše stike s svojimi kupci. Razvoj - inovacija je del celotne strategije, ki mora realizacijo podpreti.

Potreba po povečanju dodane vrednosti – po inoviranju, znižanju proizvodnih stroškov in ustvarjanju proizvodov in procesov z določeno mero drugačnosti – ekskluzivnosti (mali lahko preživijo le z drugačnostjo, pa tudi veliki ustanavljajo manjše fleksibilne enote, ki so sposobne za drugačnost), po skrajšanju časa za tržno realizacijo (time to market) in morda najvažnejše po sledenju spremembam – vse hkrati poudarja osrednjo **pomembnost znanosti in tehnološkega razvoja.**

Z vse manj marketinškimi in razvojnimi kadri morajo biti podjetja sposobna pregledati in analizirati čedalje več podatkov in iz njih izluščiti tiste, ki so za inoviranje njihovih programov ključni. Nadzorovanje tehnološkega razvoja je tako del sistema upravljanja z znanjem. Zajema zbiranje, ustvarjanje, sintezo, prilagoditev, posredovanje in uporabo znanj za poslovni uspeh. Sodelovanje strokovnjakov najrazličnejših področij in vključevanje zunanjih sodelavcev je nujno, da se vključijo vsa potrebna znanja.

Zlasti mala podjetja imajo premalo strokovnjakov, ki so tudi preveč usmerjeni in preobremenjeni z obilico raznega dela, da bi lahko sledili poznavanju konkurenčnega položaja, poznavanju bodočih trendov, ugotavljanju priložnosti in nevarnosti, preorientaciji razvoja, koncentraciji razvoja na zares nova področja itd. Zato so potrebne primerne povezave s sorodnimi in komplementarnimi podjetji kot tudi z raziskovalnimi ustanovami.

Nadzorovanje tehnološkega razvoja zagotavlja input načrtom in scenarijem tehnološkega načrtovanja in strateškega planiranja ob izvajanju analiz možnosti in zmožnosti realizacije, ohranjanja ali doseganja konkurenčnih prednosti in zadostnega dobička.

Gre torej za del strateškega vodenja s poudarkom na opazovanju sprememb zahtev trga in novih organizacijskih, tehničnih in tehnoloških znanj, ki bi jih lahko uporabili za ohranitev ali pridobitev konkurenčnih prednosti.

Nadzorovanje tehnološkega razvoja ima le malo vrednost, dokler ni polno vključeno v celotno strateško planiranje in poslovanje. Odkrivanje porajajočih se tehnologij nima pomena, če poslovni del ni zmožen uporabiti tega znanja.

Nadzorovanje tehnološkega razvoja se ukvarja s:

- poslovnim okoljem, kupci: kateri in kakšni trgi bodo obstajali?
- obnašanjem konkurence: kje in kako naj tekmujemo?
- proizvodnjo / ponudbo: kakšne proizvode in tehnologije moramo imeti?
- razpoložljivostjo znanj: katera nova znanja bi nam pomagala zadržati konkurenčne prednosti?

Odgovorom na gornja vprašanja mora ustrezati naše nadzorovanje tehnološkega razvoja. Informacije, znanja in priporočila naj ustrezajo okoljem in organizacijam. To je input za izdelavo ali spremembo strategije podjetja – njeno preverjanje skozi izdelavo poslovnih načrtov – povratne informacije in spreminjanje načrtov.

Zavedati se moramo, da nadzorovanje tehnološkega razvoja ne sme sloneti na ustaljenih vzorcih in paradigmah. Razmišljanje mora biti inovativno, preskočiti mora ustaljene miselne vzorce.

Zaposleni, ki ustvarjajo in spremljajo inovacije, morajo biti vključeni in motivirani za spoznavanje in reagiranje na spremembe.

Vodstvo mora spoznati prednosti nadzorovanja tehnološkega razvoja in ga podpreti.

Koraki v procesu nadzorovanja tehnološkega razvoja:

- definicija cilja nadzorovanja
- ugotovitev virov podatkov in informacij
- zbiranje podatkov
- izbor podatkov
- analiza podatkov
- priprava informacij - priporočil
- posredovanje informacij in njihovo skladiščenje

– redefiniranje ciljev nadzorovanja tehnološkega razvoja

Le zakaj vodstva vodilnih firm stalno premlevajo teme strateškega vodenja?

Tudi oni so ljudje, ki bi jim bilo ljubše v miru in v nedogled perfektno proizvajati vpeljane proizvode na obvladan način. A tudi oni so na udaru. Tako lastniki kot zaposleni se vse bolj zavedajo, da lahko le vedno aktualna, usposobljena, atraktivna in konkurenčna proizvodnja z zadostno dodano vrednostjo dolgoročno zagotavlja profitnost kapitala in stabilnost zaposlitve. Zato bogati toliko »zapravljajo« za razvoj.

Pri nas se običajno vprašamo: »**Smo tako bogati, da si lahko privoščimo rizičen razvoj nečesa novega?**« (kar pa v primeru uspeha pomeni višjo dodano vrednost in pobiranje smetane na trgu).

Pravilneje bi se bilo vprašati: »**Smo toliko bogati in drzni, da si lahko privoščimo tiščati glavo v pesek in predolgo zadrževati ali celo uvajati zrele morda celo preživele izdelke in tehnologije?**« (kjer so pokritja čedalje manjša, konkurenco pa zdrže le največji).

Odgovor je gotovo v osveščenosti lastnikov in vodstva in zadostnem poznavanju trga, obstoječi ponudbi in predvidenih in porajajočih se potrebah ter obnašanju konkurence ter o obstoječih in porajajočih se novih znanjih, ki nas lahko pripeljejo do proizvodov z višjo dodano vrednostjo in ki jih moramo biti sposobni trgu primerno ponuditi.

Potreben je torej stalen nadzor poslovanja, analiza, poznavanje okolja ter trendov in razmišljanje o možnostih in ocena zmožnosti, kar nam bo omogočilo usmeritve v donosne programe, pri čemer je ugotovitev nadzorovanja tehnološkega razvoja vhodni podatek.

Organizirajmo si torej nadzorovanje tehnološkega razvoja svojim potrebam, možnostim in zmožnostim primerno!

Igor Pompe
januar 2000

Pozdravni govor ob odprtju analitskega elektronskega mikroskopa JEM-2010 F,

dne 22. junija 2000 na Institutu Jožef Stefan v Ljubljani

Gospe in gospodje,

Dobrodošli na slavnostnem delu odprtja novega **analitskega elektronskega mikroskopa JEM-2010 F** na Odseku za keramiko Instituta Jožef Stefan.

Danes je za skupino za mikroskopijo na odseku za keramiko, ki je obenem vključena v Nacionalni center za mikrostrukturno in površinsko analizo, za vse sodelavce Odseka za keramiko, za mnoge ostale sodelavce IJS, pa tudi za mnoge druge v raziskovalni sredini in industriji, ki delajo na materialih, velik dan. Nova oprema, ki z jutrišnjim dnem začne uradno delovati, omogoča namreč analize strukture in sestave na nano nivoju. Mnogi od vas, ki delate na področju materialov, veste, da je srž lastnosti, ki omogočajo delovanje različnih elementov ne le v neki poprečni strukturi in kemijski sestavi, pač pa prav v specifični strukturi in sestavi majhnih področij. Za to si danes ne moremo zamisliti niti raziskovalnega niti razvojnega dela brez tovrstne opreme. Brez nje smo raziskovalci preprosto slepi. Tega se seveda na Odseku za keramiko dobro zavedamo in v skladu s tem imamo kar nekaj primerne opreme.

O novem zmogljivejšem analitskem elektronskem mikroskopu smo začeli sanjati že davno leta 1995. Vložili smo prijavo na MZT in po mnogih utemeljitvah dobili odobritev sofinanciranja. K nakupu so prispevali sredstva še Kemijski institut, Ljubljana, Institut za kovinske materiale in tehnologije, Ljubljana, Naravoslovno-tehniška fakulteta, Ljubljana, in nekateri Odseki IJS: Odsek za fiziko trdne snovi, Odsek za tanke plasti in površine ter Odsek za fizikalno in organsko kemijo.

Vsem se za to toplo zahvaljujem.

Taka oprema je seveda velika prednost, obenem pa tudi velika odgovornost in obremenitev. Resnično bi bili veseli, da bi tovrstna oprema delovala znotraj centrov, ki upam, da bodo tako kot v svetu zaživeli tudi pri nas.

Za to nabavo seveda stoji mnogo ljudi na MZT, na Institutu Jožef Stefan, na Odseku za keramiko, vendar dovolite, da posebej omenim naše kolege iz skupine Elektronska mikroskopija materialov, ki jo vodi dr. Miran Čeh, in ki so speljali izbiro, ureditev prostora, montažo, skratka vse, da lahko danes mikroskop deluje. Če me občutek ne vara, dr. Miran Čeh v zadnjih dveh letih niti enega dne ni preživel brez tega mikroskopa.

Še nekomu gre zahvala, pa je žal ne more slišati. Našemu učitelju, prof. Kolarju, ki nas je učil vrednosti analitskih rezultatov pri našem delu. On bi bil verjetno danes najbolj vesel. Naj bo njegovemu spominu posvečeno vsaj nekaj trenutkov današnje slovesnosti.

Hvala na pozornosti.

Vodja Odseka za keramiko:
prof. dr. Marija Kosec

VESTI - NEWS

News from European Semiconductor

Malaysia kits up fabs

Malaysia's attempts to enter the league of Taiwan and Singapore in the foundry market have entered the tool-buying phase. Prominent in the recent announcements have been automation companies Asyst, Brooks Automation and PRI Automation.

Asyst received two multi-million dollar orders for "fab-wide automation solutions" based on its standard mechanical interface (SMIF) and other products: Silterra is to get equipment installed in July; 1st Silicon's is due in May.

Silterra plans to start operation in Q4, ramping to 30,000 200 mm wafers/month by 2002.1st Silicon's PAS start-up is planned for Q3, also aiming for 30,000 200 mm wafers/month from its 8000 m^2 cleanroom (beginning with 0.25 μm production and moving to 0.18 μm).

Silterra has also been buying products from both Brooks and PRI. From Brooks, Silterra will be getting software - MES, workcell control, equipment comms, computerised maintenance management and data analysis. PRI's contribution will be wafer transport and planning software.

ASM Lithography is to supply Silterra's all scanner-based semiconductor manufacturing facility. Silterra has selected ASML's PAS 5500/400 i-line and 5500/700 deep UV step and scan systems.

Photonic switching

Agilent Technologies has developed a "Photonic Switching Platform", designed to route communications traffic without converting photons to electrons and back again.

The photonic switch combines inkjet and planar lightwave circuit technology. The first commercial usage is in a 32 x 32 port switch and a dual 16 x 32 port switch. The technology is already under trial with customers for integration into communication systems.

The switch is composed of a vertical and horizontal array of permanently aligned waveguides. Light is transmitted across a horizontal path from input to output until a switch command is issued.

The switch command creates a bubble (the inkjet technology) at the intersection of two waveguides, reflecting the light down a vertical path to the switched port.

32.9% IC boost

The US Semiconductor Industry Association reports a 32.9% increase on 1999 in January's IC sales. The $14.8 bn total spilts as: Americas $4.49 bn (up 25.1%); Europe $3.14 bn (21.5%); Japan $3.29 bn (43.2%); Asia Pacific $3.84 (45.9%). Product leaders were telecoms ICs, Flash memory and DSPs.

Diamond μmachines

Sandia National Laboratories in the US has created comb drive micromachine from amorphous diamond. The technique used is compatible with silicon chip and surface micromachining.

Among the properties of the material is its hardness, resistance to stiction (combination of stickiness and friction) and biocompatibility. Potential medical uses are envisaged. Researchers are seeking to develop a layering technology to increase the life and performance of micromachines through coating a silicon-based structure. Another possibility is to replace silicon altogether.

"One estimate in the literature claims that diamond should last 10,000 times longer than polysilicon in wear applications," observes Sandia researcher Tom Friedmann.

3D ICs?

University of Leeds chemistry researchers plan to create 3D chips, using a technique that "grows" interconnects between stacks of ICs from conductive molecular layers.

Their work is based on disc-shaped liquid crystals created and patented by professors Bushby and Neville Boden. These discs form stacks with a central core of conducting carbon surrounded by a rim of insulating hydrocarbons.

The research is being carried out jointly with the University College of London, the University of Strathclyde and universities in France and The Netherlands.

The scientists are aiming to emulate the 3D structure and function of the human retina and visual cortex. Bushby says the work is still at the "futuristic stage". Marketable results are not expected for a decade.

News from IMEC

1 Mbit HIMOS® Flash memory with 1 million program/erase cycles

The reliability evaluation of a 1 Mbit Flash memory based on IMEC´s patented HIMOS® technology, has revealed impressive endurance and retention results. While conventional embedded Flash technologies typically compromise in terms of performance, IMEC's solution exhibits 1 million program/erase cycles and more than 100 years of data retention. The 0.35 μm HIMOS® technology adds only 30% to the cost of standard digital CMOS (5 additional masking steps) and yet exceeds the performance of other embedded Flash solutions. An interesting feature of this technology is that the program and erase operations do not require any verification functions nor special algorithms on chip for obtaining these characteristics. Also the use

of error correction code (ECC) is redundant in IMEC's solution due to the intrinsic robustness of the HIMOS® cell concept. This is the first time that IMEC has demonstrated the feasibility of the concept on such a large memory block, which was entirely designed and processed at IMEC's facilities.

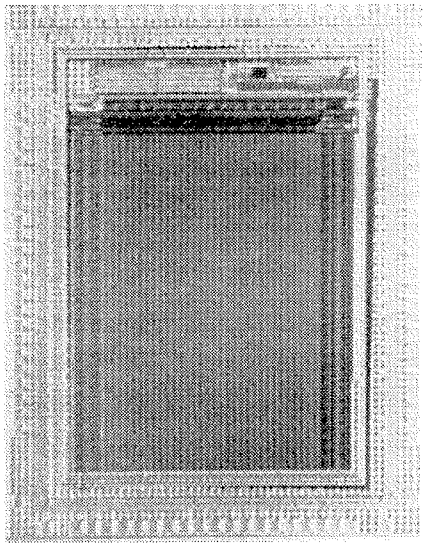

1 Mbit HIMOS® Flash memory in 0.35 μm CMOS

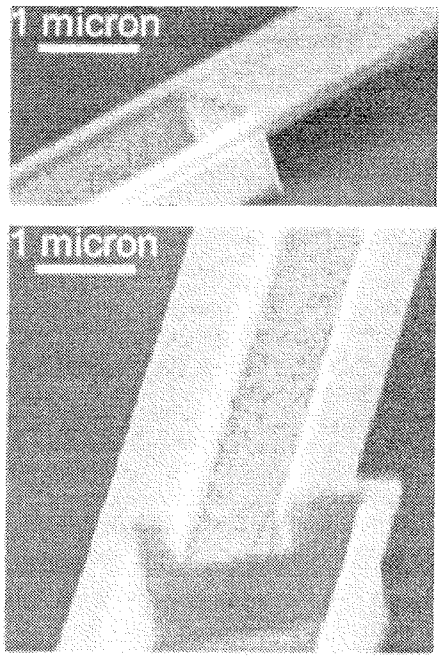

Detail of a traditional support beam and its anchoring point (top) compared to the new U-shaped support beam (bottom)

New construction techniques for sub-micron MEMS

IMEC patented the use of U-profiles in surface micromachining. The resulting mechanical stiffness enables the development of very thin micromachined actuators and sensors, such as uncooled bolometers.

Surface micromachining is a powerful and promising method for the fabrication of Si-based micro-electromechanical systems (MEMS). The basic processing concept is simple: first a sacrificial layer is deposited, patterned and etched to define the "anchor" points of the device. In a second step, the actual device layer is deposited on top of this sacrificial layer. Finally, the sacrificial layer is removed by etching, which results in a suspended device structure. An infrared bolometer is a typical example of MEMS. Its operation relies on a temperature rise of the resistive sensor. This can only be achieved by ultra-high thermal isolation. Infrared bolometers have previously been realized at IMEC using long supporting beams with sub-micron dimensions, consisting of a material with low thermal conductance such as polycrystalline SiGe. Although these sub-micron dimensions were routine in our pilot line, it was the first demonstration of sub-micron MEMS structuring. Ideally the sensor and its support beams should be as thin as possible to maximize sensitivity and speed. However, this makes the sensor element extremely fragile, both during processing and during use. Any stress gradients in the composing layers cause bending of the device and leads to failure. To date, this has limited the material choice and minimal thickness for a host of surface-micromachined sensors and actuators. IMEC has found and patented a fundamental solution to the above problems: U-shaped profiles. These profiles have very high mechanical stiffness at reduced weight and can be easily produced using surface micromachining. Compared to a solid beam with the same dimensions, the stiffness increases by up to three orders of magnitude. This gain in mechanical strength allowed fabrication of very thin bolometers (as thin as 0.1 μm), which are still capable to cope with the destructive forces during the etch process and effectively solve the problem of residual strain gradients in the material. Furthermore, the thermal loss through the two support beams is even lower than the radiative heat loss of the sensor. The benefits of this new approach are evidently not limited to bolometers since increased stiffness is relevant for a large number of surface-micromachined devices.

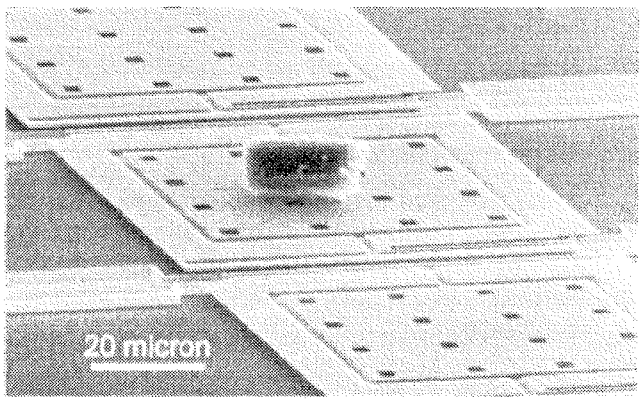

Suspended bolometer pixels featuring U-profiles in beams and sensor. Even accidental debris landing on the device (a lucky shot!) does not result in bending or failure of the device

High-k dielectrics for deep sub-micron technologies

IMEC and ASMI collaborate on the development of Atomic Layer CVD technology for applications in advanced silicon device manufacturing.

Scaling down the SiO_2 gate layer thickness in advanced CMOS devices is reaching its limits, both from the point of view of gate leakage current limitation as well as from intrinsic reliability Recent IMEC research, indicates that below 2.5-nm effective oxide thickness (EOT), the reliability of conventional thin oxide dielectrics is worse than previously expected. Consequently, alternative gate insulators with higher electrical permittivity than SiO_2 must be investigated for their potential applications as gate dielectric layers. The introduction of alternative gate insulators will be unavoidable for process technologies beyond 100 nm. Development in such a critical layer in an IC is only possible through large-scale international collaboration. IMEC, in collaboration with its strategic partner ASMI, has set up an Industrial Affiliation Program to develop gate dielectrics and gate electrodes for (sub)-100 nm devices. Within this program, IMEC wants to develop a manufacturable process for thin films (EOT< 1.5 nm) with low defect density and accurate thickness control.

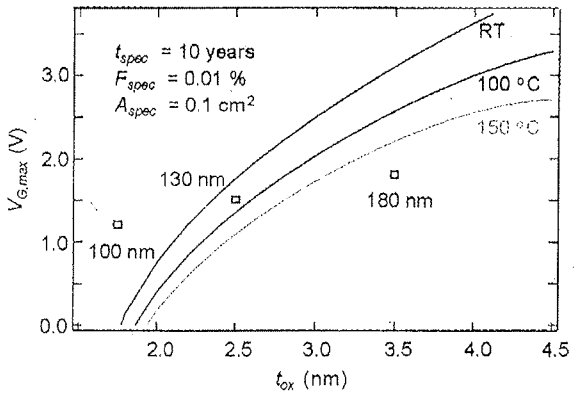

Reliability limit for thickness scaling

IMEC and ASMI aim to use this technique to deposit very thin high-k dielectric layers, such as (but not limited to) Al_2O_3, ZrO_2, HfO_2, and their silicates for use as alternative gate dielectrics. In terms of deposition techniques, atomic layer CVD offers some unique advantages over competitive approaches. It results in perfect thickness and uniformity, as well as composition control over large substrates.

SBT ferroelectric memory cells

IMEC and STMicroelectronics collaborate in the development and integration of SBT (Strontium-Bismuth-Tantalate) ferroelectric memory cells.

The integration of ferroelectric memories with deep sub-micron technologies, becomes an attractive alternative for on-chip-memories. New emerging applications, such as contactless smartcards, require low-power, fast programming speed and a large number of re-write cycles. Ferroelectric memories can offer such performance, as well as the potential for competitive cell size, cost and compatibility with sub-micron technologies. IMEC and ST have signed an agreement to jointly develop a ferroelectric SBT non-volatile memory module to be integrated into ST's current advanced 0.35 μm CMOS technology and compatible with more advanced processes in development. The collaboration will benefit from ST´s experience in smartcard ICs and non-volatile, as well as from IMEC´s work on integration and optimization of non-volatile memory based on the ferroelectric material PZT (lead-zirconate-titanate). SBT will be used as ferroelectric material because of its high endurance and superior voltage scalability compared to PZT.

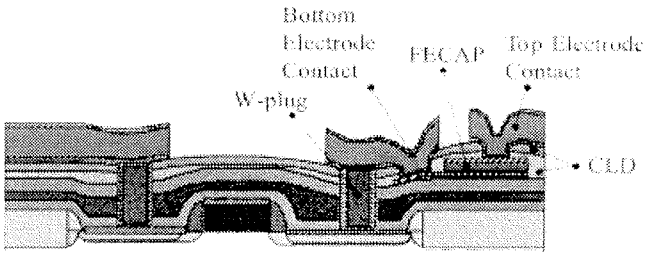

Schematic cross section of an FeRAM structure.

IMEC image sensors register popularity in Technopolis

Technopolis, the first Flemish "do center" on science and technology was officially opened on February 26, 2000. The center is an initiative of the Flemish Government to bring science and technology closer to people. Technopolis starts from the familiar living environment and thrashes out the underlying scientific and technological principles. Visitors can learn the technologies from 227 different "do expositions" in a playful way. An observation system was developed in cooperation with IMEC to assess the popularity of the different expositions. The sophisticated system is the first of its kind in the world. Several IBIS image sensors were mounted in the sealing. The sensors are connected through an internal network and deliver color images indicating the number of visitors of each exhibition. This system allows evaluation of the interest in the different expositions on each moment of the day.

TECHNOPOLIS

News from AMS

Austria Mikro Systeme International invests EUR 305 million into the construction of a new 200 mm production line

Austria Mikro Systeme International is going to build one of the most modern production lines for the production of application-specific integrated circuits (ASICs) and standard products (ASSPs) for automotive, industrial and communications applications in Unterpremstätten. Total investment for the project is EUR 305 million, construction is going to start in the second quarter of 2000. It is planned to finish the clean room during the first six months of 2001, i.e. after 12 months of construction. Process and production optimization with test wafer runs is scheduled for the second half of 2001, industrial volume production will be taken up in the 2nd quarter 2002. The new production line is of essential strategic and economic importance to the Company, for the following reasons:

- **Technology:**

Technological development is heading towards increasingly small structure widths (deep submicron) and the integration of complete electronic systems on one single chip (system-level integration). Looking forward, this can only be done on a 200 mm line. The special processes developed by Austria Mikro Systeme International, such as high-voltage, BiCMOS and SiGe-BiCMOS are unique from a technical point of view. The availability of the new production line will allow these special technologies to be made in structure widths of 0.6μm and 0.35 μm. Moreover, the new production line is going to offer a sound basis from which to develop and produce the next technology generation down to 0.18 μm in the near future.

- **Capacity:**

Within the next few years, the new production line will offer a capacity of at least 2,000 wafer starts per week on a clean room floor area of 2,600 m^2, thus significantly increasing existing inhouse production capacity. Sufficient capacity will therefore be available at Austria Mikro Systeme International and its production partners to support customer growth.

Financing

EUR 222.2 million of the total investment costs of EUR 305.2 million will be spent on building, infrastructure and equipment, and EUR 83.0 million on related investment such as assembly, test facilities, information technology as well as research & development. Financing is comprised of 48% equity funding, 11 % subsidies and 41% outside funds. Noteworthy are the Company's high cash reserves of EUR 72.7 million, available immediately at the start of construction. Utilisation of external resources will thus not become relevant until 2001. The financing structure of the project is a balanced one. In particular the shareholders'equity / total liabilities ratio is both appropriate and in line with industry average. Due to the Company's excellent financial position, the shareholders equity ratio will be above the industry level of 40% throughout the period.

WORKSHOPS IN ELECTRONICS PACKAGING

Chalmers University of Technology
in collaboration with
IEEE/CPMT Sweden Chapter, IVF

Gothenburg, Sweden

001 **Life Cycle Analysis for Environmentally Compatible Electronics (0.5 day)**
(Jun.15, 2000)
Anders Andrae, Ericsson Business Networks, Sweden

002 **Processing of Die Attach Adhesives & Underfill Resins (1 day)**
(Jun.16, 2000)
Raymond A. Pearson, Lehigh University, USA

003 **Conductive Adhesives for Electronics Packaging (1.5 days)**
(Jun.27-28/Aug.29-30/Oct.24-25/Dec. 13-14, 2000)
Johan Liu, Chalmers University of Technology Sweden

004 **Polymers for Electronics Packaging (2 days)**
(Aug.21-22, 2000)
C.P.Wong, Georgia Institute of Technology, USA

005 **Substrate Based Semiconductor Packaging (1 day)**
(Sep.8, 2000)
Charles E. Bauer, Techlead Corporation, USA

006 **Flip Chip Application & Bumping Technologies (1 day)**
(Sep.14/Nov.14, 2000)
Peter Elenius, Flip Chip Technologies, USA

007 **Thermomechanical Reliability of Micro-electronic Packages (1 day)**
(Sep.15/Dec.7, 2000)
Jianmin Qu, Georgia Institute of Technology, USA

008 **Anisotropically Conductive Adhesives for Flip Chip Applications (1 day)**
(Oct, 3, 2000)
Johan Liu, Chalmers University of Technology, Sweden & Martin Böttcher, Delo GmbH, Germany

009 **Lead Free Solders (1 day)**
(Nov. 7, 2000)
Johan Liu, Chalmers University of Technology, Sweden; Gordon C. Whitten, Delphi Delco Electronics Systems, USA & Patrice Rollet, Dehon Group, France

010 **Adhesion Science & Technology (2 days)**
(Nov.9-10, 2000)
Kash Mittal, Consultant, former IBM senior staff, USA

011 **Virtual Reliability Prediction for Electronics Packaging (1 day)**
(Date to be advised)
Sheng Liu, Wayne State University, USA

012 **Conductive Adhesives**
(Date to be advised)
James Morris, State University of New York, Binghamton, USA

013 **ACA Joining Technology in Electronics Packaging (1 day)**
(Date to be advised)
Johan Liu, Chlamers University of Technology, Sweden & T. Sugiyama, Sony Chemical

014 **An Introduction to the Thermal Design of Electronic Products**
(Sept.19, 2000/Feb, 2001)
David Whalley, Loughborough University, UK

Workshop Enquiries

Contact:	Grace Zhou
Tel:	46-31-706-6229
Fax:	46-31-706-6244
Email:	zhou@pe.chalmers.se

For details, please visit
Http://www.pe.chalmers.se/org/elprod/

KOLEDAR PRIREDITEV - CALENDAR OF EVENTS

MAY

MAY 1-3, 2000
7TH INTERNATIONAL SYMPOSIUM & TECHNICAL EXHIBITION, ID, USA
"Roadmap Challenges: Staying ahead of the technology curve" is the theme of the symposium. The two-day format will also include panel discussions and workshops. Contact SCP Global Technologies
Tel: +1208 375 4540
e-mail: mbarker@scpglobal.com
web: www.scpglobal.com

MAY 1-4, 2000
2000 GAAS MANTECH CONFERENCE,
WASHINGTON, DC, USA Contact GaAs Mantech
Tel: +1202 234, 0700
Fax: +1202 265 5333
web: www.gaasmantech.org

MAY 8 - JUNE 2, 2000
ITU WORLD RADIOCOMMUNICATION CONFERENCE (WRC 2000), ISTANBUL, TURKEY
A four-week conference, held every two to three years
Contact ITU
Tel: +4122 730 5111
Fax: +4122 733 7256
web: www.itu.int/newsroom/wrc2000/

MAY 22-24, 2000
FIFTH INTERNATIONAL SYMPOSIUM ON PLASMA PROCESS-INDUCED DAMAGE (P2ID00),
SANTA CLARA, CA, USA
Technical co-sponsors: IEEE/Electron Devices Society, American Vacuum Society and Japan Society of Applied Physics. Contact Northern Californian Chapter of the American Vacuum Society
Tel: +1408 246 3600
Fax: +1408 246 7700
e-mail: della@vacuum.org
web: www.vacuum.org/nccavs/p2id.html

MAY 22-23 2000
ACCESSING THE NANOSCALE, NEUCHÂTEL, SWITZERLAND
Two-day course providing an overview of advanced methods for accessing the nanometre lengthscale.
Contact Swiss Foundation for Research in Microtechnology
Tel: +4132 720 09 00
Fax: +4132 720 09 90
e-mail: fsrm@fsrm.ch
web: www.fsrm.ch

MAY 22-27 2000
ACHEMA 2000, FRANKFURT, GERMANY
Exhibition and symposia bringing together professionals in chemical engineering, environmental protection and biotechnology, Contact Dechema
Tel: +49 69 7564 0
Fax:+49 69 7564 201
e-mail: achema@dechema.de
web: www.achema.de

JUNE

JUNE 6-8 2000
VACUUM 2000, GRENOBLE, FRANCE
Contact SFV
Tel: +33 1 53 01 90 30
Fax: +33 1 42 78 63 20
e-mail: sfv@vide.org
web: www.vide.org

JUNE 6-8 2000
PCIM CONFERENCE, NÜRNBERG, GERMANY
International conference for power conversion, intelligent motion and power quality; plus pre-conference seminars June 4-5 2000.
Contact ZM Communications
Tel: +49 9119817 40
Fax: +49 9119817 445
e-mail: conference@zm-com.com
web: www.zm-com.com

JUNE 13-14, 2000
SEMICONDUCTOR 2000,
EDINBURGH, SCOTLAND, UK
Contact Elaine Townsend, JEMI UK
Tel: +44131472 4704
Fax: +44131662 4678
e-mail: elaine.townsend@ed.ac.uk
web: www.semiconductor2k.com

JUNE 13-16, 2000
BLUETOOTH 2000, MONTE CARLO
Contact Kathryn Redmond, IBC Global Conferences
Tel: +44171453 5452
Fax: +441716361976
e-mail: kathryn.redmond@ibcuk.co.uk
web: www.bluetoothcongress.com

JUNE 19-21, 2000
WORLD ENGINEERS' CONVENTION, HANOVER, GERMANY
Taking place during the World Exposition EXPO 2000, the congress on 'The Future of work' is organised by The Association of Engineers (VDI).
Contact The Association of Engineer
Tel: +49 2116214 0
Fax: +49 2116214 575
e-mail: wec-expo2000@vdi.de
web: wwwvdi.de

JULY

JULY 10-14, 2000
SEMICON WEST, CA, USA
The 30th Semicon West takes place in San Francisco from July 10-12, focusing on wafer processing; and in San Jose from July 12-14, focusing on test, assembly and packaging.
Contact Yumi Higa, SEMI
Tel: +1650 940 6924
Fax: +1650 940 7953
e-mail: yhiga@semi.org
web: www.semi.org